博士論文

Model Study on the Water Addition Reaction to Quinone Methide Intermediates during Lignin Biosynthesis

（リグニン生合成過程におけるキノンメチド中間体への水付加反応に関するモデル研究）

ZHU　XUHAI

朱　旭海

Model Study on the Water Addition Reaction to Quinone Methide Intermediates during Lignin Biosynthesis

（リグニン生合成過程におけるキノンメチド中間体への水付加反応に関するモデル研究）

ZHU　XUHAI

朱　旭海

Advisor: 松本 雄二

Wood Chemistry Laboratory

Department of Biomaterial Sciences

Graduate School of Agricultural and Life Sciences

The University of Tokyo

2019

Contents

Chapter 1

Introduction

1.1 Formation and structure of lignin

Lignin is a class of phenolic natural polymers with a broad composition and a variety of linkages between building units, like monolignols and a few carbohydrate moieties.[1-3] For decades, considerable work has been done on the detailed biosynthesis and structural characterization of these complex natural polymers. Its structural diversity arises mainly from the combination of three phenylpropane derivatives, *p*-coumaryl, coniferyl, and sinapyl alcohols, depicted in **Figure 1.1**.[4] These main building blocks of complex architecture of lignin, often referred to as monolignol or C_6–C_3 units, different in the number of methoxy substitutions at the 3 and 5 positions of aromatic ring. The naming of building blocks was based on the traditional numbering system for lignin rather than the systematic IUPAC numbering scheme.[5] In detail, the attachment of the aliphatic side chain to the aryl ring is at C–1. The phenol oxygen is attached at C–4 and the numbering around the ring follows a rule that we use low numbers, e.g. the only one methoxyl group of coniferyl alcohol will be on C–3 (not C–5). The side-chain carbons are assigned as α, β, and γ and C–α is the one attached to the aromatic ring at its C–1 position.).

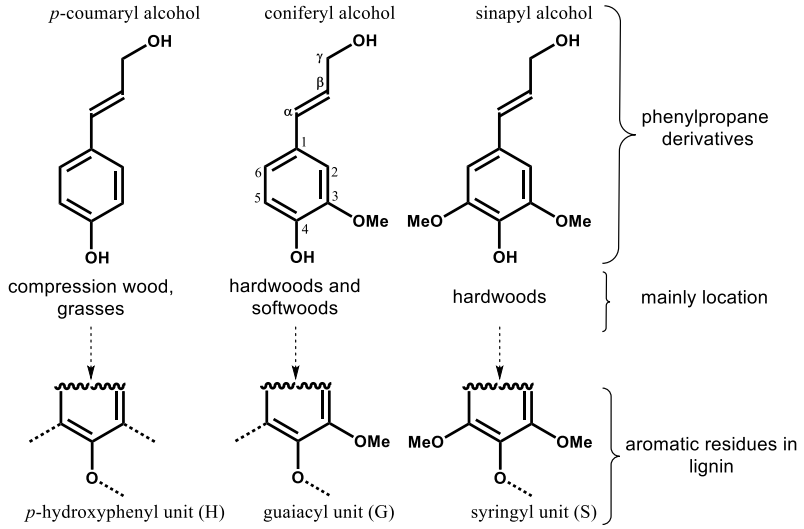

Figure 1.1 Lignin monomeric building blocks and generic lignin units.

When these three monolignols generate the native lignin through radical coupling reaction, each monolignols is constituent *p*-hydroxyphenyl (**H**), guaiacyl (**G**), and syringyl (**S**) units, respectively，in lignin polymer. The guaiacyl units have one aryl-methoxy group and are derived from coniferyl

alcohol, syringyl units have two aryl-methoxy groups and are derived from sinapyl alcohol, and *p*-hydroxyphenyl units have no methoxy groups and are derived from *p*-coumaryl alcohol.[2, 4] Whereas softwood lignins contain primarily G units, together with low levels of H units. Hardwood lignins additionally contain S units in different amounts depending on the wood species.[5] For the H units, however, is more prominent in grasses and compression wood (which develops eccentric radial growth in the lower side of the leaning woody stem and branch of coniferous gymnosperms in response to longitudinal growth stress).[4, 6]

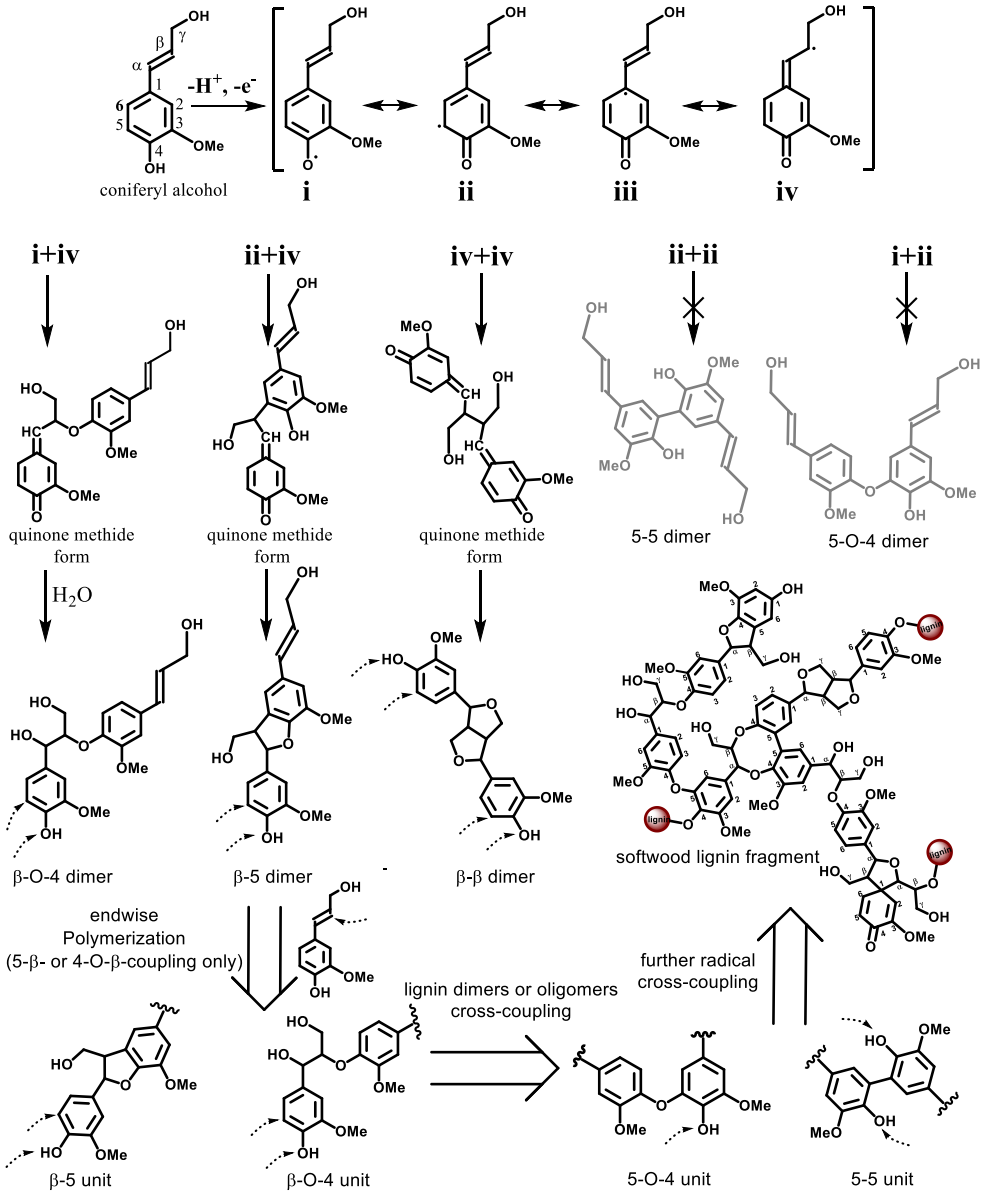

Figure 1.2 Dehydrodimerization of coniferyl alcohol followed by polymerization to produce a softwood lignin fragment. Dashed arrows represent sites where further radical coupling can occur during lignification.

Not only the existence of different monolignols but also the different ways in which these building blocks connect with each other contribute the structural diversity of lignin. Native lignin polymerization initially arises via radical coupling reaction of two monolignol radicals with each other, but further radical cross-coupling reaction between a monolignol and the growing polymer, or between two lignin oligomers give rise to macromolecular lignins.[7] Due to the fact that the monolignol radicals have different resonance structures (**Figure 1.2**), a large number of possible intermonomeric linkages between these three structural units of lignin exist. The frequent linkages found in lignins are β-O-4 (β-aryl ether), β-5 (phenylcoumaran), β-β (resinol), 5-5 (biaryl), β-1 (spirodienone) and 5-O-4 (diaryl ether) (**Figure 1.2**).[4] The phenoxy C–β position seems to be the most reactive. As indicated, the dominant linkage in both softwood and hardwood is the β-O-4 linkage, consisting of approximately 0.45/ C_6–C_3 of spruce linkages and 0.60/ C_6–C_3 of birch linkages.[5, 8, 9] The content of β-5 type structure in spruce lignin was estimated to be 0.09-0.12 by an acidolysis.[10] The total of resinol structures (syringaresinol, pinoresinol, and their analogous structures) were quantitatively estimated to be present at the order of 10% of C_6–C_3 units by the acidolysis of birch lignin.[11] The β-1 structure is relatively minor and less often discussed, in part because it is more complex. Recently authenticated via ^{1}H-NMR studies, β-1 linkages are more prevalent in high-syringyl, which was estimated to be 0.01-0.02/ C_6–C_3 in spruce MWL and 0.05/ C_6–C_3 in birch MWL based on the signal of H-β.[12]

Lignification and monolignol dimerization are substantially different processes.[2, 6, 8, 13] An example of an oxidative coupling of coniferyl alcohol followed by polymerization to produce lignins is shown in **Figure 1.2**. Initially dimerization produces only three dimers, in each of which at least one of the coniferyl alcohol radicals is coupled at its favored β-position. The often shown 4−O−5- or 5−5-coupled dimers in some literatures do not arise from coniferyl alcohol in dimerization reactions. Further cross-coupling occurs between coniferyl alcohol, invariably at its β-position, and the dimer (or higher oligomers) at the 5− or 4−O-position. As lignification progresses, coupling of dimers and higher oligomers can produce the 4−O−5-units or 5−5-linked units (that go on to form dibenzodioxocins), which are important because, in principle, they lead to chain branching.

During this process, quinone methide intermediates from one coupling accept additions of nucleophiles, resulting in the post-coupling re-aromatization reaction.[2, 14] This is an important aspect

of ligninfication.

1.2 Quinone methide in lignification

Quinone methides are reactive electrophilic species that are involved in the biosynthesis of a variety of natural products.[14] The quinone methides are generally formed as transient species, and stabilized by the addition of a nucleophile such as hydroxy group, and amino group at exocyclic methylene or methine group to produce benzylic adducts with aromatization of the ring,[15] whereas relatively stable quinone methides of diterpenoids and triterpenoids have been isolated from plants.[16, 17]

Also, the para- quinone methides are formed as intermediates during the biosynthesis of lignins. The rearomatization step of the quinone methide has a great impact on the resulting chemical structure and the reactivity of the lignins. It was thought to be responsible for the formation of different isomeric forms of major structures in the lignin polymer and for the formation of lignin-carbohydrate bonds.[14, 18] As shown in **Figure 1.2**, three quinone methide forms **1-3** generated by radical coupling of two coniferyl alcohols are subsequently rearomatized by proton-assisted nucleophilic addition reactions. The β-O-4-bonded quinone methide form **1** is the key point discussed in this paper, which will be directly referred as **QM** in the rest parts. This form is generally rearomatized by simple water addition. The resultant β-O-4 structures has two distinct, chemically different, isomeric forms, referred to as *erythro*- and *threo*-isomers.[19] With respect to them, the present knowledge will be described in next sections. It is also suggested that the formation of LCC (lignin carbohydrate complexes) take place when carbohydrates react with β-O-4-bonded **QM**.[20] The quinone methide form **2** produces the trans-phenylcoumaran (β-5 dimer) by internal trapping with the available phenolic hydroxyl group. The quinone methide form **3** produced by β-β coupling are also internally trapped by the γ-OH to produce the bicyclic resinol β-β dimer. The various quinone methide intermediates from β-O-4- or β-5-cross-coupling between a radical monolignol and the growing polymer are also rearomatized by the water addition or internal trapping.[20] In the special case (**Figure 1.3**) of β–1-coupling between a coniferyl alcohol at its β-position and a β-O-4-ether end unit at its 1-position give rise to a quinone methide that

is internally trapped by the α-OH on the original β-O-4-ether unit, to form novel spirodienone structures (β-1 units) in the lignin.[2]

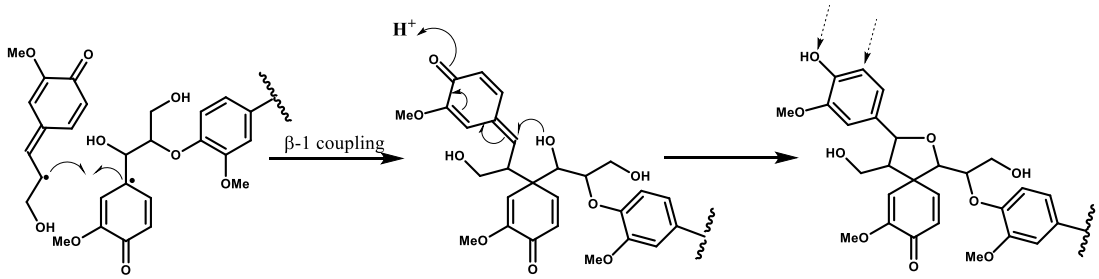

Figure 1.3 The formation of β-1-linked units between a coniferyl alcohol and a lignin β-O-4-ether end-unit.

Dashed arrows represent sites where further radical coupling can occur during lignification.

The **QM** can be thought of a limiting resonance stabilization by electron donation from a *p*-oxygen anion substituent to the cationic α-C as shown in **Figure 1.4**.[21] Nucleophilic addition is therefore easily happen at the electron-deficient α-C position. Addition reactions of **QM** can occur in either basic, neutral or mildly acidic condition. However, the reaction mechanisms are different within pH.[14] For example, as shown in **Figure 1.4**, additions of water to the β-O-4-bonded **QM** can realize via the protonated **QM** at low pH, by direct nucleophilic attack on the α-C at high pH, and possible via a general acid-catalysed process under fairly neutral condition.[14, 22] Whereas, **QM** does react extremely rapidly with softer nucleophiles like, amines, anthranol and anthrahydroquinone, at room temperature[14, 23, 24, 25] or hard nucleophiles such as HO^- and HS^- at high temperature without protonation.[26] Thus, it is generally thought that HO^- will not add to **QM** under room temperature[27] and the conversion of a β-O-4-ether unit from **QM** by water addition may be an acid-catalysed process.[28]

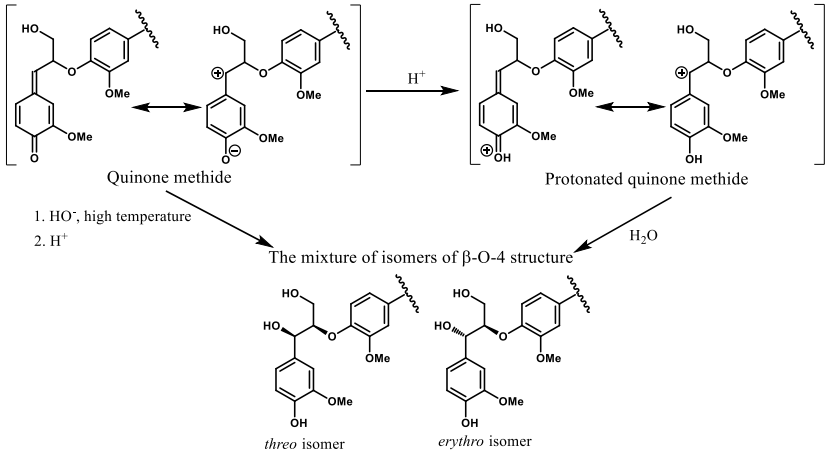

Figure 1.4 Quinone methide protonation and water addition in acidic and basic condition

Evidences suggest that slow rearomatization of **QM** can limit polymerization since further radical coupling reactions cannot occur until the phenol is regenerated.[14] Brunow et al. reported that syringyl-type **QM** dimer was significantly less reactive than the guaiacyl-type during the water addition.[29] This could be explained that the two electron-donating methoxy groups in the syringyl-type **QM** reduce the positive charge density at the α-position. Therefore the enzymatic dehydrogenative polymerizations of sinapyl alcohol afforded artificial lignin (dehydrogenation polymer: **DHP**) in extremely low yields due to the low reactivity of the syringyl-type **QMs**, whereas the polymerizations of coniferyl alcohol or *p*-coumaryl alcohol gave their corresponding **DHP**s in high yields.[30] The radical coupling mechanism for the ligninfication in cell wall is a rather well-accepted theory. Nevertheless, some challenges like how to achieve a satisfactory synthetic **DHP**s structurally resembling native lignins still remain. Thus, significant areas of research into the lignification required further investigation.

1.3 Stereochemistry of lignin

Lignins have the stereo-chemical characters, which gives one chance to the elucidation of the biosynthesis of lignins. It is generally thought that two carbons at the α- and β-positions of monolignols are transformed into asymmetric carbons during the lignin formation. As shown in **Figure 1.5**, the β-carbon becomes the chiral center of an intermediate such as a QM by a radical coupling reaction arising from a monolignol (coupling at its β-positon) and the phenolic end of growing polymer/oligomer. The

chiral centers are formed at α-carbon position on the intermediate when it is attacked by a water molecule or the other hydroxy group from β-O-4, β-β, β-5 coupling structures and carbohydrate. The α- and β-asymmetric carbons have either *R*- or *S*-configuration. Therefore, there are 4 possible stereoisomeric forms in the side-chain part of lignin.[31, 32] Among them, the enantiomeric pairs of β-O-4, β-β or β-5 structures originating from the β-asymmetric carbon are formed in equal amount (racemate).[31-36] Whereas, their diastereomeric pairs, like β-O-4 structures (*erythro* and *threo* forms) and β-5 structures (*trans* and *cis* forms) origin from the formation of the α-asymmetric carbon. The distribution of these diastereomers in lignins appears to be chemically controlled, differing from result of eventual thermodynamic equilibrium.[37, 38] These results reinforce the opinion that "random" polymerization of *p*-hydroxycinnamyl alcohols via radicals plays a role in the biosynthesis of lignins.

1.3.1 Optical activity of lignin

Even though lignification occurs within a chiral matrix (all polysaccharides and proteins are chiral), the potential for optical induction exists, lignins have long been still thought to be optically inactive in a variety of studies over decades.[2, 31-37] For example, Nimz et al. and Freudenberg et al. ever isolated racemic crystals of β-β linkage type compounds.[33, 34] The (±)-Syringaresinol and (±)-pinoresinol were separately released from beech wood meal and spruce wood by a mild hydrolysis with methanol containing 0.5% of HCl at 20 °C for 48h. Ogiyama and Kondo also isolated (±)-*Cis*-dis-γ-lactone of α, β-bis-(hydroxymethyl)-succinic acid ($[\alpha]_D^{20}$ = 0 in $CHCl_3$) originated from β-β linkage type by nitric acid oxidation of cedar lignin prepared from extractive-free wood meal.[35] Ralph et al. verified that β-5 and β-β type products collected from pine lignin by the DFRC (derivatization followed by reductive cleavage) chemical degradation method was optically inactive.[36] This method fully retained optical activity in chiral compounds. They also showed that no optical activity could be detected by the circular dichroism of isolated lignins from pine, kenaf, or maize.[36] In addition, dimers, eg. dehydro-diconiferylalcohol (β-5), pinoresinol (β-β), and the analogous compound (β-β) obtained by the enzymatic oxidation of coniferyl alcohol *in vitro*, were also optically inactive.[39] For the β-O-4 structures, accounting for the most predominant linkages types in lignins, are also determined to be essentially racemic. Through investigating the proportion of *erythro*- and *threo*-forms of β-O-4-

structures and their enantiomeric compositions in hardwood lignin by applying the ozonation method to birch wood meal, Akiyama et al. showed that approximately equal amounts of enantiomeric forms of **QM**s were produced by the β-O-4-coupling reaction during lignification and that the subsequent rearomatization step, water addition, was also racemic.[31, 32]

Therefore, the correctness of the non-stereoselective radical coupling in lignin formation has been confirmed by the structural evidences of some linkage types of lignins.

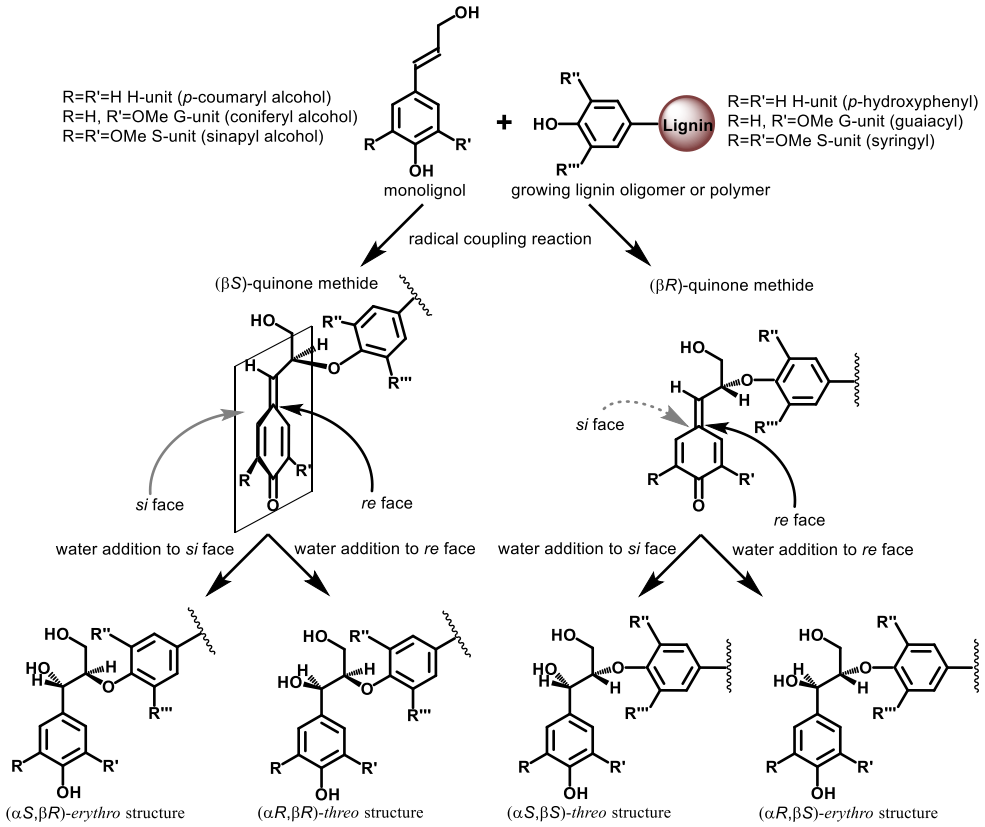

Figure 1.5 Stereoisomeric forms of β-O-4 structures formed by radical coupling

1.3.2 Diastereomeric forms of β-O-4 structures

It is important to note that the appearance of "racemic" structural elements in lignins by no means excludes an uneven distribution of different diastereomeric forms. For all hardwood species, although the proportion of *erythro*- and *threo*-forms of β-O-4 structures in lignins varied widely depending on wood species, the *erythro*-form of β-O-4 structures predominated without exception.[40] This was

elucidated by ^{1}H-NMR studies of birch, oak, alder, maple, sycamore, chestnut and cherry MWLs,[41-43] by ozonation analysis of birch, beech, yellow poplar, ulin, sonokeling, eucalyptus, hackberry wood meals etc.,[40, 44] and by ^{31}P-NMR studies of cherry MWL.[45] In contrast, around 50:50 *erythro*-: *threo*-forms ratio of β-O-4 structures are in softwood, which was determined by ^{1}H-NMR studies of spruce MWL[46] and ozonation analysis of spruce, cedar, maidenhair tree, red pine, agathist, sachalin fir wood meals.[40, 47]

According to the above mentioned hypothesis for the formation of β-O-4 structures in lignin, the proportion of *erythro*- or *threo*- forms is determined in the stereo-preferential water addition to the β-O-4-bonded **QM** intermediate (**Figure 1.5**). Syringyl/guaiacyl (**S/G**) ratio of aromatic nuclei seems to be one of the factors governing the *erythro/threo* ratio, which has been indicated by structural characterization of lignins[40, 48, 49] and by the *in vitro* experiment of the water addition to syringyl-type QM model compounds mimicking hardwood lignin formation.[29] In their structural studies with chemical degradation methods, positive correlations between **S/G** ratio and the *erythro/threo* ratio was found among the lignins of different wood species[40, 48] and were also observed as distributions within a reaction wood stem.[48, 50, 51] Moreover, in the ^{13}C-NMR study of beech MWL and 2D-INADEQUATE experiments of ^{13}C-enriched aspen MWL,[49, 52] the *erythro*-form of β-syringyl ether structures was found to be the predominant type in the four related structural types, the *erythro*- and *threo*-forms of β-guaiacyl or β-syringyl ethers. Depending on the ^{13}C-NMR 2D-INADEQUATE spectrum, the proportion of the *erythro*-form of β-syringyl ether structures were firstly estimated to be ca. 55% in four structural types. These finding evidenced that syringyl-unit influences on the diastereoselective water addition reaction, and induces the *erythro*-preferential formation of β-O-4 structures in hardwood lignins.

There was a case, however, that the *erythro/threo* ratio is not 50:50 for softwood lignin in spite of the absence of syringyl unit.[48, 53] Previous studies of reaction wood lignin showed that β-O-4 structures in compression wood were slightly predominant in *erythro*-form whereas the *erythro/threo* (**E/T**) ratio in the opposite wood was 50:50. The distribution of the **E/T** ratio in the reaction wood disc was positively correlated with that of *p*-hydroxyphenyl/guaiacyl (**H/G**) ratio, implying that the *erythro*-preferential formation occurred during lignin biosynthesis, and is related to the **H**-unit of

aromatic ring type.[48]

1.3.3 Possible factors controlling the proportion of *erythro* and *threo* forms of β-O-4 structures

Mechanism of the diastereo-differentiating water addition to a quinone methide

In the formation of β-O-4 structures, the isomers distribution is kinetically determined by which face of the QM reacts faster with water.[2] The alternative thermodynamic control may also occur when the products are allowed to chemically equilibrate, reflecting the relative stability of the two isomers. However, isomers ratios in lignins differs from the result of the equilibrium state, implying that the formed isomers do not subsequently interconvert to each other during lignification. Through analysis lignin in wood and model compound experiment, β-O-4 guaiacyl ethers are produced around in a 50:50, *erythro*/*threo* ratio, whereas β-O-4 syringyl ethers are produced in a 75:25 ratio in the acidic condition, versus the equilibrium distribution of ～55:45.[29, 40] Therefore, this re-aromatization of **QMs** give rise to a chiral center at the α-position (benzylic position) is under kinetic chemical control rather than thermodynamic control.

As shown in **Figure 1.6**, in the water addition to **QM1**, the enantiomer (**2)** would be produced by addition from the above plane of drawing **QM1** (*si* face), and the enantiomer (**3)** by addition from below (*re* face), since the water addition is in the non-chiral environment, the formation of (**2)** and (**3)** must be exactly equal in rate, giving racemic mixture.

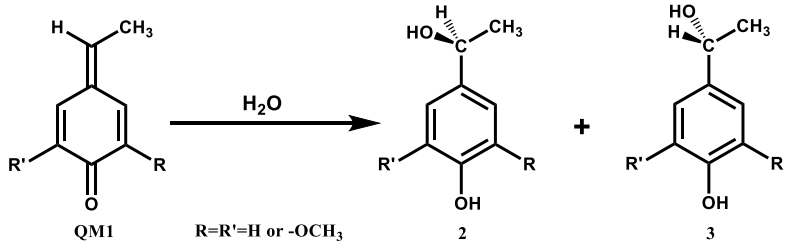

Figure 1.6 Non stereoselective water addition to quinone methide[54]

However, as shown in **Figure 1.7**, once the β-asymmetric carbon is introduced to the β-O-4

bonded **QM** (**4**) before water addition at its electron-deficient α-carbon position, one possible stereoisomeric product can be produced in excess. For example, since the products from water addition to **(*βS*)-QM** are diastereomeric, the transition states of each products are also diastreomeric. Their activation energy can be different and then the diastereomeric products (**5** and **6**) can be formed in different rate. For the *erythro*-form dominates in the hardwood lignin, an asymmetric carbon may influence the stereoselective water addition to the prochiral α-carbon of QM intermediate. In addition to the β-asymmetric carbon of QM, the presence of other asymmetric carbons, like in the carbohydrates and already existing lignin polymer, may affect this process. Based on the results from applying the ozonation method to birch wood meal, an approximately equal amounts of enantiomeric forms of QMs were produced by the β-O-4 coupling reaction during lignin biosynthesis and that the subsequent rearomatization step is also racemic, i.e. the enantiomeric composition of *erythro*- or *threo*-isomers is 50:50.[31, 32] This result implies that, during hardwood lignin biosynthesis, the *erythro*-preferential water addition occurs in the same way both in (*βS*)- and (*βR*)-QM under the influence of the neighboring β-asymmetric carbon that makes the *re*- and *si*-faces uneven toward the water addition.

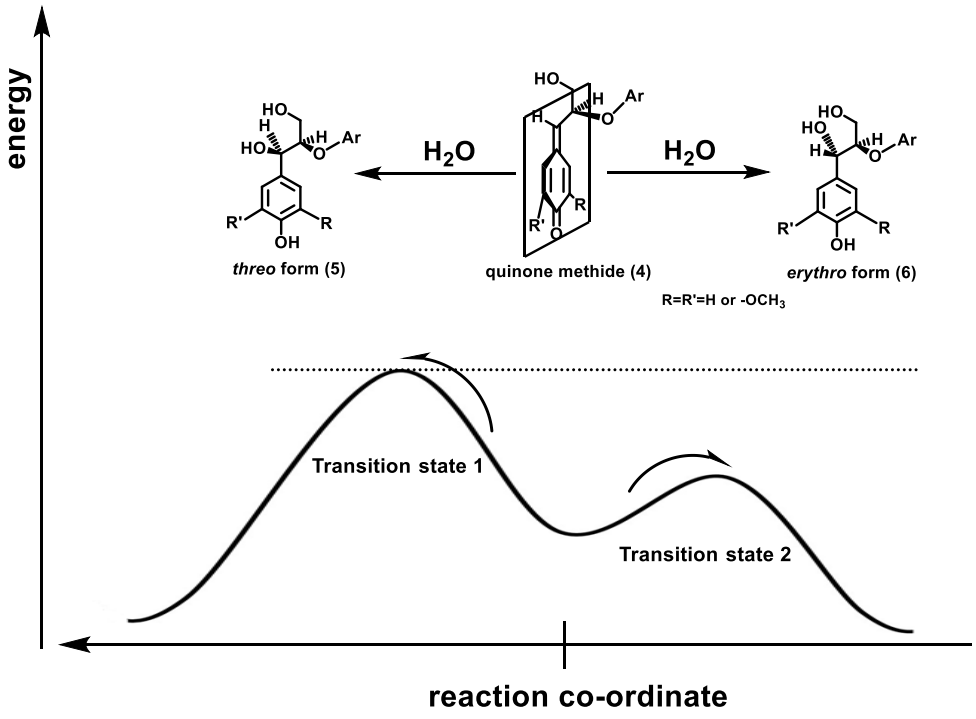

Figure 1.7 Diastereo-differentiating water addition to quinone methide[54]

Model experiment for diastereo-differentiating water addition to quinone methides

Among alternative lignin analysis in wood, model experiment hold great promise for diastereo-differentiating water addition to **QMs**. Through model experiments mimicking the differentiating step of *erythro* and *threo* form from water addition to β-O-4 bonded **QMs**, the degree of stereospecificity and the predominant product isomer appear to depend on the reaction condition (effect of solvent and pH) and the aromatic ring type (guaiacyl, syringyl and *p*-hydroxyphenyl units) of **QM** moiety (A-ring) and etherified aromatic-ring (B-ring).

In a study of the reaction of **QM** in chloroform with catalytic amount of acid, Nakatsubo et al.[55] concluded that *erythro* isomers of guaiacylglycerol-β-guaiacyl ether (**GG**) are produced more than its *threo* ones from the corresponding **QM**. Whereas, *threo* isomers tend to be produced in excess in water. In detail, the *erythro*/*threo* ratio was about 0.5 in dioxane/water (1:9) and 0.4 in dioxane/water (1:1), respectively. Interestingly, these values did not change when buffer solution was used instead of water, or when reaction temperature was changed from 20 ^{o}C to 50 ^{o}C. These results indicate that the *erythro*/*threo* ratio is determined by the difference of solvent.[22]

Brunow et al.[29] performed water addition to three types of β-O-4 bonded QMs prepared from corresponding β-O-4 dimer models: guaiacylglycerol-β-guaiacyl ether (**GG**), guaiacylglycerol-β-syringyl ether (**GS**), and syringylglycerol-β-syringyl ether (**SS**), respectively. The *erythro/threo* ratio of **GG**, and **GS** decreased from 1.0 to 0.5, and from 2.0 to 0.8 as the increase of pH (3 to 7) in dioxane-water solution (1:1, v/v). These results indicate the effect of pH. In addition, not only the A-ring but also the B-ring could influence the ratio of *erythro* and *threo* forms according to the result on higher *erythro*/*threo* ratio (3.0) of SS from water addition to its QM at pH 3 than that of GS (2.0) in the same condition.

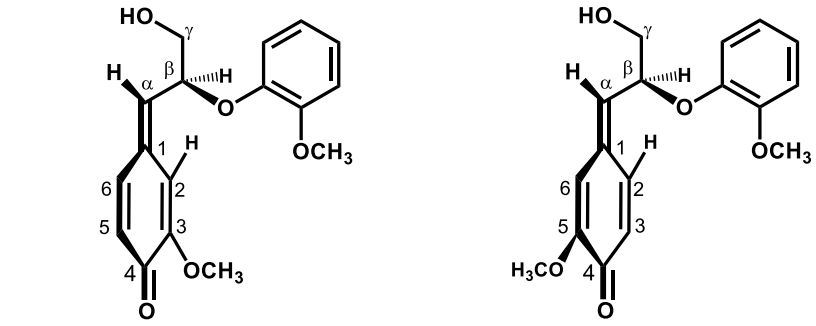

Figure 1.8 Guaiacyl-type quinone methide

Stereoisomeric quinone methide

Two geometric isomers of the guaiacyl-type **QM** are present, as shown in **Figure 1.8**, one in which the side chain is *syn* to the methoxyl group and one in which it is *anti*. Based on the ^{1}H and ^{13}C NMR data and nuclear overhauser effect data, they were distinguished showing that the ratio is typically ～70:30 *syn*/*anti* during preparation.[14, 27] Previous studies indicate that these isomers were non-interconverting at room temperature, even at 170 ^{o}C.[56] They have different stabilities. It also showed that each isomer rearomatizes by nucleophilic addition to α position at a different rate. In the addition of amines to guaiacyl-type **QM**, the *anti*-isomer reacted slightly faster than *syn*-isomer. Ede et al. proposed that the *anti*-isomer was under greater steric strain then the *syn*-isomer based on that internuclear distance between H_{β} and H_2 in *anti*-form **(8)** is smaller than that between H_{β} and H_2 *syn*-form (**7)** observed by NMR.[57] This steric compression is also reflected in an enlargement of angles, C(2)-C(1)-C(α) [123.6^{o}] and C(1)-C(α)-C(β) [122.5^{o}], as shown in *syn*-form 9 of **Figure 1.9**.[58] Therefore, the difference in the effect of these two isomers on *erythro*/*threo* ratio should be taken into consideration. The uneven water addition to each diastereomeric faces (*Re* and *Si* faces of *syn* or *anti* isomer) may happen.

The conformations of QM also can cause the different proportion of *erythro* and *threo* form of β-O-4 structure. If the QM did not have a preferential conformation, i.e., its C_{α}-C_{β} bond rotates freely, water can attack either *Re* or *Si* face equally. On the other hand, when the conformation of QM is stabilized in a certain position, different frequency of attacking on the *Re* and *Si* faces of QM may result the *erythro* and *threo* forms in the different amounts. For example, as shown in **Figure 1.10**,

Nakatsubo et. al.[55] proposed three limited conformations of the *anti* isomer of guaiacyl-type QM in which the QM moisty takes *trans* orientation for each of γ-hydroxymethyl group (**10**), β-hydrogen (**11**) and β-phenoxy group (**12**), respectively. In these conformations, (**11**) may not stable due to the large steric hindrance existing between QM moiety and γ-hydroxymethyl or β-phenoxy group. Left side preferentially attacked to conformation (**12**) may happen producing *threo* isomer because of steric hindrance between nucleophiles and γ-hydroxymethyl group in the right side. By a similar steric factor, *erythro* isomer may be produced predominantly via conformation (**10**), which is attacked from its right side.

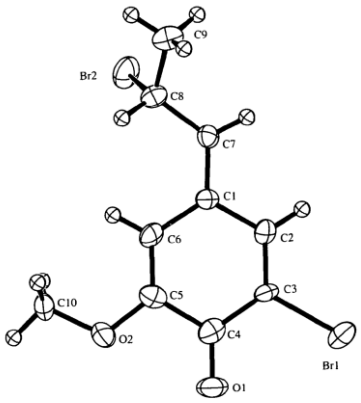

Figure 1.9 A perspective drawing of molecule *syn*-form of guaiacyl-type quinone methide (**9**), picture from the reference [58]

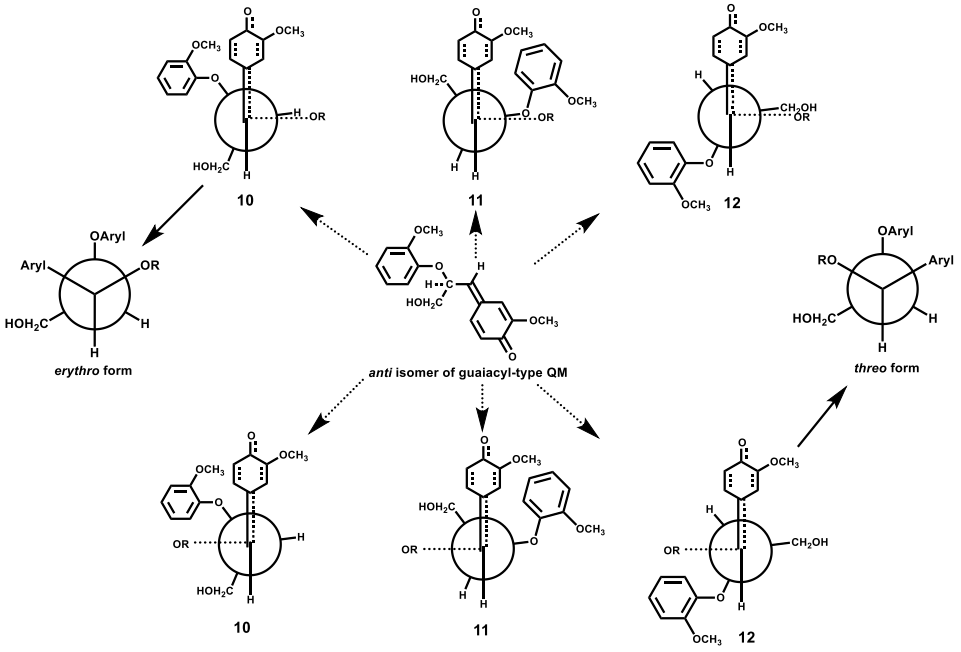

Figure 1.10 Possible conformations of quinone methide in transition state

The crystal structure of β-O-4 dimeric model compounds

If the conformations of transition states during water addition to **QM**s are similar to the crystal structures of β-O-4 product, some same factors influencing the energy of conformation of the β-O-4, like hydrogen bonding, local steric interaction could be taken into consider on the stability of its transition state from QM. Therefore, the conformational preferences of the *threo* and *erythro* diastereomeric forms of β-O-4 dimer have been investigated in detail.[59, 60] The conformation of β-O-4 dimer is largely determined by two torsion angles: C_{aryl}-C_α-C_β-O and C_{aryl}-O-C_β-C_α. As shown in isomers with R-configuration at C_α in **Figure 1.11**, in all the *erythro* forms of β-guaiacyl ethers and β-phenyl ether (**13**, **14**, **15**), the A-ring is gauche to B-ring, i.e., the C_{aryl}-C_α-C_β-O angle is abount 60^o and the angle C_{aryl}-O-C_β-C_α is roughly -140^o. In crystal structures of the *threo* forms of β-guaiacyl ethers (**16**, **17**, **18**), the A-ring is antiperiplanar to B-ring showing the angle C_{aryl}-C_α-C_β-O is about 180^o and the C_{aryl}-O-C_β-C_α angles are ranging from 105^o to 165^o. In the respect to β-syringyl ether model, the aromatic rings of both *erythro* compound (**19**) and *threo* compound (**20**) are interrelated in a similar way: the C_{aryl}-C_α-C_β-O angle is abount 60^o and the angle C_{aryl}-O-C_β-C_α is roughly -150^o. However, the conformations of the *erythro* form of β-syringyl ether models (**21**) and (**22**) are different from that of compound (**19**): their two aromatic rings are almost as far apart as possible showing the angle C_{aryl}-C_α-C_β-O is abount 180^o and the C_{aryl}-O-C_β-C_α angles are about -80^o.

Different intramolecular H-bond can coexist in guaiacyl, syringyl and *p*-hydroxyphenyl β-O-4 dimers.[61,62] Based on the computed and experimental results, a highly directional strong intramolecular H-bond between either the α or γ hydroxyl hydrogen and the methoxy oxygen of the B-ring is present in all the low energy conformers of β-O-4 dimers. An additional intramolecular H-bond, involving only the α and γ hydroxyl groups, can also be detected in some conformational families, but its existence depends on the orientation about the Cα-Cβ bond. Finally, a third H-bond, between the α or γ hydroxyl hydrogen and the β-ether oxygen, is also present in each low energy conformers. The first H-bond constitutes the predominate stabilizing interaction. The same H-bonding patterns with identical optimal geometries are present in the guaiacyl and syringyl structures. As a consequence, the same anticlinal orientation of the B-ring is retained. For the *p*-hydroxyphenyl structure, the B-ring is preferentially locked in an antiperiplanar orientation rather than in an anticlinal

orientation. This can be mainly attributed to the lack of strong first type H-bond, rather than resulting from a simple steric effect due to the absence of methoxy groups. Also, previous molecular modeling on all β-O-4 structures predicted that the energetic ranking of the low-energy conformers is predominantly governed by steric interactions rather than by differences in the H-bonding patterns.[62]

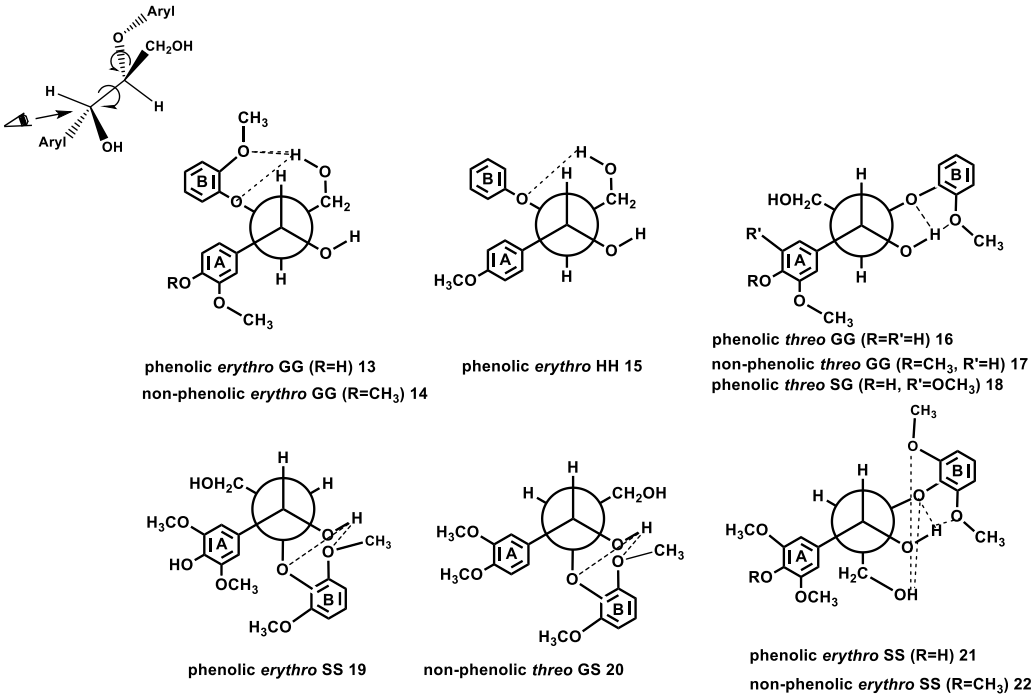

Figure 1.11 Crystal structures of β-O-4 model compounds

1.4 Objectives of this work

As described in the previous section, stereochemical studies on lignins have shown that the ratio of *erythro* and *threo* forms is close to 50:50 in softwood lignins and that the *erythro* form dominates in hardwood lignins. For *erythro* or *threo* isomer to be produced in excess during lignin biosynthesis, stereo-preferential water addition must occur to the β-O-4 aryl ether QM intermediate. What governs the ratio of the two isomers during lignification? Syringyl/guaiacyl (S/G) ratio of aromatic nuclei seems to be one of the factors governing the *erythro/threo* (E/T) ratio, which was evidenced by the positive correlation between these ratios among different wood species and was also indicated by a model study of water addition to syringyl-type QM mimicking hardwood lignin formation.

There was a case, however, that the *erythro/threo* ratio is not 50:50 for softwood lignin in spite of the absence of S-units. Previous studies of reaction wood lignin showed that β-O-4 structures in compression wood were slightly predominant in *erythro* form whereas the E/T ratio in the opposite wood was 50:50. The distribution of the E/T ratio in the reaction wood disc was positively correlated with that of *p*-hydroxyphenyl/guaiacyl (H/G) ratio, implying that the *erythro*-preferential formation occurred during lignin biosynthesis, and is related to the H-unit of aromatic ring type. Nevertheless, direct model experimental evidence on this phenomenon has not been studied in detail.

Therefore, targets of this work are as following:

1. To prepare the clean and stable β-O-4 bonded quinone methide models carrying *p*-hydroxyphenyl units and guaiacyl units. Also, to prepare the related diastereomers of β-O-4 models with different structures. **Chapter 2 & Chapter 3**

2. To investigate the effect of reaction condition and chemical structure of QM moiety (A-ring) and etherified aromatic-ring (B-ring) on the formation of *p*-hydroxyphenyl- and guaiacyl-type β-O-4 structures from the corresponding quinone methides. **Chapter 3**

3. To verify the factors influencing the proportion of *erythro* and *threo* form of β-O-4 structure from quinone methide through preparation of artificial lignins (Synthetic dehydrogenation polymers, DHP). **Chapter 4**

1.5 References

[1] Ragauskas, A. J., Beckham, G. T., Biddy, M. J., Chandra, R., Chen, F., Davis, M. F., ..., Langan, P. 2014. Lignin valorization: improving lignin processing in the biorefinery. Science, 344(6185), 1246843.

[2] Ralph, J., Lundquist, K., Brunow, G., Lu, F., Kim, H., Schatz, P. F., ..., Boerjan, W. 2004. Lignins: natural polymers from oxidative coupling of 4-hydroxyphenyl-propanoids. Phytochemistry Reviews, 3(1-2), 29-60.

[3] Calvo-Flores, F. G., Dobado, J. A., Isac-García, J., Martín-Martínez, F. J. 2015. Lignin and lignans as renewable raw materials: chemistry, technology and applications. John Wiley & Sons, pp 11-12.

[4] Heitner, C., Dimmel, D., Schmidt, J. 2016. Lignin and lignans: advances in chemistry. CRC press, pp 2-3.

[5] Sarkanen, K. V., Ludwig, C. H. 1971. Lignins. Occurrence, formation, structure, and reactions. Wiley-Interscience, New York, pp 43-94.

[6] Nanayakkara, B., Manley-Harris, M., Suckling, I. D., Donaldson, L. A. 2009. Quantitative chemical indicators to assess the gradation of compression wood. Holzforschung, 63(4), 431-439.

[7] Boerjan, W., Ralph, J., Baucher, M. 2003. Lignin biosynthesis. Annual review of plant biology, 54(1), 519-546.

[8] Adler, E. 1977. Lignin chemistry—past, present and future. Wood Science and Technology, 11(3), 169-218.

[9] Neish, A. C. 1968. Monomeric intermediates in the biosynthesis of lignin. Constitution and Biosynthesis of lignin, pp 3-43.

[10] Adler, E., Lundquist, K. 1963. Spectrochemical estimation of phenylcoumaran elements in lignin. Acta Chemica Scandinavica, 17(1), 13-26.

[11] Lignin, B. 1973. Acid degradation of lignin. Acta Chemica Scandinavica, 27(7), 2597-2606.

[12] Lundquist, K. 1987. On the occurrence of β-1 structures in lignins. Journal of Wood Chemistry and Technology, 7(2), 179-185.

[13] Yue, F., Lu, F., Ralph, S., Ralph, J. 2016. Identification of 4–O–5-units in softwood lignins via

definitive lignin models and NMR. Biomacromolecules, 17(6), 1909-1920.

[14] Ralph, J., Schatz, P. F., Lu, F., Kim, H., Akiyama, T., Nelsen, S. F. 2009. Quinone methides in lignification. Quinone Methides, pp 385-420.

[15] Andersen, S. O. 2010. Insect cuticular sclerotization: A review. Insect Biochemistry and Molecular Biology, 40(3), 166-178.

[16] Kupchan, S. M., Karim, A., Marcks, C. 1968. Tumor inhibitors. XXXIV. Taxodione and taxodone, two novel diterpenoid quinone methide tumor inhibitors from Taxodium distichum. Journal of the American Chemical Society, 90(21), 5923-5924.

[17] Gunatilaka, A. L., Fernando, H. C., Kikuchi, T., Tezuka, Y. 1989. ^{1}H and ^{13}C NMR analysis of three quinone-methide triterpenoids. Magnetic Resonance in Chemistry, 27(8), 803-807.

[18] Sipilä, J., Brunow, G. 1991. On the mechanism of formation of non-cyclic benzyl ethers during lignin biosynthesis Part 3. The reactivity of a β-O-4 type quinone methide with methyl-α-D-glucopyranoside in competition with vanillyl alcohol. The formation and the stability of benzyl ethers between lignin and carbohydrates. Holzforschung, 45(s1), 3-8.

[19] Akiyama, T., Goto, H., Nawawi, D. S., Syafii, W., Matsumoto, Y., Meshitsuka, G. 2005. *Erythro*/*threo* ratio of β-O-4 structures as an important structural characteristic of lignin. Part 4: Variation in the *erythro*/*threo* ratio in softwood and hardwood lignins and its relation to syringyl/guaiacyl ratio. Holzforschung, 59(3), 276-281.

[20] Freudenberg, K. 1968. Constitution and biosynthesis of lignin. Constitution and Biosynthesis of Lignin, pp 43-129.

[21] Toteva, M. M., Moran, M., Amyes, T. L., Richard, J. P. 2003. Substituent effects on carbocation stability: The pK_R for *p*-quinone methide. Journal of the American Chemical Society, 125(29), 8814-8819.

[22] Ralph, J., Young, R. A. 1983. Stereochemical aspects Op addition reactions involving lignin model quinone methides. Journal of Wood Chemistry and Technology, 3(2), 161-181.

[23] Landucci, L. L., Ralph, J. 1982. Adducts of anthrahydroquinone and anthranol with lignin model quinone methides. 1. Synthesis and characterization. The Journal of Organic Chemistry, 47(18), 3486-3495.

[24] Landucci, L. L. 1981. Formation of carbon-linked anthrone-lignin and anthrahydroquinonelignin adducts. Journal of Wood Chemistry and Technology, 1, 61–74.

[25] Ralph, J., Landucci, L. L. 1986. Adducts of anthrahydroquinone and anthranol with lignin model quinone methides. 9, 10-^{13}C Labelled Anthranol-Lignin Aeducts; Examination of adouct formation and stereochemistry in the polymer. Journal of Wood Chemistry and Technology, 6(1), 73-88.

[26] Ralph, J. 1985. Lignin model quinone methides—facts and fallacies. In Proceedings of the Third International Symposium of Wood and Pulping Chemistry, Vancouver, BC, Canada.

[27] Ralph, J. 1982. Reactions of lignin model quinone methides and NMR studies of lignins. Ph. D. thesis, University of Wisconsin—Madison, University Microfilms #DA 82-26987.

[28] Durbeej, B., Eriksson, L. A. 2003. Formation of β-O-4 lignin models-A theoretical study. Holzforschung, 57(5), 466-478.

[29] Brunow, G., Karlsson, O., Lundquist, K., Sipilä, J. 1993. On the distribution of the diastereomers of the structural elements in lignins: the steric course of reactions mimicking lignin biosynthesis. Wood Science and Technology, 27(4), 281-286.

[30] Tobimatsu, Y., Takano, T., Kamitakahara, H., Nakatsubo, F. 2008. Azide ion as a quinone methide scavenger in the horseradish peroxidasecatalyzed polymerization of sinapyl alcohol. Journal of Wood Science, 54(1), 87-89.

[31] Akiyama, T., Magara, K., Matsumoto, Y., Meshitsuka, G., Ishizu, A., Lundquist, K. 2000. Proof of the presence of racemic forms of arylglycerol-β-aryl ether structure in lignin: Studies on the stereo structure of lignin by ozonation. Journal of Wood Science, 46(5), 414-415.

[32] Akiyama, T., Magara, K., Meshitsuka, G., Lundquist, K., Matsumoto, Y. 2015. Absolute configuration of β-and α-asymmetric carbons within β-O-4-structures in hardwood lignin. Journal of Wood Chemistry and Technology, 35(1), 8-16.

[33] Nimz, H., Gaber, H. 1965. Isolierung von dl-Syringaresinol aus Buchenholz. Chemische Berichte, 98(2), 538-539.

[34] Freudenberg, K., Chen, C. L., Harkin, J. M., Nimz, H., Renner, H. 1965. Observation on lignin. Chemical Communications, (11), 224-225.

[35] Ogiyama, K., Kondo, T. 1966. On the pinoresinol type of structural units in lignin. Tetrahedron

Letters, 7(19), 2083-2088.

[36] Ralph, J., Peng, J., Lu, F., Hatfield, R. D., Helm, R. F. 1999. Are lignins optically active ?. Journal of Agricultural and Food Chemistry, 47(8), 2991-2996.

[37] Lundquist, K., Langer, V., Li, S., Stomberg, R. 2003. Lignin stereochemistry and its biosynthetic implications. In 12th International Symposium on Wood and Pulping Chemistry, Madison, Wisconsin, USA, Vol. 1, pp 239-244.

[38] Lundquist, K., Rolf, S. 1988. On the occurrence of structural elements of the lignan type (β-β Structures) in lignins-The crystal structures of (+)-pinoresinol and (±)-trans-3, 4-divanillyltetrahydrofuran. Holzforschung, 42(6), 375-384.

[39] Freudenberg, K., Rasenack, D. 1953. d, l-Pinoresinol, ein weiteres Zwischenprodukt der Ligninbildung. Chemische Berichte, 86(6), 755-758.

[40] Akiyama, T., Goto, H., Nawawi, D. S., Syafii, W., Matsumoto, Y., Meshitsuka, G. 2005. *Erythro*/*threo* ratio of β-O-4-5 structures as an important structural characteristic of lignin. Part 4: Variation in the *erythro*/*threo* ratio in softwood and hardwood lignins and its relation to syringyl/guaiacyl ratio. Holzforschung, 59(3), 276-281.

[41] Lundquist, K. 1979. NMR studies of lignine. 2. Interpretation of the Щ NMR spectrum of acetylated birch lignin. Acta Chemica Scandinavia B, 33, 27-30.

[42] Hauteville, M., Lundquist, K., von Unge, S. 1986. NMR studies of lignins. 7. ^{1}H NMR spectroscopic investigation of the distribution of *erythro* and *threo* forms of β-O-4 structures in lignins. Acta Chemica Scandinavica, 31-35.

[43] Tollier, M. T., Monties, B., Lapierre, C., Herve du Penhoat, C., Rolando, C. 1986. Inhomogeneity of angiosperm lignin: Comparison of the monomeric composition of lignin fractions isolated from different wood species. Holzforschung, Suppl 40:75-79.

[44] Matsumoto, Y. 1993. Structural study on lignin by ozonation. The *erythro* and *threo* ratio of the β-O-4 structure indicates how lignin polymerizes. Mokuzai Gakkaishi, 39, 734-736.

[45] Saake, B., Argyropoulos, D. S., Beinhoff, O., Faix, O. 1996. A comparison of lignin polymer models (DHPs) and lignins by ^{31}P NMR spectroscopy. Phytochemistry, 43(2), 499-507.

[46] Lundquist, K. N. U. T. 1980. NMR studies of lignins. 4. Investigation of spruce lignin by ^{1}H NMR

spectroscopy. Acta Chemica Scandinavica, 34, 21-26.

[47] Matsumoto, Y. 1986. Studies on chemical structure of lignin by ozonation. Holzforschung, 40, 81-85.

[48] Nawawi, D. S., Akiyama, T., Syafii, W., Matsumoto, Y. 2017. Characteristic of β-O-4 structures in different reaction wood lignins of Eusideroxylon zwageri T. et B. and four other woody species. Holzforschung, 71(1), 11-20.

[49] Bardet, M., Robert, D., Lundquist, K., von Unge, S. 1998. Distribution of *erythro* and *threo* forms of different types of β-O-4 structures in aspen lignin by ^{13}C NMR using the 2D INADEQUATE experiment. Magnetic Resonance in Chemistry, 36(8), 597-600.

[50] Akiyama, T., Matsumoto, Y., Okuyama, T., Meshitsuka, G. 2003. Ratio of *erythro* and *threo* forms of β-O-4 structures in tension wood lignin. Phytochemistry, 64(6), 1157-1162.

[51] Nawawi, D. S., Syafii, W., Akiyama, T., Matsumoto, Y. 2016. Characteristics of guaiacyl-syringyl lignin in reaction wood in the gymnosperm Gnetum gnemon L. Holzforschung, 70(7), 593-602.

[52] Bardet, M., Gagnaire, D., Nardin, R., Robert, D., Vincendon, M. 1986. Use of ^{13}C enriched wood for structural NMR investigation of wood and wood components, cellulose and lignin, in solid and in solution. Holzforschung, 17-24.

[53] Yeh, T. F., Braun, J. L., Goldfarb, B., Chang, H. M., Kadla, J. F. 2006. Morphological and chemical variations between juvenile wood, mature wood, and compression wood of loblolly pine (Pinus taeda L.). Holzforschung, 60(1), 1-8.

[54] Akiyama, T. 2003. Stereochemistry of β-O-4 structure in lignin. Ph. D. thesis, University of Tokyo, 1(4), 11-12.

[55] Nakatsubo, F., Sato, K., Higuchi, T. 1976. Enzymic dehydrogenation of *p*-coumaryl alcohol, 4: Reactivity of quinonemethide. Mokuzai Gakkaishi, 22, 29–33.

[56] Ralph, J., Elder, T. J., Ede, R. M. 1991. The stereochemistry of guaiacyl lignin model quinone methides. Holzforschung, 45(3), 199-204.

[57] Ede, R. M., Main, L., Ralph, J. 1990. Evidence for increased steric compression in *anti* compared to *syn* lignin model quinone methides. Journal of Wood Chemistry and Technology, 10(1), 101-110.

[58] Li, S., Lundquist, K., Soubbotin, N., Stomberg, R. 1995. 2-Bromo-4-[2-bromo-(E)-propylidene]-

6-methoxy-2, 5-cyclohexadien-1-one. Acta Crystallographica Section C, 51(11), 2366-2369.

[59] Lundquist, K., Langer, V., Li, S., Stomberg, R. 2003. Lignin stereochemistry and its biosynthetic implications. In 12th International Symposium on Wood and Pulping Chemistry, Madison, Wisconsin, USA, Vol. 1, pp 239-244.

[60] Langer, V., Lundquist, K., Parkås, J. 2007. The stereochemistry and conformation of lignin as judge by X-ray crystallographic investigations of lignin model compounds: Arylglycerol β-guaiacyl ethers. BioResources, 2(4), 590-597.

[61] Besombes, S., Robert, D., Utille, J. P., Taravel, F. R., Mazeau, K. 2003. Molecular modeling of lignin β-O-4 model compounds. Comparative study of the computed and experimental conformational properties for a guaiacyl β-O-4 dimer. Holzforschung, 57(3), 266-274.

[62] Besombes, S., Robert, D., Utille, J. P., Taravel, F. R., Mazeau, K. 2003. Molecular modeling of syringyl and *p*-hydroxyphenyl β-O-4 dimers. Comparative study of the computed and experimental conformational properties of lignin β-O-4 model compounds. Journal of Agricultural and Food Chemistry, 51(1), 34-42.

Chapter 2

Synthesis of Lignin β-O-4 Models and Related Compounds

2.1 Introduction

The lack of extensive experimental information on the biosynthesis of *p*-hydroxyphenyl type β-O-4 structure requires the use of model compounds and simulations to provide further insight into the reactivity and diastereo-preferential formation of this type β-O-4 structure from water addition to quinone methide.

In this work, six different phenolic β-O-4 models carrying guaiacyl units (**G**), syringyl units (**S**), and/or *p*-hydroxyphenyl (**H**) units in their two aromatic rings were synthesized according to Adler's method,[1] as shown in **Figure 2.1** to **2.3**. They were guaiacylglycerol-β-guaiacyl ether (**GG**), guaiacylglycerol-β-*p*-hydroxyphenyl ether (**GH**), guaiacylglycerol-β-syringyl ether (**GS**), *p*-hydroxyphenylglycerol-β-guaiacyl ether (**HG**), *p*-hydroxyphenylglycerol-β-*p*-hydroxyphenyl ether (**HH**). In addition, β-O-4 trimeric model which carry a **HH**-type biphenyl unit in β-aryl etherified moiety (**H-HH$_{biphenyl}$**). The separation of *erythro* and *threo* isomers of each β-O-4 dimers (**GG**, **GH**, **GS**, **HG**, **HH**) were carried out using ion-exchange chromatography using a borate solution as the eluent. The *erythro* and *threo* isomers of **H-HH$_{biphenyl}$** were separated each other with flash chromatography. The configuration of each isomers of the β-O-4 models (*erythro* or *threo*) was determined by ozonation method, in which erythronic and threonic acid are obtained from the *erythro* and *threo* isomers, respectively.

Phenolic β-O-4 models were used as the starting material to prepare the β-O-4 bonded quinone methide (**QM**) models. The synthesized β-O-4 model was also used to identify and quantify the β-O-4 products obtained by water addition experiment to **QM**s in chapter 3.

2.2 Experimental

2.2.1 General

All chemicals were purchased from Wako Pure Chemical Industries, Ltd. (Osaka, Japan), Tokyo Chemical Industry Co., Ltd. (Tokyo, Japan) or Sigma-Aldrich (Tokyo, Japan) and used as supplied. The thin-layer chromatography (TLC) was conducted on silica gel plate (Kieselgel 60 F_{254}, Merck)

with solvent system. Silica gel chromatography was performed on a Biotage Isolera One (Biotage, Charlottesville, VA) flash-chromatography instrument, using prepacked (or re-packed) SNAP cartridges (50 or 100 g of silica gel). All synthesized compounds were characterized by the usual array of NMR. NMR spectra were acquired on a JEOL JNM-A500 500 MHz spectrometer. Spectra were processed using JEOL's Alice 1D and 2D software. Standard JEOL programs of one-and two-dimensional (proton, carbon, DEPT-135, ^{1}H-^{1}H COSY, ^{1}H-^{13}C HSQC, and ^{1}H-^{13}C HMBC) NMR experiments were used for routine structural assignments of synthesized compounds. The conditions used for all samples were 10-20 mg in 0.5 mL NMR solvent, with the central solvent peak (δ_H 7.26, δ_c 77.0 ppm for $CDCl_3$, δ_H 2.04, δ_c 29.8 ppm for acetone-*d*$_6$, δ_H 5.32, δ_c 53.8 ppm for CD_2Cl_2) used as an internal reference. For samples that encountered multiplicity problems with hydroxyl group protons, a drop of D_2O was added for the OH-OD exchange prior to analysis. The traditional numbering system for lignin[2, 3] was used rather than the systematic IUPAC numbering scheme.

2.2.2 Synthesis of β-O-4 model compounds

Guaiacylglycerol-β-guaiacyl ether (GG)

The synthetic route of β-O-4 model **GG** is shown in **Figure 2.1**.

Synthesis of 3-methoxy-4-benzyloxyacetophenone (1$_G$). A solution of anhydrous DMF (200 ml), acetovanillone (33.23 g, 200 mmol, 1 equiv), potassium iodide (2.32 g, 14 mmol, 0.07 equiv) and powdered potassium carbonate (38.70 g, 280 mmol, 1.4 equiv) were prepared in a 500 ml round bottom flask, then refluxed at 90 °C in an oil bath while stirring magnetically. Benzyl chloride (35.44 g, 280 mmol, 1.4 equiv) was added dropwise into the suspension. The progress of the reaction was monitored by TLC [hexane-EtOAc=2:1, R_f (starting material, s/m)=0.15, R_f (target material, t/m)=0.24]. After 3 hours, the reaction mixture was cooled down to room temperature and poured into approx. 150 g of ice with stirring. When all of the ice melted, the resulting white solids were isolated by suction filtration and washed three times with water and once with hexane. The collected residue was then dissolved in hot ethanol and allowed to cool, affording crystalline compound **1$_G$** (42.6 g, 83% yield). **Compound 1$_G$** ^{1}H NMR (acetone-*d*$_6$, 500 MHz), δ_H: 2.50 (3H, s, β), 3.87 (3H, s, A3-OMe), 5.21 (2H,

s, $PhCH_2$), 7.10-7.59 (8H, m, aromatic). ^{13}C NMR (acetone-d_6, 125 MHz) δ_C: 26.4 (β), 56.2 (A3-OMe), 71.2 ($PhCH_2$), 111.6, 113.3, 123.8, 128.6, 128.9 and 129.4 (aromatic, -CH), 131.7, 138.0, 150.5 and 153.5 (aromatic, quaternary C), 196.5 (α).

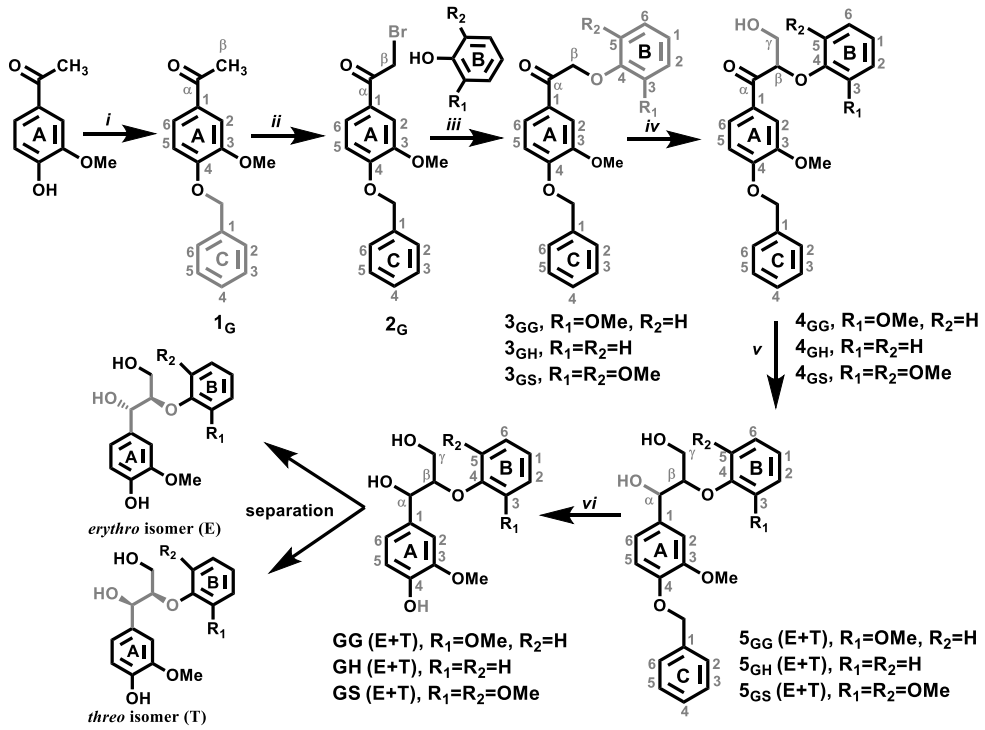

Figure 2.1 Synthetic route of β-O-4 model **GG**, **GH** and **GS**. Reagents and conditions were as follows: (*i*) BnCl, KI, K_2CO_3, anhydrous DMF, 90 °C, (*ii*) Br_2, EtOH, rt, (*iii*) K_2CO_3, acetone, 40 °C, (*iv*) HCHO, THF, K_2CO_3, 40 °C, (*v*) $NaBH_4$, THF-EtOH (v/v, 1:2), rt (mixture of *erythro* and *threo* isomers), (*vi*) 10% Pd/C, H_2, THF, rt (mixture of *erythro* and *threo* isomers).

Synthesis of 3-methoxy-4-benzyloxy-α-bromoacetophenone (2_G). Compound $\mathbf{1_G}$ (12.82 g, 50 mmol, 1 equiv) was dissolved in 400 ml of ethanol at 60 °C, and nitrogen gas was slowly bubbled through the solution. After the solution was cooled down to room temperature, bromine (9.59 g, 60 mmol, 1.2 equiv) was quickly added with stirring at room temperature. In approximately 20 minutes later a precipitate began to form as the solution faded from dark red-orange to a clear pale yellow. The progress of the reaction was monitored by TLC [hexane-EtOAc=2:1, R_f (s/m)=0.27, R_f (t/m)=0.35]. After around 1.5 hours, the starting material completely disappeared. The precipitate in the reaction mixture was collected by suction filtration and washed with small amount of cold ethanol and hexane, successively. The resulting crude product was recrystallized from ethanol, then needle crystals of compound $\mathbf{2_G}$ was obtained (12.4 g, 74% yield). **Compound 2_G** ^1H NMR (acetone-d_6, 500 MHz), δ_H:

3.09 (3H, s, A3-OMe), 3.88 (2H, s, β), 4.56 (2H, s, $PhCH_2$), 6.36-6.89 (8H, m, aromatic). ^{13}C NMR (acetone-d_6, 125 MHz) δ_C: 32.7 (β), 56.3 (A3-OMe), 71.3 ($PhCH_2$), 112.3, 113.3, 124.5, 128.7, 129.0 and 129.4 (aromatic, -CH), 128.4, 137.8, 150.5 and 154.2 (aromatic, quaternary C), 190.8 (α).

Synthesis of 3-methoxy-4-benzyloxy-α-(3-methoxyphenoxy)-acetophenone (3_{GG}). To a stirred solution of anhydrous acetone (60 ml), compound $\mathbf{2_G}$ (12.36 g, 37 mmol, 1 equiv), and guaiacol (5.49 g, 44 mmol, 1.2 equiv) charged in a 200 ml of round bottom flask, powdered potassium carbonate (10.19 g, 74 mmol, 2 equiv) was added and the reaction mixture was kept at 40 °C for 1.5 hours. The progress of the reaction was monitored by TLC [hexane-EtOAc=2:1, R_f (s/m)=0.37, R_f (t/m)=0.18]. The reaction mixture was concentrated under reduced pressure. The resulting residue was then extracted with dichloromethane, washed twice with aqueous 0.1 M NaOH, once with H_2O, and once with brine. The organic layer was dried over Na_2SO_4 and the solvent was evaporated in *vacuo*. The residue was dissolved in hot methanol and allowed to cool to afford crystalline compound $\mathbf{3_{GG}}$ (12.0 g, 86% yield). **Compound 3_{GG}** ^1H NMR ($CDCl_3$, 500 MH), δ_H: 3.87 (3H, s, B3-OMe), 3.94 (3H, s, A3-OMe), 5.23 (2H, s, $PhCH_2$), 5.27 (2H, s, β), 6.82-7.62 (12H, m, aromatic). ^{13}C NMR ($CDCl_3$, 125 MHz) δ_C: 56.1 (B3-OMe), 56.3 (A3-OMe), 71.0 ($PhCH_2$), 72.1 (β), 111.0, 112.3, 112.4, 114.9, 121.0, 122.5, 122.7, 127.4, 128.3 and 128.9 (aromatic, -CH), 128.2, 136.3, 147.8, 149.9, 149.9 and 153.1 (aromatic, quaternary C), 193.4 (α).

Synthesis of 3-methoxy-4-benzyloxy-α-(3-methoxyphenoxy)-β-hydroxypropiophenone (4_{GG}). To a magnetically stirred solution of tetrahydrofuran (THF) (100 ml) in a 200 ml of round bottom flask, compound $\mathbf{3_{GG}}$ (7.57 g, 20 mmol, 1 equiv), formaldehyde (6.01 g, 200 mmol, 10 equiv) and potassium carbonate (2.76 g, 20 mmol, 1 equiv) were added together and the reaction mixture was set to 40 °C. The progress of the reaction was monitored by TLC [hexane-EtOAc=1:1, R_f (s/m)=0.47, R_f (t/m)=0.14]. After 55 min, the starting material completely disappeared. The reaction was then stopped by added 1 M HCl to adjust the pH value of reaction mixture into 7. The reaction mixture were extracted by dichloromethane, washed twice with H_2O, and once with brine. The organic layer was dried over Na_2SO_4 and the solvent was evaporated in *vacuo*. The residue was then dissolved in hot methanol and allowed to cool, which afforded crystalline compound $\mathbf{4_{GG}}$ (7.2 g, 88% yield). **Compound 4_{GG}** ^1H NMR ($CDCl_3$+ D_2O (1 drop), 500 MH), δ_H: 3.84 (3H, s, B3-OMe), 3.91 (3H, s,

A3-OMe), 4.05 (2H, d, J = 5.2 Hz, γ), 5.22 (2H, s, $PhCH_2$), 5.40 (1H, t, J = 5.2 Hz, β), 6.79-7.68 (12H, m, aromatic). ^{13}C NMR ($CDCl_3$, 125 MHz) δ_C: 56.0 (B3-OMe), 56.2 (A3-OMe), 63.9 (γ), 71.0 ($PhCH_2$), 84.4 (β), 111.5, 112.3, 112.4, 118.0, 121.3, 123.5, 123.6, 127.4, 128.3 and 128.9 (aromatic, -CH), 136.2, 147.1, 149.8, 150.4 and 153.3 (aromatic, quaternary C), 195.1 (α).

Synthesis of 1-(4-benzyloxy-3-methoxyphenyl)-2-(3-methoxyphenoxy)-1, 3-propanediol ($\mathbf{5_{GG}}$). To a magnetically stirred solution mixture of THF/EtOH (100 ml : 100 ml) dissolving with $\mathbf{4_{GG}}$ (10.10 g, 25 mmol, 1 equiv), excess of $NaBH_4$ (1.87 g, 50 mmol, 2 equiv) was added slowly over 5 min. The reaction suspension was stirred at room temperature for 1 day and the completion of the reaction was checked by TLC [CH_2Cl_2-MeOH=100:4, R_f (s/m)=0.60, R_f (t/m)=0.45]. 1 M HCl was added dropwise to quench the remaining $NaBH_4$ under an ice-water bath. The reaction mixture was extracted with dichloromethane, washed twice with H_2O, and once with brine. The organic layer was dried over Na_2SO_4 and concentrated under vacuum, affording mixture of *erythro* isomer (**E**) and *threo* isomer (**T**) of compound $\mathbf{5_{GG}}$ as syrup (10 g, 99% yield). The configurations of each isomer (*erythro* or *threo*) in compound $\mathbf{5_{GG}}$ were determined based on ozonation result and isomers ratio of its debenzylated product, **GG**. **Compound $\mathbf{5_{GG}}$** (**E**/**T** = 1.61) ^1H NMR (acetone-d_6, 500 MHz), δ_H: **major isomer (*erythro*)**, 3.69 (1H, m, γ_1), 3.75 (1H, t, J = 5.2 Hz, γ-OH), 3.83 (1H, m, γ_2), 3.80 (6H, s, A3-OMe and B3-OMe), 4.29 (1H, m, β), 4.60 (1H, d, J = 4.6 Hz, α-OH), 4.91 (1H, t, J = 4.6 Hz, α), 5.08 (2H, s, $PhCH_2$), 6.78-7.48 (12H, m, aromatic). **minor isomer (*threo*)**, 3.50 (1H, m, γ_1), 3.61 (1H, t, J = 5.8 Hz, γ-OH), 3.83 (1H, m, γ_2), 3.85 (6H, s, A3-OMe and B3-OMe), 4.21 (1H, m, β), 4.47 (1H, d, J = 4.6 Hz, α-OH), 4.91 (1H, t, J = 4.6 Hz, α), 5.08 (2H, s, $PhCH_2$), 6.79-7.48 (12H, m, aromatic). ^{13}C NMR (acetone-d_6, 125 MHz) δ_C: **major isomer (*erythro*)**, 56.2 (A3-OMe), 56.4 (B3-OMe), 61.9 (γ), 71.6 ($PhCH_2$), 73.8 (α), 86.7 (β), 112.3, 113.6, 114.7, 119.7, 119.9, 120.1, 122.0, 123.4, 128.5 and 129.3 (aromatic, -CH), 136.3, 138.8, 148.7, 149.1, 150.7 and 152.1 (aromatic, quaternary C). **minor isomer (*threo*)**, 56.2 (A3-OMe), 56.4 (B3-OMe), 61.9 (γ), 71.6 ($PhCH_2$), 73.8 (α), 88.3 (β), 112.3, 113.5, 114.7, 119.7, 119.9, 120.1, 122.0, 123.5, 128.5 and 128.6 (aromatic, -CH), 135.9, 138.8, 148.8, 149.7, 150.7 and 152.1(aromatic, quaternary C).

Synthesis of 1-(3-methoxyphenyl)-2-(3-methoxyphenoxy)-1, 3-propanediol (GG). A mixture of compound $\mathbf{5_{GG}}$ (mixture of diastereomers, 7.00 g, 17 mmol, 1 equiv) and palladium on activated-

carbon (0.7 g) in THF (380 ml) was fitted with a hydrogen-gas-filled balloon. The reaction suspension was kept stirring overnight at room temperature. The completion of the reaction was monitored by TLC [CH_2Cl_2-MeOH=100:4, R_f (s/m)=0.45, R_f (t/m)=0.27]. After reaction, the catalyst was removed through a glass filter with the aid of Celite, and washed with acetone and the filtrate was concentrated under vacuum. The crude product was purified by flash silica gel chromatography using CH_2Cl_2-MeOH (100:10) at multiple times to afford the mixture of **E** and **T** isomers of **GG** as a pale yellow syrup (4 g, 73% yield). The resulting **E** and **T** isomers of **GG** model were separated from each other via anion exchange chromatography in an aqueous ethanol solution containing potassium borate. Each isomer was subjected to ozonation in order to determine the *erythro* or *threo* stereoconfiguration. Procedures for the separation, stereoconfiguration determination and NMR characterization of the diastereomers will be described in Section 2.2.3, 2.2.4 and 2.3.3, respectively.

Guaiacylglycerol-β-*p*-hydroxyphenyl ether (GH)

The synthetic route of β-O-4 model **GH** is shown in **Figure 2.1**.

Synthesis of 3-methoxy-4-benzyloxy-α-(phenoxy)-acetophenone (3_{GH}). Compound $\mathbf{3_{GH}}$ was synthesized in the same manner as the synthesis of compound $\mathbf{3_{GG}}$. A solution of anhydrous acetone (75 ml) dissolving compound $\mathbf{2_G}$ (16.76 g, 50 mmol, 1 equiv) was mixed with powdered potassium carbonate (13.83 g, 100 mmol, 2 equiv) in a 200 ml-round bottom flask. Then phenol (5.65 g, 60 mmol, 1.2 equiv) was added to reaction mixture with stirring at 50 °C. After12 hours, solvent was partially removed from the reaction mixture with the vacuum evaporator. The resulting residue was then extracted with dichloromethane. The organic layer was washed twice with 0.1 M NaOH, once with H_2O, once with brine, and dried over Na_2SO_4. After filtrating, the solvent in the filtrate was evaporated in *vacuo*. The residue was then dissolved in hot EtOH/EtOAc (50:1) solution mixture and allowed to cool, which gave crystals of compound $\mathbf{3_{GH}}$ (16.8 g, 97% yield). **Compound $\mathbf{3_{GH}}$** ^{1}H NMR ($CDCl_3$, 500 MH), δ_H: 3.94 (3H, s, A3-OMe), 5.21 (2H, s, $PhCH_2$), 5.24 (2H, s, β), 6.91-7.60 (13H, m, aromatic). ^{13}C NMR ($CDCl_3$, 125 MHz) δ_C: 56.3 (A3-OMe), 70.9 (β), 71.0 ($PhCH_2$), 111.0, 112.4, 115.0, 121.7, 122.8, 127.4, 128.4, 129.0 and 129.7 (aromatic, -CH), 128.2, 136.3, 150.0, 153.2 and 158.3 (aromatic, quaternary C), 193.3 (α).

Synthesis of 3-methoxy-4-benzyloxy-α-(phenoxy)-β-hydroxypropiophenone (4_{GH}). Compound $\mathbf{4_{GH}}$ was synthesized by the same procedures as compound $\mathbf{4_{GG}}$. Compound $\mathbf{4_{GH}}$ was synthesized from compound $\mathbf{3_{GH}}$ (15.68 g, 45 mmol, 1 equiv), which was reacted with formaldehyde (13.51 g, 450 mmol, 10 equiv) and potassium carbonate (6.22 g, 45 mmol, 1 equiv) in THF (250 ml) at 55 °C. The progress of the reaction was monitored by TLC [hexane-EtOAc=2:1, R_f (s/m)=0.38, R_f (t/m)=0.12]. The crude products were purified by crystallization from methanol to affording crystalline compound $\mathbf{4_{GH}}$ (13.4 g, 79% yield). **Compound 4_{GH}** ^{1}H NMR ($CDCl_3$+ D_2O (1 drop), 500 MH), δ_H: 3.89 (3H, s, A3-OMe), 4.08 (1H, broad-dd, J = 12, 6 Hz, γ_1), 4.12 (1H, br-dd, J = 12, 4 Hz, γ_2), 5.23 (2H, s, $PhCH_2$), 5.51 (1H, br-dd, J = 6, 4 Hz, β), 6.88-7.69 (13H, m, aromatic). ^{13}C NMR ($CDCl_3$, 125 MHz) δ_C: 56.2 (A3-OMe), 63.7 (γ), 71.0 ($PhCH_2$), 81.0 (β), 111.4, 112.3, 115.4, 122.1, 123.4, 127.4, 128.4, 128.9, 129.9 and 136.2 (aromatic, -CH), 128.1, 136.2, 149.9, 153.5 and 157.5 (aromatic, quaternary C), 195.07 (α).

Synthesis of 1-(4-benzyloxy-3-methoxyphenyl)-2-(phenoxy)-1, 3-propanediol (5_{GH}). Compound $\mathbf{5_{GH}}$ was synthesized in the same manner as compound $\mathbf{5_{GG}}$. To a magnetically stirred solution of THF/EtOH (143 ml:143 ml) dissolving compound $\mathbf{4_{GH}}$ (13.48 g, 36 mmol, 1 equiv), excess of $NaBH_4$ (2.70 g, 71 mmol, 2 equiv) was added slowly over 5 min. The reaction suspension was stirred at room temperature for 1 day and the completion of the reaction was monitored by TLC [CH_2Cl_2-MeOH=100:4, R_f (s/m)=0.63, R_f (t/m)=0.41]. With the same work-up of the synthesis of compound $\mathbf{5_{GG}}$, the mixture of **E** and **T** isomers of compound $\mathbf{5_{GH}}$ were finally obtained as syrup (13g, 96% yield). The configurations of each isomer (*erythro* or *threo*) in compound $\mathbf{5_{GH}}$ were determined based on ozonation result and isomers ratio of its debenzylated product, **GH**. **Compound 5_{GH}** (**E**/**T** = 0.40) ^{1}H NMR (acetone-d_6, 500 MHz), δ_H: **major isomer (*threo*)**, 3.55 (1H, m, γ_1), 3.79 (3H, s, B3-OMe), 3.83 (1H, m, γ_2), 3.86 (1H, m, γ-OH), 4.46 (1H, broad-d, J = 5 Hz, α-OH), 4.48 (1H, m, β), 4.98 (1H, br-t, J = 5 Hz, α), 5.07 (2H, s, $PhCH_2$), 6.86-7.48 (13H, m, aromatic). **minor isomer (*erythro*)**, 3.78 (3H, s, B3-OMe), 3.80-3.88 (2H, m, γ), 4.47 (1H, m, β), 4.64 (1H, br-d, J = 5 Hz, α-OH), 4.93 (1H, br-t, J = 5 Hz, α), 5.06 (2H, s, $PhCH_2$), 6.86-7.48 (13H, m, aromatic). **^{13}C NMR** (acetone-d_6, 125 MHz) δ_C: **major isomer (*threo*)**, 56.2 (B3-OMe), 61.8 (γ), 71.6 ($PhCH_2$), 73.3 (α), 84.0 (β), 112.2, 114.7, 117.1, 117.2, 120.0, 121.6, 128.5, 129.3 and 130.2 (aromatic, -CH), 138.9, 148.6,

150.6 and 160.1 (aromatic, quaternary C).

Synthesis of 1-(3-methoxyphenyl)-2-(phenoxy)-1, 3-propanediol (GH). Compound **GH** was synthesized in the same manner as the synthesis of compound **GG**. A mixture of compound $\mathbf{5_{GH}}$ (mixture of diastereomers, 6.00 g, 16 mmol, 1 equiv) and 10 % palladium-activated carbon (0.6 g) in THF (320 ml) was fitted with a hydrogen-gas-filled balloon. The reaction suspension was kept stirring overnight at room temperature. The completion of the reaction was monitored by TLC [CH_2Cl_2-MeOH=100:4, R_f (s/m)=0.37, R_f (t/m)=0.20]. After the same work-up as compound **GG**, the crude product was purified by flash chromatography using CH_2Cl_2-EtOAc (1:1) to afford the mixture of **E** and **T** isomers of compound **GH** as a pale yellow syrup (4 g, 87% yield). Procedures for the separation, stereoconfiguration determination and NMR characters of these diastereomers will be described in Section 2.2.3, 2.2.4 and 2.3.3, respectively.

Guaiacylglycerol-β-syringyl ether (GS)

The synthetic route of β-O-4 model **GS** is shown in **Figure 2.1**.

Synthesis of 3-methoxy-4-benzyloxy-α-(3, 5-dimethoxyphenoxy)-acetophenone ($\mathbf{3_{GS}}$). To a stirred anhydrous acetone (15 ml) in a 30 ml of round bottom flask, compound $\mathbf{2_G}$ (3.35 g, 10 mmol, 1 equiv), syringol (1.85 g, 12 mmol, 1.2 equiv) contained, and powdered potassium carbonate (2.76 g, 20 mmol, 2 equiv) were added. The reaction mixture was kept at 50 °C for 2 hours. The progress of the reaction was monitored by TLC [hexane-EtOAc=2:1, R_f (s/m)=0.47, R_f (t/m)=0.20]. The work-up was same as the synthesis of compound $\mathbf{3_{GG}}$. The crude products were dissolved in hot EtOAc/hexane (5:8) solution mixture and allowed to cool, which gave crystals of compound $\mathbf{3_{GS}}$ (3.3 g, 81% yield). **Compound $\mathbf{3_{GS}}$** ^{1}H NMR (acetone-d_6, 500 MHz), δ_H: 3.78 (6H, s, B3-OMe and B5-OMe), 3.89 (3H, s, A3-OMe), 5.03 (2H, s, $PhCH_2$), 5.22 (2H, s, β), 6.66 (2H, broad-d, J = 8 Hz, B2 and B6), 7.00 (1H, br-t, J = 8 Hz, B1), 7.14 (1H, d, J = 8.6 Hz, A5), 7.33 (1H, br-t, J = 7 Hz, C4), 7.39 (2H, br-t, J = 7 Hz, C3 and C5), 7.50 (2H, br-d, J = 7 Hz, C2 and C6), 7.68 (1H, d, J = 1.8 Hz, A2), 7.80 (1H, dd, J = 1.8, 8.6 Hz, A6). ^{13}C NMR (acetone-d_6, 125 MHz) δ_C: 56.3 (A3-OMe), 56.5 (B3-OMe and B5-OMe), 71.3 (β), 76.0 ($PhCH_2$), 106.6, 112.4, 113.4, 124.1, 125.0, 128.6, 128.9 and 129.4 (aromatic, -CH), 129.7, 137.7, 138.0, 150.5, 153.8 and 154.5 (aromatic, quaternary C), 194.1 (α).

Synthesis of 3-methoxy-4-benzyloxy-α-(3, 5-dimethoxyphenoxy)-β-hydroxypropiophenone

(4_{GS}). A mixture of compound $\mathbf{3_{GS}}$ (3.27 g, 8 mmol, 1 equiv), formaldehyde (0.24 g, 80 mmol, 10 equiv) and potassium carbonate (1.11 g, 8 mmol, 1 equiv) were added in a 100 ml of round bottom flask containing THF (50 ml) and the reaction mixture was set to 55 °C. The progress of the reaction was monitored by TLC [hexane-EtOAc=1:1, R_f (s/m)=0.78, R_f (t/m)=0.42]. After 8 hours, the reaction was stopped by added 1 M HCl aqueous to the neutral condition. Following the same work-up with the compound $\mathbf{4_{GG}}$, the resulting products were purified with flash chromatography (hexane-EtOAc=1:1) to give pale yellow crystalline $\mathbf{4_{GS}}$ (2.8 g, 80% yield). **Compound 4_{GS}** ^{1}H NMR (acetone-d_6, 500 MHz), δ_H: 3.71 (6H, s, B3-OMe and B5-OMe), 3.82-3.89 (2H, m, γ), 3.87 (3H, s, A3-OMe), 5.14 (1H, m, β), 5.22 (2H, s, $PhCH_2$), 6.67 (2H, broad-d, *J* = 8 Hz, B2 and B6), 7.01 (1H, br-t, *J* = 8 Hz, B1), 7.12 (1H, d, *J* = 8.6 Hz, A5), 7.33 (1H, m, C4), 7.39 (2H, m, C3 and C5), 7.50 (2H, m, C2 and C6), 7.68 (1H, d, *J* = 2.0 Hz, A2), 7.77 (1H, dd, *J* = 8.6, 2.0 Hz, A6). ^{13}C NMR (acetone-d_6, 125 MHz) δ_C: 56.2 (A3-OMe), 56.3 (B3-OMe and B5-OMe), 63.7 (γ), 71.1 ($PhCH_2$), 86.9 (β), 106.3, 112.5, 113.1, 124.1, 124.8, 128.5, 128.8 and 129.3 (aromatic, -CH), 130.3, 137.4, 137.8, 150.3, 153.5 and 153.8 (aromatic, quaternary C), 195.5 (α).

Synthesis of 1-(4-benzyloxy-3-methoxyphenyl)-2-(3, 5-dimethoxyphenoxy)-1, 3-propanediol (5_{GS}). Excess of $NaBH_4$ (0.39 g, 10 mmol, 2 equiv) was added slowly to the compound $\mathbf{4_{GS}}$ (2.28 g, 5 mmol, 1 equiv) dissolved in THF/EtOH (21 ml : 21 ml). The reaction was monitored by TLC [hexane-EtOAc=1:3, R_f (s/m)=0.43, R_f (t/m)=0.36]. The work-up almost same as the compound $\mathbf{5_{GG}}$, was used to afford the mixture of **E** and **T** isomers of compound $\mathbf{5_{GS}}$ as syrup (around 2.2 g, 96 % yield). The configurations of each isomer (*erythro* or *threo*) in compound $\mathbf{5_{GS}}$ were determined based on ozonation result and isomers ratio of its debenzylated product, **GS**. Compound $\mathbf{5_{GS}}$ (**E**/**T** = 0.41) ^{1}H NMR (acetone-d_6, 500 MHz), δ_H: **major isomer (*threo*)**, 3.33 (1H, m, γ_1), 3.57 (1H, m, γ_2), 3.89 (9H, s, OMe×3), 4.13 (1H, m, β), 4.35 (1H, s, α-OH), 5.04 (1H, d, *J* = 8.9 Hz, α), 5.14 (2H, s, $PhCH_2$), 6.62-7.43 (11H, m, aromatic); **minor isomer (*erythro*)**, 3.15 (1H, m, γ_1), 3.49 (1H, m, γ_2), 3.87 (9H, s, OMe×3), 5.13 (2H, s, $PhCH_2$), 6.62-7.43 (11H, m, aromatic). ^{13}C NMR (acetone-d_6, 125 MHz) δ_C: **major isomer (*threo*)**, 56.1 (OMe×3), 60.4 (γ), 71.0 ($PhCH_2$), 74.0 (α), 88.9 (β), 105.2, 110.8, 113.9, 119.7, 124.4, 127.2, 127.7 and 128.4 (aromatic, -CH), 133.2, 135.2, 137.1, 147.8, 149.6 and 153.2 (aromatic, quaternary C); **minor isomer (*erythro*)**, 56.0 (OMe×3), 60.5 (γ), 71.0 ($PhCH_2$), 72.4 (α),

86.9 (β), 105.2, 109.5, 114.0, 118.0, 124.4, 127.2, 127.7 and 128.4 (aromatic, -CH), 132.6, 135.2, 137.1, 147.2, 149.7 and 153.5 (aromatic, quaternary C).

Synthesis of 1-(3-methoxyphenyl)-2-(3, 5-dimethoxyphenoxy)-1, 3-propanediol (GS). The compound was prepared in the same manner as the compound **GG**. A mixture of compound $\mathbf{5_{GS}}$ (mixture of diastereomers, 2.80 g, 6.36 mmol, 1 equiv) and 10% palladium-activated carbon (0.28 g) in THF (127 ml) was fitted with a hydrogen gas-filled balloon. The reaction suspension was kept stirring overnight at room temperature. The completion of the reaction was monitored by TLC [Hexane-EtOAc=1:1, R_f (s/m)=0.18, R_f (t/m)=0.11]. After reaction, the catalyst was removed through a glass filter with an aid of Celite, and washed with acetone and the filtrate was concentrated under vacuum pressure. The crude product was purified by flash chromatography using CH_2Cl_2-MeOH (100:10) to afford the mixture of **E** and **T** isomers of lignin model **GS** as a pale yellow syrup (1.9 g, 85% yield). Procedures for the separation, stereoconfiguration determination and NMR characters of these diastereomers will be described in Section 2.2.3, 2.2.4 and 2.3.3, respectively.

p-Hydroxyphenylglycerol-β-guaiacyl ether (HG)

The synthetic route of β-O-4 model **HG** is shown in **Figure 2.2**.

Synthesis of 4-benzyloxyacetophenone ($\mathbf{1_H}$). A solution of anhydrous DMF (200 ml), compound *p*-hydroxyacetophenone (27.23 g, 200 mmol, 1 equiv), potassium iodide (2.32 g, 14 mmol, 0.07 equiv) and powdered potassium carbonate (38.70 g, 280 mmol, 1.4 equiv) were mixed in a 500 ml round bottom flask, then refluxed at 90 °C in an oil bath with magnetically stirring. Benzyl chloride (35.44 g, 280 mmol, 1.4 equiv) was added drop-wise into the suspension. The progress of the reaction was monitored by TLC [hexane-EtOAc=2:1, R_f (s/m)=0.17, R_f (t/m)=0.37]. After 1.5 hours, the reaction mixture was cooled down to room temperature and poured into approx. 150 g of ice with stirring. When all of the ice melted, the appeared white solids were isolated by suction filtration and washed three times with water and once with hexane. The resulting residue was then dissolved in hot ethanol and allowed to cool, affording crystalline compound $\mathbf{1_H}$ (40.6 g, 91% yield). **Compound $\mathbf{1_H}$**, ^{1}H NMR (acetone-d_6, 500 MHz), δ_H: 2.50 (3H, s, β), 5.21 (2H, s, $PhCH_2$), 7.09-7.96 (9H, m, aromatic). ^{13}C NMR (acetone-d_6, 125 MHz) δ_C: 26.5 (β), 70.7 ($PhCH_2$), 115.5, 128.6, 128.9, 129.4 and 131.3, (aromatic, -CH), 131.6, 137.8 and 163.6, (aromatic, quaternary C), 196.4 (α).

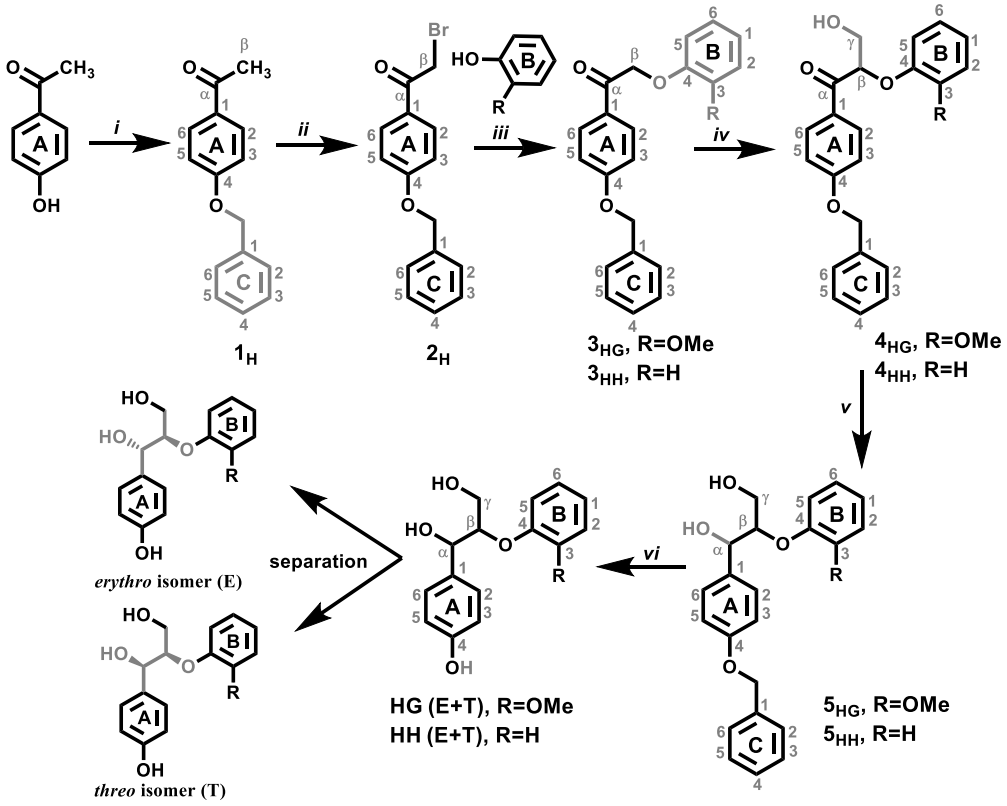

Figure 2.2 Synthetic route of β-O-4 model **HG**. Reagents and conditions were as follows: (*i*) BnCl, KI, K_2CO_3, anhydrous DMF, 90 °C, (*ii*) Br_2, EtOH, rt, (*iii*) K_2CO_3, acetone, 40 °C, (*iv*) HCHO, THF, K_2CO_3, 40 °C, (*v*) $NaBH_4$, THF-EtOH (v/v, 1:2), rt (mixture of *erythro* and *threo* isomers), (*vi*) 10% Pd/C, H_2, THF, rt (mixture of *erythro* and *threo* isomers).

Synthesis of 4-benzyloxy-α-bromoacetophenone (2_H). Compound $\mathbf{1_H}$ (12.32 g, 55 mmol, 1 equiv) was dissolved in 385 ml of ethanol at 60 °C, and nitrogen gas was slowly bubbled through the solution. After the solution was cooled down to room temperature, bromine (10.55 g, 66 mmol, 1.2 equiv) was quickly added with stirring at room temperature. The progress of the reaction was monitored by TLC [hexane-EtOAc=2:1, R_f (s/m)=0.44, R_f (t/m)=0.52]. In approximately 25 minutes the solution faded from dark red-orange to a clear pale yellow. At this point, the starting material $\mathbf{1_H}$ completely disappeared, and the reaction mixture was poured into approx. 200 g of ice. White precipitate began to form with continuously stirring. After all of the ice melted, these white precipitates were isolated by suction filtration and washed three times with water and once with hexane. The resulting residue was crystallized from EtOH to afford compound $\mathbf{2_H}$ (16.5 g, 98% yield). **Compound $\mathbf{2_H}$** ^{1}H NMR (acetone-d_6, 500 MHz), δ_H: 3.88 (2H, s, β), 4.46 (2H, s, $PhCH_2$), 6.36-7.25 (9H, m, aromatic). ^{13}C NMR (acetone-d_6, 125 MHz) δ_C: 32.7 (β), 70.9 ($PhCH_2$), 115.8, 128.66, 129.0, 129.5

and 132.1 (aromatic, -CH), 12.2, 137.7 and 164.3, (aromatic, quaternary C), 196.4 (α).

Synthesis of 4-benzyloxy-α-(3-methoxyphenoxy)-acetophenone (3_{HG}). The compound 2_H (10.60 g, 35 mmol, 1 equiv), powdered potassium carbonate (9.67 g, 70 mmol, 2 equiv) and guaiacol (5.21 g, 42 mmol, 1.2 equiv) were added to a stirred anhydrous acetone (210 ml). The reaction mixture was kept at 40 °C for 7 hours. The progress of the reaction was monitored by TLC [hexane-EtOAc=2:1, R_f (s/m)=0.50, R_f (t/m)=0.33]. The work-up was same as the compound 3_{GG}, affording crystalline compound 3_{HG} (11.2 g, 92% yield). **Compound 3_{HG}** ^{1}H NMR ($CDCl_3$, 500 MH), δ_H: 3.88 (3H, s, -OMe), 5.14 (2H, s, $PhCH_2$), 5.28 (2H, s, β), 6.83-8.03 (13H, m, aromatic). ^{13}C NMR ($CDCl_3$, 125 MHz) δ_C: 56.1 (-OMe), 70.3 ($PhCH_2$), 72.1 (β), 112.3, 114.9, 115.0, 121.0, 122.5, 127.6, 128.5, 128.9 and 130.7, (aromatic, -CH), 128.1, 136.2, 147.8, 149.9 and 163.3 (aromatic, quaternary C), 193.3 (α).

Synthesis of 4-benzyloxy-α-(3-methoxyphenoxy)-β-hydroxypropiophenone (4_{HG}). To a THF solution (138 ml) of compound 3_{HG} **(**10.65 g, 31 mmol, 1 equiv**),** formaldehyde (9.30 g, 310 mmol, 10 equiv) and K_2CO_3 (4.28 g, 31 mmol, 1 equiv) were added. The reaction mixture was set to 45 °C. The progress of the reaction was monitored by TLC [hexane-EtOAc=2:1, R_f (s/m)=0.36, R_f (t/m)=0.10]. After 30 min, the reaction was then stopped by adding 1 M HCl aqueous to adjust the pH value of reaction mixture into 7. The products were extracted by dichloromethane and then evaporated in *vacuo*. The pure compound 4_{HG} (9.5 g, 81% yield) was obtained by crystallization from ethanol. **Compound 4_{HG}** ^{1}H NMR ($CDCl_3$+ D_2O (1 drop), 500 MH), δ_H: 3.85 (3H, s, -OMe), 4.05 (2H, d, J = 5.2 Hz, γ), 5.13 (2H, s, $PhCH_2$), 5.39 (1H, t, J = 5.2 Hz, β), 6.79-8.08 (13H, m, aromatic). ^{13}C NMR ($CDCl_3$, 125 MHz) δ_C: 56.0 (-OMe), 63.8 (γ), 70.4 ($PhCH_2$), 84.9 (β), 112.5, 115.0, 118.8, 121.3, 123.8, 127.7, 128.5, 128.9 and 131.5 (aromatic, -CH), 128.3, 136.2, 147.1, 150.7 and 163.4 (aromatic, quaternary C), 195.2 (α).

Synthesis of 1-(4-benzyloxyphenyl)-2-(3-methoxyphenoxy)-1, 3-propanediol (5_{HG}). The excess of $NaBH_4$ (1.13 g, 30 mmol, 2 equiv) was added slowly to a magnetically stirred solution of compound 4_{HG} (5.82 g, 15 mmol, 1 equiv) dissolved in THF/EtOH (63 ml : 63 ml). The reaction suspension was stirred at room temperature for 1 day and the completion of the reaction was monitored by TLC [CH_2Cl_2-MeOH=100:4, R_f (s/m)=0.48, R_f (t/m)=0.38]. Finally, with the similar work-up as the compound 5_{GG}, mixture of **E** and **T** isomers of compound 5_{HG} (5.8 g) were obtained as syrup. The

configurations of each isomer (*erythro* or *threo*) in compound **5_{HG}** were determined based on ozonation result and isomers ratio of its debenzylated product, **HG**. **compound 5_{HG}** (**E**/**T** = 1.86) ^{1}H NMR (acetone-d_6+D_2O (1 drop), 500 MHz), δ_H: **major isomer (*erythro*)**, 3.68 (1H, broad-dd, *J* = 12, 4 Hz, γ_1), 3.76 (3H, s, -OMe), 3.82 (1H, br-dd, *J* = 12, 4 Hz, γ_2), 4.27 (1H, m, β), 4.91 (1H, d, *J* = 5.4 Hz, α), 5.06 (2H, s, $PhCH_2$), 6.77-7.44 (13H, m, aromatic); **minor isomer (*threo*)**, 3.45 (1H, br-dd, *J* = 12, 4 Hz, γ_1), 3.71 (1H, br-dd, *J* = 12, 4 Hz, γ_2), 3.81 (3H, s, -OMe), 4.27 (1H, m, β), 4.94 (1H, d, *J* = 5.7 Hz, α), 5.06 (2H, s, $PhCH_2$), 6.77-7.44 (13H, m, aromatic). ^{13}C NMR (acetone-d_6, 125 MHz) δ_C: **major isomer (*erythro*)**, 56.4 (-OMe), 61.8 (γ), 70.4 ($PhCH_2$), 73.6 (α), 87.1 (β), 113.7, 115.1, 120.2, 122.0, 123.6, 128.5, 128.6, 129.0 and 129.3 (aromatic, -CH), 135.4, 138.6, 149.1, 152.2 and 159.1 (aromatic, quaternary C); **minor isomer (*threo*)**, 56.4 (-OMe), 61.9 (γ), 70.5 ($PhCH_2$), 73.7 (α), 88.8 (β), 113.5, 115.2, 120.5, 122.1, 123.7, 128.5, 128.7, 129.0 and 129.2 (aromatic, -CH), 134.9, 138.6, 149.8, 152.0 and 159.3 (aromatic, quaternary C).

Synthesis of 2-(3-methoxyphenoxy)-1-phenyl-1, 3-propanediol (HG). The procedures were same as those for the synthesis of model **GG**. A mixture of compound **5_{HG}** (mixture of diastereomers, 6.64 g, 17 mmol, 1 equiv) was debenzylated by hydrogen in the THF (350 ml) with palladium on charcoal (0.66 g) for overnight at room temperature. The completion of the reaction was monitored by TLC [CH_2Cl_2-EtOAc=1:1, R_f (s/m)=0.51, R_f (t/m)=0.28]. The crude product was purified by flash chromatography using CH_2Cl_2-MeOH (100:10) at multiple times to afford the mixture of **E** and **T** isomers of lignin model **HG** as a pale yellow syrup (3.9 g, 80% yield). Procedures for the separation, stereoconfiguration determination and NMR characters of these diastereomers will be described in Section 2.2.3, 2.2.4 and 2.3.3, respectively.

p-Hydroxyphenylglycerol-β-*p*-hydroxyphenyl ether (HH)

The synthetic route of β-O-4 model **HH** is shown in **Figure 2.2**.

Synthesis of 4-benzyloxy-α-(phenoxy)-acetophenone (3$_{HH}$). The compound **2_H** (10.60 g, 35 mmol, 1 equiv), powdered potassium carbonate (9.67 g, 70 mmol, 2 equiv) and phenol (3.95 g, 42 mmol, 1.2 equiv) were mixed together in anhydrous acetone (210 ml) at 40 °C and stirred for 12 hours. The progress of the reaction was monitored by TLC [hexane-EtOAc=2:1, R_f (s/m)=0.51, R_f (t/m)=0.49]. The same work-up described in the compound **3_{GG}** was used. Crude product was

crystallized from EtOH to afford compound **3_{HH}** (8.2 g, 74% yield). **Compound 3_{HH}** ^{1}H NMR ($CDCl_3$, 500 MH), δ_H: 5.15 (2H, s, $PhCH_2$), 5.21 (2H, s, β), 6.94-8.02 (14H, m, aromatic). ^{13}C NMR ($CDCl_3$, 125 MHz) δ_C: 70.4 ($PhCH_2$), 70.9 (β), 114.9, 115.0, 121.7, 127.7, 128.5, 128.9, 129.7 and 130.7, (aromatic, -CH), 128.0, 136.2, 158.3 and 163.3 (aromatic, quaternary C), 193.2 (α).

Synthesis of 4-benzyloxy-α-(phenoxy)-β-hydroxypropiophenone (4_{HH}). The procedures were same as those described for the synthesis of compound **4_{GG}.** The compound **3_{HH}** (7.63 g, 24 mmol, 1 equiv), THF (106 ml), formaldehyde (7.20 g, 240 mmol, 10 equiv) and potassium carbonate (3.31 g, 24 mmol, 1 equiv) were added to a 200 ml of round bottom flask. The reaction suspension was stirred at 40 °C for 5 hours. The progress of the reaction was monitored by TLC [hexane-EtOAc=2:1, R_f (s/m)=0.55, R_f (t/m)=0.30]. The reaction products were then extracted with dichloromethane. After evaporation in vacuum, the residue was then dissolved in hot ethanol and allowed to cool to afford crystalline compound **4_{HH}** (6.8 g, 81% yield). **Compound 4_{HH}** ^{1}H NMR (acetone-d_6, 500 MHz), δ_H: 4.03-4.11 (2H, m, γ), 4.34 (1H, t, J = 6.3 Hz, γ-OH), 5.22 (2H, s, $PhCH_2$), 5.62 (1H, m, β), 6.87-8.14 (14H, m, aromatic). ^{13}C NMR (acetone-d_6, 125 MHz) δ_C: 64.1 (γ), 70.9 ($PhCH_2$), 82.6 (β), 115.7, 116.1, 122.0, 128.7, 129.0, 129.5, 130.4 and 132.0 (aromatic, -CH), 137.7, 159.0, 163.9 and 195.8 (aromatic, quaternary C), 195.8 (α).

Synthesis of 1-(4-benzyloxyphenyl)-2-(phenoxy)-1, 3-propanediol (5_{HH}). The procedures were same as those described for the synthesis of compound **5_{GG}.** To a magnetically stirred solution of **4_{HH}** (6.8 g, 20 mmol, 1 equiv) dissolved in THF/EtOH (75 ml : 75 ml), excess of $NaBH_4$ (1.48 g, 39 mmol, 2 equiv) was added slowly over 5 min. The reaction suspension was stirred at room temperature for 1 day and the completion of the reaction was monitored by TLC [CH_2Cl_2-MeOH=100:4, R_f (s/m)=0.57, R_f (t/m)=0.40]. With the same work-up of the synthesis of compound **5_{GG}**, the mixture of **E** and **T** isomers of compound **5_{HH}** were obtained as syrup (6.5 g, 95% yield). The configurations of each isomer (*erythro* or *threo*) in compound **5_{HH}** were determined based on ozonation result and isomers ratio of its debenzylated product, **HH**. **Compound 5_{HH} (E/T** = 0.67) ^{1}H NMR (acetone-d_6 + D_2O (1 drop), 500 MHz), δ_H: **major isomer (*threo*)**, 3.49 (1H, broad-dd, J = 12, 5 Hz, γ_1), 3.79 (1H, m, γ_2), 4.45 (1H, m, β), 4.98 (1H, d, J = 4.9 Hz, α), 5.07 (2H, s, $PhCH_2$), 6.83-7.45 (14H, m, aromatic); **minor isomer (*erythro*)**, 3.79 (1H, m, γ_1), 3.85 (1H, br-dd, J = 12, 5 Hz, γ_2), 4.42 (1H,

m, β), 4.92 (1H, d, *J* = 5.8 Hz, α), 5.06 (2H, s, $PhCH_2$), 6.83-7.45 (14H, m, aromatic). ^{13}C NMR (acetone-d_6, 125 MHz) δ_C: **major isomer (*threo*)**, 68.1 (γ), 70.5 ($PhCH_2$), 73.2 (α), 84.2 (β), 115.2, 117.2, 121.7, 128.5, 128.7, 129.0, 129.3 and 130.2 (aromatic, -CH), 135.3, 138.6, 159.2 and 160.2 (aromatic, quaternary C); **minor isomer (*erythro*)**, 68.1 (γ), 70.5 ($PhCH_2$), 73.7 (α), 83.9 (β),, 115.2, 117.4, 121.7, 128.5, 128.7, 129.1, 129.3 and 130.2 (aromatic, -CH), 135.6, 138.6, 159.1 and 159.9 (aromatic, quaternary C).

Synthesis of *p*-hydroxyphenylglycerol-β-*p*-hydroxyphenyl ether (HH). The procedures used were same as those for the debenzylation of model $\mathbf{5_{GG}}$, the debenzylation of compound $\mathbf{5_{HH}}$ (mixture of diastereomers, 6.0 g, 17 mmol, 1 equiv) was performed by the treatment with hydrogen and palladium on charcoal (0.6 g) in THF (350 ml) overnight at room temperature. The completion of the reaction was monitored by TLC [CH_2Cl_2-EtOAc = 1:1, R_f (s/m) = 0.53, R_f (t/m)=0.34]. The crude product was purified by flash chromatography using CH_2Cl_2-EtOAc (3:1) to afford the mixture of **E** and **T** isomers of lignin model **HH** as a pale yellow syrup (4.3 g, 98% yield). Procedures for the separation, stereoconfiguration determination and NMR characters of these diastereomers will be described in Section 2.2.3, 2.2.4 and 2.3.3, respectively.

p-Hydroxyphenylglycerol-β-biphenyl ether ($\mathbf{H\text{-}HH_{biphenyl}}$)

The synthetic route of β-O-4 model $\mathbf{H\text{-}HH_{biphenyl}}$ is shown in **Figure 2.3**.

Synthesis of 2-methoxy-2′-hydroxybiphenyl (biphenol-OMe). 2, 2′-biphenol (12 g, 64 mmol, 1 equiv) was dissolved in anhydrous acetone (200 ml), potassium carbonate (10.67 g, 77 mmol, 1.2 equiv) and methyl iodide (10.98 g, 77 mmol, 1.2 equiv) were added to the solution and stirred under room temperature for 20 hours. The progress of the reaction being followed by TLC [hexane-EtOAc = 2:1, R_f (s/m) = 0.34, R_f (t/m) = 0.38]. The reaction mixture was concentrated with the vacuum evaporator to partially remove acetone. The resulting residue was then extracted with dichloromethane, washed once with H_2O, and once with brine. The organic layer was dried over Na_2SO_4 and the solvent was evaporated in *vacuo*. The residue was purified with flash chromatography (elute hexane-EtOAc=2:1) to give compound **biphenol-OMe** as syrup (11.3 g, 88% yield). **Compound biphenol-OMe** ^1H NMR ($CDCl_3$, 500 MHz), δ_H: 3.91 (3H, s, C4-OMe), 6.24 (0.9H, s, B4-OH), 7.04 (1H, broad-td, *J* = 7, 1 Hz, B1), 7.06 (1H, br-dd, *J* = 7, 1 Hz, B3), 7.07 (1H, br-dd, *J* = 7, 1 Hz, C3), 7.14 (1H, br-

td, *J* = 7, 1 Hz, C1), 7.28 (1H, br-dd, *J* = 7, 2 Hz, B6), 7.32 (1H, br-td, *J* = 7, 2 Hz, B2), 7.36 (1H, br-dd, *J* = 7, 2 Hz, C6), 7.41 (1H, br-td, *J* = 7, 2 Hz, C2). **^{13}C NMR** ($CDCl_3$, 125 MHz) δ_C: 56.2 (C4-OMe), 111.6 (C3), 117.4 (B3), 120.9 (B1), 122.2 (C1), 126.2 (B5), 127.1 (C5), 129.2 (B2), 129.3 (C2), 131.3 (B6), 132.5 (C6), 153.7 (B4), 155.5 (C4).

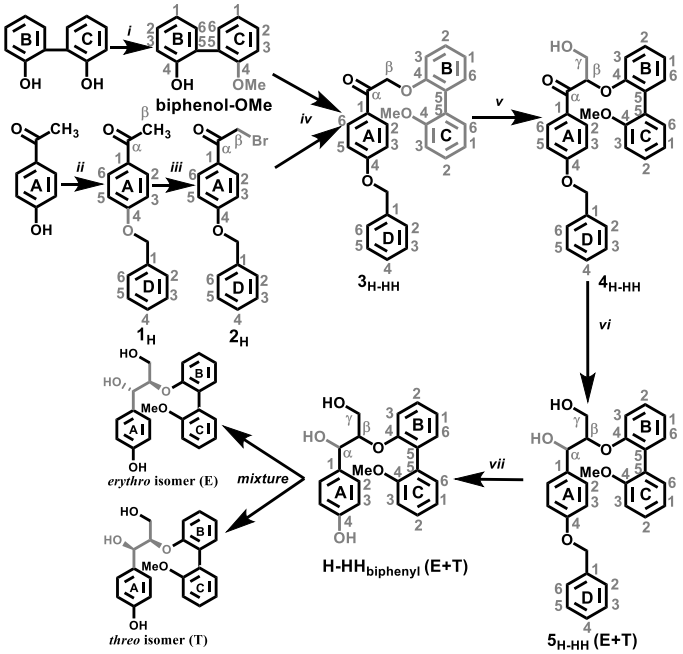

Figure 2.3 Synthetic route of **H-HH$_{biphenyl}$** trimer. Reagents and conditions were as follows: (i) CH_3I, K_2CO_3, acetone, rt , (ii) BnCl, KI, K_2CO_3, anhydrous DMF, 90 °C, (iii) Br_2, EtOH, rt, (iv) K_2CO_3, acetone, 40 °C, (v) HCHO, THF, K_2CO_3, 40 °C, (vi) $NaBH_4$, THF-EtOH (v/v, 1:2), rt (mixture of *erythro* (**E**) and *threo* (**T**) isomers), (vii) 10% Pd/C, H_2, THF, rt (mixture of *erythro* and *threo* isomers).

Synthesis of 1-(4-benzyloxyphenyl)-2-(2-methoxy-1, 1′-biphenyl-2′-yloxy)ethanone ($3_{H\text{-}HH}$). To a 500 ml of round bottom flask charged with solution of anhydrous acetone (182 ml), compound **2_H** (11.02 g, 36 mmol, 1 equiv), compound **biphenol-OMe** (8.20 g, 41 mmol, 1.2 equiv), and powdered potassium carbonate (6.03 g, 44 mmol, 1.1 equiv) were added. The reaction mixture was stirred at 50 °C for 15 hours. The progress of the reaction was monitored by TLC [hexane-EtOAc = 2:1, R_f (s/m) = 0.48, R_f (t/m) = 0.44]. The acetone was evaporated in *vacuo*, then the resulting residue was extracted with dichloromethane, washed twice with aqueous 0.1 M NaOH, once with H_2O, and once with brine. The organic layer was dried over Na_2SO_4 and the solvent was evaporated in *vacuo*. At last, the residue was dissolved in hot EtOH and allowed to cool to afford crystalline compound **$3_{H\text{-}HH}$** (14.2 g, 93% yield). **Compound $3_{H\text{-}HH}$** ^{1}H NMR ($CDCl_3$, 500 MHz), δ_H: 3.71 (3H, s, C4-OMe),

5.08 (2H, s, β), 5.13 (2H, s, $PhCH_2$), 6.93 (2H, d, *J* = 8.9 Hz, A3 and A5), 6.93 (2H, broad-d, *J* = 7 Hz, C3 and B3), 6.99 (1H, br-td, *J* = 7, 1 Hz, C1), 7.05 (1H, br-td, *J* = 7, 1 Hz, B1), 7.27 (1H, br-dd, *J* = 7, 2 Hz, B6), 7.28 (1H, br-td, *J* = 7, 2 Hz, B2), 7.29 (1H, br-dd, *J* = 7, 2 Hz, C6), 7.32 (1H, br-td, *J* = 7, 2 Hz, C2), 7.36 (1H, m, D4), 7.42 (2H, m, D3 and D5), 7.42 (2H, d, *J* = 8.6 Hz, D2 and D6), 7.89 (2H, d, *J* = 8.9 Hz, A2 and A6). ^{13}C NMR ($CDCl_3$, 125 MHz) δ_C: 55.6 (C4-OMe), 70.1 ($PhCH_2$), 72.3 (β), 110.9 (C3), 113.1 (B3), 114.6 (A3 and A5), 120.2 (C1), 121.5 (B1), 127.4 (D2 and D6), 127.5 (A1and C5), 128.1 (B5), 128.2 (D4), 128.6 (B2), 128.7 (C2), 128.7 (D3 and D5), 130.9 (A2 and A6), 131.6 (C6), 131.7 (B6), 136.1 (D1), 155.7 (B4), 157.0 (C4), 162.9 (A4), 193.8 (α).

Synthesis of 3-hydroxy-1-(4-benzyloxyphenyl)-2-(2-methoxy-1, 1′-biphenyl-2′-yloxy) propanone ($4_{H\text{-}HH}$). A 500 ml of round bottom flask was charged with THF (115 ml), compound $\mathbf{3_{H\text{-}HH}}$ (9.67 g, 23 mmol, 1 equiv), and potassium carbonate (3.16 g, 23 mmol, 1 equiv). The formaldehyde (6.84 g, 228 mmol, 10 equiv) 37 w% aqueous solution was added the reaction mixture slowly. The progress of the reaction was monitored by TLC [hexane-EtOAc = 2:1, R_f (s/m) = 0.46, R_f (t/m) = 0.31]. After 16 hours stirring at 40 °C, the reaction was stopped by added 1 M HCl aqueous to adjust the pH value of reaction mixture into 7. The products were extracted by dichloromethane, washed twice with H_2O, and once with brine. The organic layer was dried over Na_2SO_4 and the solvent was evaporated in *vacuo*. The residue was purified with flash chromatography (elute hexane-EtOAc=2:1), to give pale yellow syrup compound $\mathbf{4_{H\text{-}HH}}$ (8.86 g, 85.5% yield). **Compound $4_{H\text{-}HH}$** ^1H NMR ($CDCl_3$+D_2O (1 drop), 500 MHz), δ_H: 3.76 (3H, s, C4-OMe), 3.85 (1H, broad-dd, *J* = 12, 7 Hz, γ_1), 3.91 (1H, br-dd, *J* = 12, 3 Hz, γ_2), 5.12 (2H, s, CH_2Ph), 5.37 (1H, br-dd, *J* = 7, 3 Hz, β), 6.77 (1H, br-d, *J* = 8 Hz, C3), 6.93 (2H, d, *J* = 8.9 Hz, A3 and A5), 7.02 (1H, br-d, *J* = 8 Hz, B3), 7.03 (1H, br-t, *J* = 8 Hz, C1), 7.07 (1H, br-t, *J* = 8 Hz, B1), 7.23 (1H, br-td, *J* = 8, 2 Hz, C2), 7.24 (1H, br-dd, *J* = 8, 2 Hz, C6), 7.27 (1H, br-dd, *J* = 8, 2 Hz, B6), 7.37 (1H, br-td, *J* = 8, 2 Hz, B2), 7.34-7.42 (5H, m, D-aromatic ring), 7.95 (2H, d, *J* = 8.9 Hz, A2 and A6). ^{13}C NMR ($CDCl_3$, 125 MHz) δ_C: 56.5 (C4-OMe), 63.5 (γ), 70.1 (CH_2Ph), 83.4 (β), 112.2 (B3), 113.1 (C3), 114.7 (A3 and A5), 121.3 (B1), 121.7 (C1), 127.4 (D-ring), 127.8 (A1), 128.2 (C5), 128.3 (D4), 128.6 (B5), 128.7 (D-ring), 128.8 (C2), 129.0 (B2), 131.4 (A2 and A6), 131.6 (B6 and C6), 136.0 (D1), 154.7 (B4), 156.7 (C4), 163.1 (A4), 195.0 (α).

Synthesis of 2-(2-methoxy-1, 1′-biphenyl-2′-yloxy)-1-(4-benzyloxyphenyl)propane-1, 3-diol

($5_{H\text{-}HH}$). The compound **$4_{H\text{-}HH}$** (10.29 g, 23 mmol, 1 equiv) was dissolved in THF/EtOH (91 ml : 91 ml) with stirring. Then excess of $NaBH_4$ (1.72 g, 45 mmol, 2 equiv) was added slowly into the solution. The reaction suspension was stirred at room temperature for 11 h. The completion of the reaction was monitored by TLC [hexane-EtOAc=1:1, R_f (s/m) = 0.53, R_f (*threo* isomer) = 0.48, R_f (*erythro* isomer) = 0.39]. 1 M of HCl aqueous was added dropwise to quench the remaining $NaBH_4$ under an ice-water bath. The reaction mixture was extracted with dichloromethane, washed twice with H_2O, and once with brine. The organic layer was dried over Na_2SO_4. After filtration, the filtrate was concentrated under vacuum to afford the mixture of **E** and **T** isomers of **$5_{H\text{-}HH}$** as syrup (9.74 g, 94% yield). The separation of *erythro* and *threo* isomers of compound **$5_{H\text{-}HH}$** was made with flash chromatography. The configurations of each isomers (*erythro* or *threo*) were determined by ozonation method, which yields erythronic and threonic acids from the *erythro* and *threo* isomers, respectively. The procedure of the method will be described in Section 2.2.4. The ***erythro* isomer of compound $5_{H\text{-}HH}$** ^{1}H NMR ($CDCl_3$, 500 MHz), δ_H: 3.60 (1H, m, γ_1), 3.72 (1H, broad-dd, *J* = 12, 6 Hz, γ_2), 3.74 (3H, s, C4-OMe), 4.42 (1H, m, β), 4.90 (1H, t, *J* = 4.0 Hz, α), 5.04 (2H, s, $PhCH_2$), 6.87 (2H, d, *J* = 8.6 Hz, A2 and A6), 7.02 (1H, br-d, *J* = 7 Hz, B3 and C3), 7.06 (1H, br-td, *J* = 7, 1 Hz, B1), 7.07 (1H, br-td, *J* = 7, 1 Hz, C1), 7.11 (2H, d, *J* = 8.6 Hz, A3 and A5), 7.21 (1H, br-dd, *J* = 7, 2 Hz, C6), 7.25 (1H, br-dd, *J* = 7, 2 Hz, B6), 7.32 (1H, br-td, *J* = 7, 2 Hz, B2), 7.33 (1H, m, D4), 7.39 (1H, br-td, *J* = 7, 2 Hz, C2), 7.39 (2H, br-t, *J* = 7 Hz, D3 and D5), 7.43 (2H, br-d, *J* = 7 Hz, D2 and D6). ^{13}C NMR ($CDCl_3$, 125 MHz) δ_C: 56.5 (C4-OMe), 60.3 (γ), 70.1 ($PhCH_2$), 72.3 (α), 82.2 (β), 112.0 (C3), 113.9 (B3), 114.7 (A2 and A6), 121.2 (C1), 121.5 (B1), 127.3 (A3 and A5), 127.4 (D2 and D6), 127.9 (D4), 128.3 (C5), 128.6 (D3 and D5), 128.8 (B2), 129.0 (C2), 129.4 (B5), 131.5 (C6), 131.5 (B6), 132.2 (A1), 136.9 (D1), 154.7 (B4), 156.7 (C4), 158.2 (A4). ***threo* isomers of compound $5_{H\text{-}HH}$** ^{1}H NMR ($CDCl_3$+D_2O (1 drop), 500 MHz), δ_H: 3.34 (1H, broad-dd, *J* = 12, 3 Hz, γ_1), 3.64 (1H, br-dd, *J* = 12, 3 Hz, γ_2), 3.78 (3H, s, C4-OMe), 4.37 (1H, m, β), 4.75 (1H, d, *J* = 8.0 Hz, α), 5.06 (2H, s, CH_2Ph), 6.94 (2H, br-d, *J* = 9 Hz, A2 and A6), 7.05 (1H, br-d, *J* = 7 Hz, B3 and C3), 7.07 (1H, br-td, *J* = 7, 1 Hz, B1), 7.09 (1H, br-td, *J* = 7, 1 Hz, C1), 7.24 (1H, br-dd, *J* = 7, 2 Hz, C6), 7.25 (1H, br-dd, *J* = 7, 2 Hz, B6), 7.29 (2H, br-d, *J* = 9 Hz, A3 and A5),7.32 (1H, br-td, *J* = 7, 2 Hz, B2), 7.33 (1H, br-t, *J* = 7 Hz, D4), 7.39 (2H, br-t, *J* = 7 Hz, D3 and D5), 7.39 (1H, br-td, *J* = 7, 2 Hz, C2), 7.43 (2H, br-d, *J* = 7 Hz, D2 and D6). ^{13}C NMR

($CDCl_3$, 125 MHz) δ_C: 56.4 (C4-OMe), 60.3 (γ), 70.0 ($PhCH_2$), 73.2 (α), 83.5 (β), 111.9 (C3), 113.5 (B3), 114.9 (A2 and A6), 121.4 (C1), 121.5 (B1), 127.4 (D2 and D6), 127.9 (D4), 128.3 (A3 and A5), 128.5 (D3 and D5), 128.9 (B2), 129.0 (C2), 129.1 (C5 and B5), 131.4 (C6), 131.6 (B6), 131.7 (A1), 136.9 (D1), 155.1 (B4), 156.6 (C4), 158.7 (A4).

Synthesis of 2-(2-methoxy-1, 1′-biphenyl-2′-yloxy)-1-(4-hydroxyphenyl)propane-1, 3-diol (*erythro* isomer of H-HH$_{biphenyl}$). A stirred suspension of compound *erythro* isomer of **5**$_{H\text{-}HH}$ (1.65 g, 3.62 mmol, 1 equiv) and palladium on charcoal (0.17 g) in THF (73 ml) was fitted with a hydrogen-gas-filled balloon. The reaction suspension was kept stirring overnight at room temperature. The completion of the reaction was monitored by TLC [hexane-EtOAc = 1:1, R_f (s/m, *erythro* form) = 0.45, R_f (t/m, *erythro* form) = 0.35]. After reaction, the insoluble catalyst was separated from THF solution by a glass filter with the aid of Celite, and washed with acetone. The filtrate was concentrated under vacuum. The crude product was purified by flash chromatography using hexane-EtOAc=1:1 at multiple times to afford the *erythro* isomer of **H-HH**$_{biphenyl}$ as syrup (1.3 g, 98% yield). The configurations of resulting *erythro* isomer of **H-HH**$_{biphenyl}$ was determined by ozonation method, of which experimental procedures will be described in Section 2.2.4.

Synthesis of 2-(2-methoxy-1, 1′-biphenyl-2′-yloxy)-1-(4-hydroxyphenyl)propane-1, 3-diol (*threo* form of H-HH$_{biphenyl}$). Similar with the debenzylated method described above**,** *threo* isomer of **5**$_{H\text{-}HH}$ (5.57 g, 12.21 mmol, 1 equiv) was also reduced by hydrogen in THF (245 ml) with the aid of palladium on charcoal (0.56 g) for overnight at room temperature. The completion of the reaction was monitored by TLC [hexane-EtOAc = 1:1, R_f (s/m, *threo* form) = 0.56, R_f (t/m, *threo* form) = 0.42]. With the same work-up, the resulting crude products were purified by flash chromatography using hexane-EtOAc = 1:1 at multiple times to afford the *threo* isomer of **H-HH**$_{biphenyl}$ as syrup (4.4 g, 98% yield). The configurations of resulting *threo* isomer of **H-HH**$_{biphenyl}$ was determined by ozonation method, of which experimental procedures will be described in Section 2.2.4.

2.2.3 Separation of diastereomers of β-O-4 model compounds

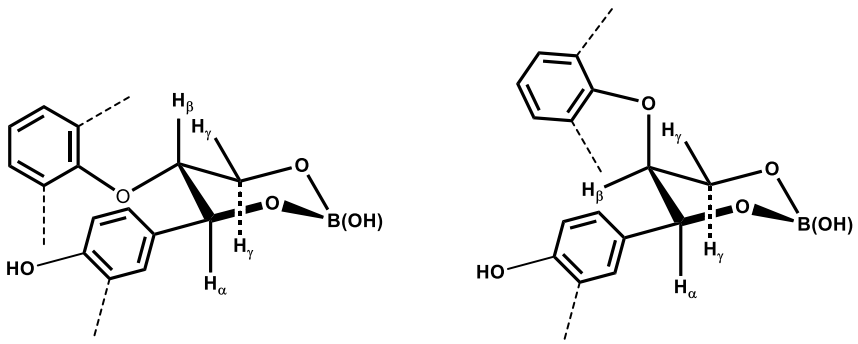

Figure 2.4 borate complexes for the diastereomers of lignin β-O-4 models

The *erythro* and *threo* mixture of each β-O-4 model (**GG**, **GH**, **GS**, **HG** or **HH**) were separated by ion-exchange chromatography with borate solution as eluent according to the method developed by Lundquist's group (**Figure 2.4**).[4-6] The separation was carried out on an anion-exchange column (around 220 ml QAE-Sephadex A-25, size 40-120 μm, Pharmacia; column dimensions: 2.5×50 cm) using 0.06 M $K_2B_4O_7$ in ethanol-water (1/4, v/v) as the eluent. Around 0.7 g of samples were stirred in the 2 ml eluent for 2 hours, then the resulting suspension was dissolved in a small amount of ethanol. After the sample solution was injected into the anion-exchange column at the top, a peristaltic pump (ST-1211, ATTO Co.) was used to convey the eluent from the column at the rate 1.5 ml/min. Several 13 ml glass tubes were used to collect the effluent (one tube for 500 drops, around 10 ml). The separation process was monitored by the UV monitor (UV-2075, JASCO Co., Japan) at the absorbance peak 254 nm. The effluent fractions were combined on the basis of high-performance liquid chromatography (HPLC) analysis of the each fraction. The two combined fractions containing either *erythro* or *threo* isomer were neutralized by addition of acetic acid. The each fractions neutralized were extracted six times with chloroform (50 ml × 3 times and 30 ml × 3 times), respectively. The organic layers were combined, washed twice with H_2O, once with brine, dried over Na_2SO_4. After filtration, the filtrate was evaporated to dryness in *vacuo* to afford *erythro* or *threo* isomers of β-O-4 models as syrupy or crystals.

2.2.4 Determination of stereo-configurations of separated β-O-4 model compounds

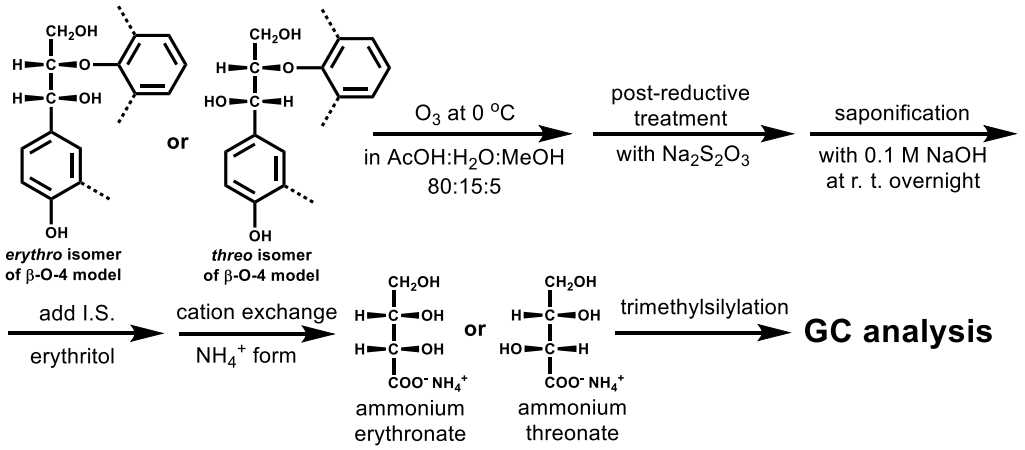

Figure 2.5 Experimental scheme for the configurations determining ozonation method

As Shown in **Figure 2.5**, the configurations of separated β-O-4 models (**E** or **T**) were determined by ozonation analysis according to the method of Akiyama et al. except for the use of 1h reaction time.[7-10] Samples (0.01 mmol) were firstly suspended in 30 ml of AcOH-H_2O-MeOH (80: 15: 5 by volume). Oxygen containing ca. 3% ozone (type ON-3-2, Nippon ozone) was then bubbled into the suspension at a rate of 0.5 L/min for 1 h with stirring in an ice bath. After bubbling oxygen for 10 minutes, 0.1 M sodium thiosulfate (300 μl) was added to consume the residual ozone. The solvent was evaporated in reduced pressure at 40°C and traces of acetic acid were removed by repeated evaporation by adding small amounts of water (1 ml×3). The products were saponified with 0.1 M NaOH (20 ml) at room temperature overnight. Erythritol (2 μmol) was added as an internal standard. The product solution was then passed through a column filled with 10–15 ml of cation-exchange resin (Dowex-50W-X4, NH_4^+ form), and the column was washed with water until the pH of eluent was neutral. A 0.1 M ammonia solution (1ml) was added to the eluent, and diluted with water to adjust the total volume of the eluent into 100 ml. An aliquot of the eluent (2 ml) was concentrated and dried in *vacuo* at 40 °C, then trimethylsilylated with hexamethyldisilazane (200 μl) and trimethylchlorosilane (100 μl) in dimethylsulfoxide (300 μl) solution at 60 °C for 30 min. The upper layer containing trimethylsilyl derivatives was subjected to gas chromatography (GC-FID: Shimadzu 17A) with an

InertCap 1 column (GL Science NB1, 0.25mm i.d. ×30 m) to determine the yields of erythronic acid or threonic acid in the ozonation product. The analytical conditions were as follows:

GC-FID: Oven temperature program: 120 ℃, 5 min-4 ℃ /min→170 ºC-10 ℃ /min→280 ℃.

Injection tem. 250 ℃; Detector temp. 280 ℃; Column flow rate of He gas 1.9 mL/min; Splitting ratio 60:1; Injection volume 1 μl;

Retention time (TMS derivatives): 15.8 min (erythritol), 16.7 min (erythronic acid), 17.2 min (threonic acid).

2.3 Results and discussion

2.3.1 Separation of diastereomers of β-O-4 model compounds

The separation of diastereomers of β-O-4 model compounds based on the stability of their borate complexes was developed by Berndtsson and Lundquist.[4-6] According to this method, *erythro* and *threo* isomers were separated from *erythro-threo* mixtures of each β-O-4 model compounds **GG**, **GH**, **GS**, **HG** and **HH**.

Table1. Elution volumes of a series of phenolic β-O-4 model compounds on ion-exchange chromatography on an anion exchanger using a borate solution as the eluent

Compound	*threo* isomer	*erythro* isomer
GG	586 ml	1774 ml
GH	1102 ml	2254 ml
GS	540 ml	1000 ml
HG	792 ml	2050 ml
HH	1530 ml	2790 ml

Although the separation took over 12 h, a large amount of phenolic β-O-4 model (～1g) was able to be separated by each separation. Lundquist's group[5] ever showed the elution volumes (ml) for

isomers separation of β-O-4 model using 0.06 M $K_2B_4O_7$ in acetone-water (1:4) as the eluent from a QAE-Sephadex A-25 column: phenolic **GG**$_{erythro}$ (630), phenolic **GG**$_{threo}$ (380), non-phenolic **GG**$_{erythro}$ (270), non-phenolic **GG**$_{threo}$ (200), non-phenolic **HG**$_{erythro}$ (300) and non-phenolic **HG**$_{threo}$ (200). The isomers separation took larger elution volume for phenolic **GG** model than non-phenolic **GG** model. Also, the elution volumes for our isomers separation of phenolic compounds are comparatively large (**Table 1**), e.g., phenolic **GG**$_{erythro}$ (1774), phenolic **GG**$_{threo}$ (586), phenolic **HG**$_{erythro}$ (2050) and phenolic **HG**$_{threo}$ (792). The two peaks observed in the separation chromatography, the firstly appeared one is from their *threo* form, the last one is from their *erythro* form. Satisfactory separation of diastereomers for all β-O-4 models were achieved although the second peak (*erythro* isomer) has the broadening and tailing problem in the separation. After extraction, the boric acid could be removed by repeated addition and evaporation of Methanol. By this treatment, *threo* isomer of **GG**, *erythro* isomer of **HH** and *erythro* isomer of **GS** were obtained as crystals. The *erythro* isomer of **GG**, *erythro* and *threo* isomers of **GH**, *threo* isomer of **GS**, *erythro* and *threo* isomers of **HG** and *threo* isomer of **HH** were obtained as syrup. The ^{1}H NMR spectrum of the each isomer (**Figure 3.4-3.8** in Chapter 3) indicated that each compound separated in this experiment was fairly pure. Any NMR peak of another isomer was not found in the NMR spectra.

2.3.2 Determination of stereo-configurations of separated lignin β-O-4 models

The ozonation of various linkage types in lignin yields low-molecular weight compounds that retain the original stereo structures of lignin side-chains (**Figure 2.5**). This ozonation analysis method developed by Matsumoto and Akiyama[7-10] has been used on stereochemical study of lignin.

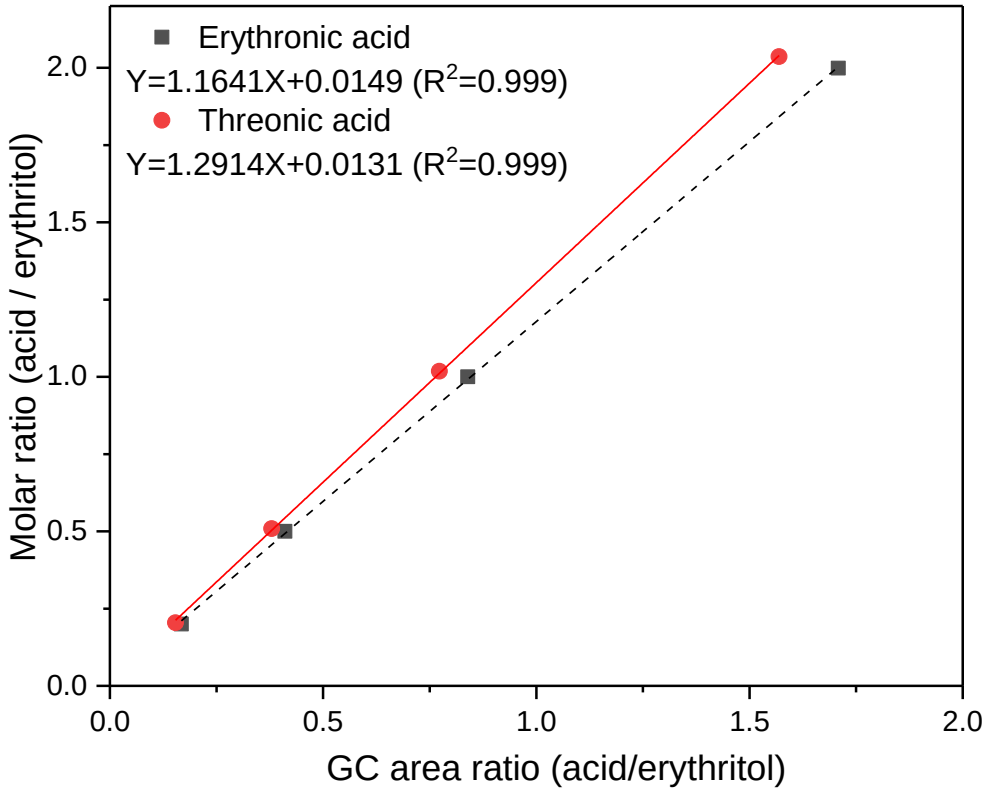

Figure 2.6 Calibration curves for the GC-FID analysis of erythronic and threonic acids with erythritol as internal standard

The calibration curves of erythronic and threonic acid with erythritol as an internal standard were fitted well with linear lines (**Figure 2.6)**. Each isomers of β-O-4 model compound (**GG**, **GH**, **GS**, **HG**, **HH** and **H-HH$_{biphenyl}$**) were subjected to ozonation analysis, and their stereo-configurations were determined by comparing the retention time of erythronic or threonic acids in ozonation products in GC chromatogram with that of their authentic compounds. The yield of erythronic and threonic acids from each isomers of β-O-4 model compound during ozonation were shown in **Table 2**. In addition to determine the stereo-configuration of each separated isomer, we also can see each compound separated was fairly pure. Only one peak of trimethylsilylated erythronic or threonic acid in ozonation products from corresponding isomers can be found in the GC chromatography.

Table 2. The yield of erythronic acid and threonic acid from each isomer of β-O-4 model compound (**GG**, **GH**, **GS**, **HG**, **HH** and **H-HH$_{biphenyl}$**) through ozonation analysis

entry	Yield of ozonation products	
	erythronic acid	threonic acid
erythro-**GG**	57%	no data
threo-**GG**	no data	55%
erythro-**GH**	65%	no data
threo-**GH**	no data	86%
erythro-**GS**	57%	no data
threo-**GS**	no data	61%
erythro-**HG**	67%	no data
threo-**HG**	no data	42%
erythro-**HH**	57%	no data
threo-**HH**	no data	49%
erythro-**H-HH$_{biphenyl}$**	36%	no data
threo-**H-HH$_{biphenyl}$**	no data	51%

2.3.3 NMR characterization of separated diastereomers of β-O-4 model compounds

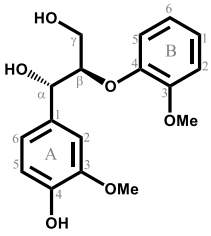

Compound GG (*erythro* isomer). ^{1}H NMR (acetone-d_6 +D_2O (1 drop), 500 MHz), δ_H: 3.68 (1H, broad-dd, J = 12, 4 Hz, γ_1), 3.78 (3H, s, A3-OMe), 3.79 (3H, s, B3-OMe), 3.81 (1H, br-dd, J = 12, 5 Hz, γ_2), 4.30 (1H, m, β), 4.87 (1H, d, J = 5.4 Hz, α), 6.74 (1H, br-d, J = 8 Hz, A5), 6.80 (1H, br-td, J = 8, 2 Hz, B6), 6.86 (1H, br-dd, J = 8, 2 Hz, A6), 6.89 (1H, br-td, J = 8, 2 Hz, B1), 6.94 (1H, br-dd, J = 8, 2 Hz, B2), 6.95 (1H, br-dd, J = 8, 2 Hz, B5), 7.07 (1H, br-d, J = 2 Hz, A2). ^{13}C NMR (acetone-d_6, 125 MHz) δ_C: 56.3 (A3-OMe), 56.4 (B3-OMe), 61.9 (γ), 73.9 (α), 86.9 (β), 111.5 (A2), 113.6 (B2), 115.2 (A5), 119.8

(B5), 120.6 (A6), 121.9 (B6), 123.4 (B1), 134.4 (A1), 146.7 (A4), 148.0 (A3), 149.2 (B4), 152.1 (B3).

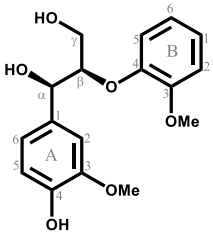

Compound GG (*threo* isomer). ^{1}H NMR (acetone-d_6 +D_2O (1 drop), 500 MHz), δ_H: 3.47 (1H, dd, J = 11.8, 5.5 Hz, γ_1), 3.69 (1H, dd, J = 11.8, 4.3 Hz, γ_2), 3.77 (3H, s, A3-OMe), 3.83 (3H, s, B3-OMe), 4.25 (1H, ddd, J = 5.7, 5.5, 4.3 Hz, β), 4.87 (1H, d, J = 5.7 Hz, α), 6.74 (1H, broad-d, J = 8 Hz, A5), 6.83 (1H, br-td, J = 8, 2 Hz, B6), 6.86 (1H, br-dd, J = 8, 2 Hz, A6), 6.90 (1H, br-td, J = 8, 2 Hz, B1), 6.97 (1H, br-dd, J = 8, 2 Hz, B2), 7.06 (1H, br-d, J = 2 Hz, A2), 7.11 (1H, br-dd, J = 8, 2 Hz, B5). ^{13}C NMR (acetone-d_6, 125 MHz) δ_C: 56.3 (A3-OMe), 56.4 (B3-OMe), 62.0 (γ), 74.0 (α), 88.8 (β), 111.5 (A2), 113.5 (B2), 115.3 (A5), 120.2 (B5), 120.7 (A6), 122.1 (B6), 123.5 (B1), 133.9 (A1), 146.9 (A4), 148.1 (A3), 149.8 (B4), 151.9 (B3).

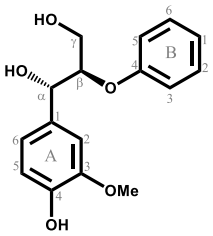

Compound GH (*erythro* isomer). ^{1}H NMR (acetone-d_6 +D_2O (1 drop), 500 MHz), δH: 3.76 (3H, s, A3-OMe), 3.78 (1H, dd, J = 11.7, 4.0 Hz, γ_1), 3.83 (1H, dd, J = 11.7, 5.2 Hz, γ_2), 4.43 (1H, m, β), 4.86 (1H, d, J = 6.0 Hz, α), 6.72 (1H, broad-d, J = 8 Hz, A5), 6.83 (1H, br-t, J = 7 Hz, B1), 6.86 (1H, br-dd, J = 8, 2 Hz, A6), 6.89 (2H, br-d, J = 9 Hz, B3 and B5), 7.03 (1H, br-d, J = 2 Hz, A2), 7.16 (2H, br-dd, J = 9, 7 Hz, B2 and B6). ^{13}C NMR (acetone-d_6, 125 MHz) δC: 56.3 (A3-OMe), 62.1 (γ), 74.0 (α), 83.8 (β), 111.5 (A2), 115.2 (A5), 117.3 (B3, B5), 120.6 (A6), 121.6 (B1), 130.1 (B2 and B6), 134.6 (A1), 146.8 (A4), 148.0 (A3), 159.9 (B1).

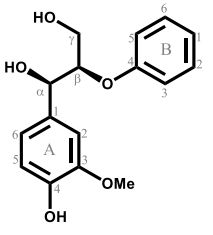

Compound GH (*threo* isomer). ^{1}H NMR (acetone-d_6 +D_2O (1 drop), 500 MHz), δ_H: 3.50 (1H, dd, J = 11.6, 5.5 Hz, γ_1), 3.77 (3H, s, A3-OMe), 3.78 (1H, dd, J = 11.6, 4.6 Hz, γ_2), 4.44 (1H, m, β), 4.91 (1H, d, J = 4.9 Hz, α), 6.74 (1H, broad-d, J = 8 Hz, A5), 6.85 (1H, br-dd, J = 8, 2 Hz, A6), 6.86 (1H, m, B1), 6.97 (2H, br-d, J = 9 Hz, B3 and B5), 7.05 (1H, br-d, J = 2 Hz, A2), 7.20 (2H, br-dd, J = 9, 8 Hz, B2 and B6). ^{13}C NMR (acetone-d_6, 125 MHz) δ_C: 56.3 (A3-OMe), 62.8 (γ), 73.5 (α), 84.2 (β), 111.5 (A2), 115.3 (A5), 117.2 (B3 and B5), 120.5 (A6), 121.6 (B1), 130.2 (B2 and B6), 134.4 (A1), 146.8 (A4),

148.1 (A3), 160.3 (B1).

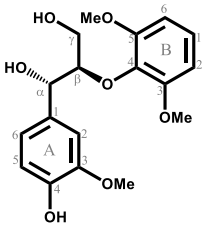

Compound GS (*erythro* isomer). ^{1}H NMR (acetone-d_6 +D_2O (1 drop), 500 MHz), δ_H: 3.42 (1H, dd, J = 12.1, 3.5 Hz, γ_1), 3.80 (3H, s, A3-OMe), 3.82 (6H, s, B3-OMe and B5-OMe), 3.83 (1H, m, γ_2), 4.16 (1H, m, β), 4.95 (1H, d, J = 4.6 Hz, α), 6.70 (2H, broad-d, J = 9 Hz, B2 and B6), 6.75 (1H, br-d, J = 9 Hz, A5), 6.80 (1H, br-d, J = 9 Hz, A6), 7.02 (1H, br-t, J = 9 Hz, B1), 7.02 (1H, s, A2). ^{13}C NMR (acetone-d_6, 125 MHz) δ_C: 56.3 (A3-OMe), 56.6 (B3-OMe and B5-OMe), 61.0 (γ), 73.4 (α), 87.9 (β), 106.6 (B2 and B6), 110.9 (A2), 115.3 (A5), 120.1 (A6), 124.9 (B1), 133.8 (A1), 136.8 (B3, B5), 146.5 (A4), 148.1 (A3), 154.6 (B4).

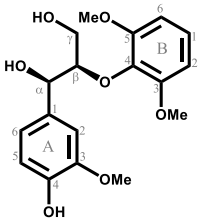

Compound GS (*threo* isomer). ^{1}H NMR (acetone-d_6 +D_2O (1 drop), 500 MHz), δ_H: 3.27 (1H, dd, J = 12.0, 3.2 Hz, γ_1), 3.63 (1H, dd, J = 12.0, 3.7 Hz, γ_2), 3.79 (3H, s, A3-OMe), 3.86 (6H, s, B3-OMe and B5-OMe), 3.93 (1H, m, β), 4.97 (1H, d, J = 7.2 Hz, α), 6.70 (2H, broad-d, J = 8 Hz, B2 and B6), 6.75 (1H, br-d, J = 8 Hz, A5), 6.88 (1H, br-dd, J = 8, 2 Hz, A6), 7.02 (1H, br-t, J = 8 Hz, B1), 7.03 (1H, br-d, J = 2 Hz, A2). ^{13}C NMR (acetone-d_6, 125 MHz) δ_C: 56.3 (A3-OMe), 56.6 (B3-OMe and B5-OMe), 64.3 (γ), 74.1 (α), 89.9 (β), 106.6 (B2 and B6), 111.5 (A2), 115.3 (A5), 120.8 (A6), 125.0 (B1), 133.8 (A1), 137.2 (B3 and B5), 146.9 (A4), 148.0 (A3), 154.3 (B4).

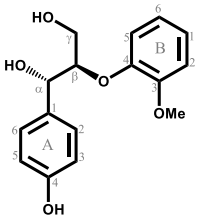

Compound HG (*erythro* isomer). ^{1}H NMR (acetone-d_6 + D_2O (1 drop), 500 MHz), δ_H: 3.67 (1H, dd, J = 12.0, 3.7 Hz, γ_1), 3.79 (3H, s, B3-OMe), 3.81 (1H, dd, J = 12.0, 5.4 Hz, γ_2), 4.25 (1H, m, β), 4.87 (1H, d, J = 5.4 Hz, α), 6.76 (2H, broad-d, J = 8 Hz, A3 and A5), 6.80 (1H, br-td, J = 8, 2 Hz, B6), 6.90 (1H, br-td, J = 8, 2 Hz, B1), 6.94 (1H, br-dd, J = 8, 2 Hz, B2), 6.95 (1H, br-dd, J = 8, 2 Hz, B5), 7.25 (2H, br-d, J = 8 Hz, A2 and A6). ^{13}C NMR (acetone-d_6, 125 MHz) δ_C: 56.4 (B3-OMe), 61.8 (γ), 73.7 (α), 87.2 (β), 113.6 (B2), 115.6 (A3 and A5), 120.2 (B5), 122.0 (B6), 123.6 (B1), 129.0 (A2 and A6), 133.8 (A1), 149.1 (B4), 152.2 (B3), 157.5 (A4).

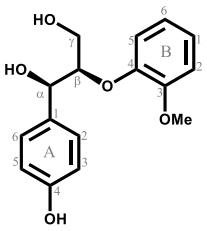

Compound HG (*threo* isomer). ^{1}H NMR (acetone-d_6+D_2O (1 drop), 500 MHz), δ_H: 3.43 (1H, dd, J = 12.0, 5.4 Hz, γ_1), 3.65 (1H, dd, J = 12.0, 4.0 Hz, γ_2), 3.84 (3H, s, B3-OMe), 4.18 (1H, m, β), 4.86 (1H, d, J = 6.3 Hz, α), 6.76 (2H, broad-d, J = 9 Hz, A3 and A5), 6.84 (1H, br-td, J = 8, 2 Hz, B6), 6.93 (1H, br-td, J = 8, 1 Hz, B1), 6.98 (1H, br-dd, J = 8, 2 Hz, B2), 7.14 (1H, br-dd, J = 8, 1 Hz, B5), 7.25 (2H, br-d, J = 9 Hz, A2 and A6). ^{13}C NMR (acetone-d_6, 125 MHz) δ_C: 56.4 (B3-OMe), 61.9 (γ), 73.9 (α), 89.2 (β), 113.5 (B2), 115.7 (A3 and A5), 120.6 (B5), 122.1 (B6), 123.7 (B1), 129.2 (A2 and A6), 133.3 (A1), 149.9 (B4), 152.0 (B3), 157.8 (A4).

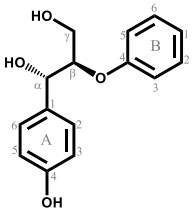

Compound HH (*erythro* isomer). ^{1}H NMR (acetone-d_6 + D_2O (1 drop), 500 MHz), δ_H: 3.77 (1H, dd, J = 11.8, 5.0 Hz, γ_1), 3.83 (1H, dd, J = 11.8, 5.0 Hz, γ_2), 4.39 (1H, m, β), 4.87 (1H, d, J = 5.7 Hz, α), 6.74 (2H, broad-d, J = 9 Hz, A2 and A6), 6.84 (1H, br-t, J = 7 Hz, B1), 6.89 (2H, br-d, J = 9 Hz, B3 and B5), 7.17 (2H, br-dd, J = 7, 9 Hz, B2 and B6), 7.25 (2H, br-d, J = 9 Hz, A3 and A5). ^{13}C NMR (acetone-d_6, 125 MHz) δ_C: 61.7 (γ), 73.5 (α), 83.8 (β), 115.5 (A2 and A6), 117.3 (B3 and B5), 121.6 (B1), 128.9 (A3 and A5), 130.1 (B2 and B6), 133.7 (A1), 157.5 (A4), 159.7 (B4).

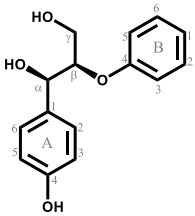

Compound HH (*threo* isomer). ^{1}H NMR (acetone-d_6+ D_2O (1 drop), 500 MHz), δ_H: 3.47 (1H, dd, J = 11.5, 5.0 Hz, γ_1), 3.76 (1H, dd, J = 11.5, 4.3 Hz, γ_2), 4.41 (1H, m, β), 4.91 (1H, d, J = 5.2 Hz, α), 6.75 (2H, broad-d, J = 9 Hz, A2 and A6), 6.87 (1H, br-t, J = 7 Hz, B1), 6.97 (2H, br-d, J = 9 Hz, B3 and B5), 7.21 (2H, br-dd, J = 7, 9 Hz, B2 and B6), 7.25 (2H, br-d, J = 9 Hz, A3 and A5). ^{13}C NMR (acetone-d_6, 125 MHz) δ_C: 62.0 (γ), 73.9 (α), 84.4 (β), 115.6 (A2 and A6), 117.4 (B3 and B5), 121.6 (B1), 129.0 (A3 and A5), 130.2 (B2 and B6), 134.0 (A1), 157.6 (A4), 160.3 (B4).

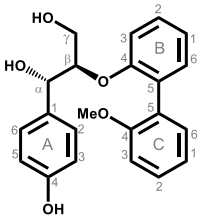

Compound H-HH$_{biphenyl}$ (*erythro* isomer). ^{1}H NMR ($CDCl_3$ + D_2O (1 drop), 500 MHz), δ_H: 3.55 (1H, broad-dd, *J* = 12, 3 Hz, γ_1), 3.69 (1H, br-dd, *J* = 12, 5 Hz, γ_2), 3.71 (3H, s, C4-OMe), 4.39 (1H, m, β), 4.84 (1H, d, *J* = 4.3 Hz, α), 6.62 (2H, br-d, *J* = 8 Hz, A2 and A6), 6.98 (2H, br-d, *J* = 8 Hz, A3 and A5), 6.99 (1H, br-d, *J* = 8 Hz, B3), 7.01 (1H, br-d, *J* = 8 Hz, C3), 7.05 (1H, br-t, *J* = 8 Hz, B1), 7.05 (1H, br-t, *J* = 8 Hz, C1), 7.19 (1H, br-dd, *J* = 8, 2 Hz, C6), 7.23 (1H, br-dd, *J* = 8, 2 Hz, B6), 7.30 (1H, br-td, *J* = 8, 2 Hz, B2), 7.36 (1H, br-td, *J* = 8, 2 Hz, C2). **^{13}C NMR** ($CDCl_3$, 125 MHz) δ_C: 56.5 (C4-OMe), 60.1 (γ), 72.2 (α), 82.0 (β), 112.2 (C3), 114.0 (B3), 115.2 (A2 and A6), 121.4 (C1), 121.6 (B1), 127.4 (A3 and A5), 128.3 (C5), 128.9 (B2), 129.0 (C2), 129.4 (B5), 131.3 (A1), 131.5 (C6), 131.6 (B6), 154.6 (B4), 155.3 (A4), 156.7 (C4).

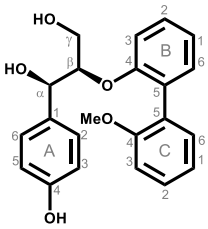

Compound H-HH$_{biphenyl}$ (*threo* isomer). ^{1}H NMR ($CDCl_3$ + D_2O (1 drop), 500 MHz), δ_H: 3.29 (1H, broad-dd, *J* = 13, 3 Hz, γ_1), 3.61 (1H, br-dd, *J* = 13, 3 Hz, γ_2), 3.74 (3H, s, C4-OMe), 4.36 (1H, m, β), 4.68 (1H, d, *J* = 8.0 Hz, α), 6.63 (2H, d, *J* = 8.6 Hz, A2 and A6), 7.04 (1H, br-d, *J* = 8 Hz, B3), 7.05 (1H, br-d, *J* = 8 Hz, C3), 7.06 (1H, br-t, *J* = 8 Hz, B1), 7.08 (1H, br-t, *J* = 8 Hz, C1), 7.13 (2H, d, *J* = 8.6 Hz, A3 and A5),7.22 (1H, br-dd, *J* = 8, 2 Hz, C6), 7.23 (1H, br-dd, *J* = 8, 2 Hz, B6), 7.32 (1H, br-td, *J* = 8, 2 Hz, B2), 7.38 (1H, br-td, *J* = 8, 2 Hz, C2). **^{13}C NMR** ($CDCl_3$, 125 MHz) δ_C: 56.6 (C4-OMe), 60.3 (γ), 73.4 (α), 83.4 (β), 112.3 (C3), 113.4 (B3), 115.6 (A2 and A6), 121.6 (C1 and B1), 128.4 (B5 and C5), 128.5 (A3 and A5), 129.0 (B2), 129.1 (C2), 130.6 (A1), 131.4 (C6), 131.7 (B6), 155.1 (B4), 156.0 (A4), 156.6 (C4).

2.4 References

[1] Adler, E., Lindgren, B. O., Saeden, U. 1952. The β-guaiacyl ether of α-veratrylglycerol as a lignin model. Svensk Papperstidn, 57(7), 245-254.

[2] Ralph, J., Lundquist, K., Brunow, G., Lu, F., Kim, H., Schatz, P. F., ... & Boerjan, W. 2004. Lignins:

natural polymers from oxidative coupling of 4-hydroxyphenyl-propanoids. Phytochemistry Reviews, 3(1-2), 29-60.

[3] Sarkanen, K. V., Hergert, H. L. 1971. In lignins: occurrence, formation, structure, and reactions, Wiley-Interscience: New York, pp 43−94.

[4] Ibrahim, W., Lundquist, K. 1994. Synthesis of *erythro* and *threo* forms of lignin models of the arylglycerol-β-guaiacyl ether type. Acta Chemica Scandinavica, 48, 149-151.

[5] Berndtsson, I., Lundquist, K. 1977. On the synthesis of lignin model compounds of the arylglycerol-β-aryl ether type. Acta Chemica Scandinavica, B31(8), 725-726.

[6] Li, S., Lundquist, K., Soubbotin, N. 1994. Separation of diastereomers of lignin model compounds of the 1, 3-diol type as borate complexes by ion-exchange chromatography. Holzforschung, 48, 509-509.

[7] Akiyama, T., Sugimoto, T., Matsumoto, Y., Meshitsuka, G. 2002. *Erythro*/*threo* ratio of β-O-4 structures as an important structural characteristic of lignin. I: Improvement of ozonation method for the quantitative analysis of lignin side-chain structure. Journal of Wood Science, 48(3), 210-215.

[8] Akiyama, T., Goto, H., Nawawi, D. S., Syafii, W., Matsumoto, Y., Meshitsuka, G. 2005. *Erythro*/*threo* ratio of β-O-4 structures as an important structural characteristic of lignin. Part 4: Variation in the *erythro*/*threo* ratio in softwood and hardwood lignins and its relation to syringyl/guaiacyl ratio. Holzforschung, 59(3), 276-281.

[9] Matsumoto, Y. 1986. Studies on chemical structure of lignin by ozonation. Holzforschung, 40, 81-85.

[10] Matsumoto, Y. 1993. Structural study on lignin by ozonation. The *erythro* and *threo* ratio of the β-O-4 structure indicates how lignin polymerizes. Mokuzai Gakkaishi, 39, 734-736.

Chapter 3

Water Addition to β-O-4 bonded Quinone Methide Models mimicking Lignin biosynthesis

3.1 Introduction

p-Quinone methides (**QMs**) are involved in lignin biosynthesis as transient intermediates, and their aromatization step has a great impact on the chemical structure of the resulting lignins.[1] In the formation of arylglycerol-β-aryl ether structures (β-O-4 structures), β-O-4-bonded **QMs** are aromatized by the attack of water to produce either *erythro* or *threo* form of β-O-4 structures (**Figure 3.1**). Their stereochemistry is determined by which face of the **QM** reacts faster with water.[2,3] The *erythro*/*threo* ratio is variable in plants, which causes the structural variation in lignins.[4-6] The ratio of *erythro* and *threo* forms is close to 50:50 in softwood lignins, whereas the *erythro* form dominates in hardwood lignins.[4,7,8] For *erythro* or *threo* form to be produced in excess during lignin biosynthesis, stereo-preferential water addition must occur to the β-O-4-bonded **QM** intermediate.[3] Syringyl/guaiacyl (**S/G**) ratio of aromatic nuclei seems to be one of the factors governing the *erythro*/*threo* ratio, which was evidenced by the positive correlation between these ratios among different wood species[4,5,9] and was also indicated by a model study of water addition to **S**-type **QM** mimicking hardwood lignin formation.[3]

There was a case, however, that the *erythro*/*threo* ratio is not 50:50 for softwood lignin in spite of the absence of **S** unit. Previous study about a compression wood lignin containing *p*-hydroxyphenyl (**H**) unit showed that *erythro* form ratio was slightly predominant.[10, 11] The distribution of this ratio was positively correlated with that of **H/G** ratio, implying that the *erythro*-preferential formation is related to the **H**-unit of aromatic ring type.[10] The aim of this chapter is to investigate factors that influence the *erythro*/*threo* ratio of β-O-4 structures during lignin biosynthesis. The main focus is put on the effect of pH condition, water-dioxane ratio in reaction solvent, and also the structures of aromatic ring type or moiety in **QM**. In this work, a series of **QMs** with different structures were synthesized, and water addition experiments were conducted to simulate the *erythro*/*threo* ratio determining step during lignin biosynthesis.

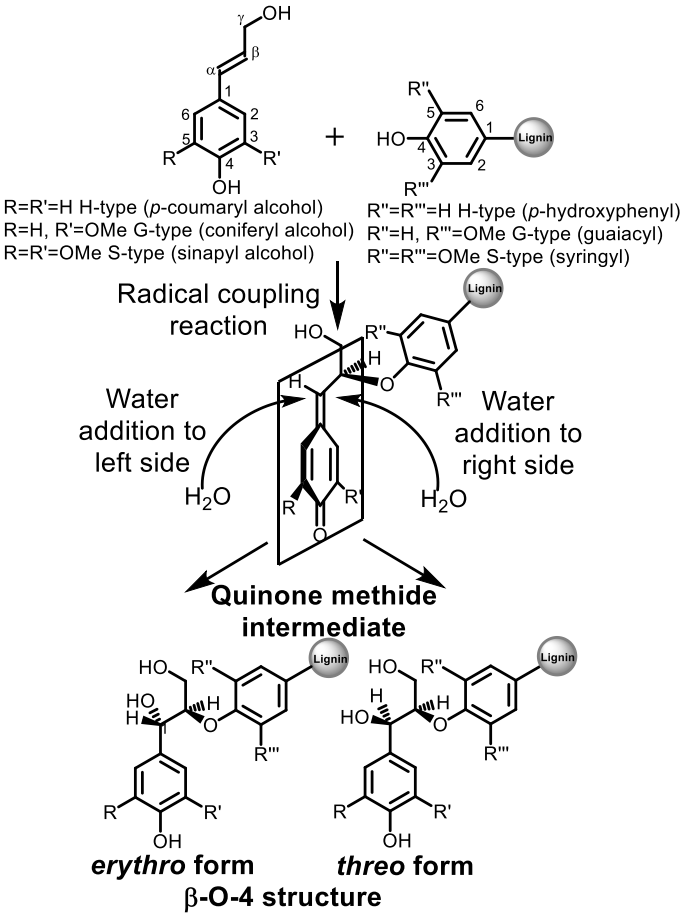

Figure 3.1 Formation of *erythro* and *threo* forms of β-O-4 structures during lignin biosynthesis.

3.2 Experimental

3.2.1 General

Reagents and solvents were purchased from Fujifilm Wako Pure Chemical Co. (Osaka, Japan), Tokyo Chemical Industry Co., Ltd. (Tokyo, Japan) or Sigma-Aldrich (Tokyo, Japan), and used as received. The pH values of buffers were measured with a HORIBA F-52 pH meter with JF15 electrode (Horiba, Kyoto, Japan). The NMR spectra of synthesized compounds were recorded with a JEOL JNM-A500 500 MHz spectrometer. The standard JEOL programs of one- and two-dimensional (proton, carbon, DEPT-135, ^{1}H-^{1}H COSY, ^{1}H-^{13}C HSQC, and ^{1}H-^{13}C HMBC) NMR experiments were performed for the structural elucidation and assignment of newly synthesized **QM** models. The central

peak of the residual solvent was used as an internal reference (δ_H 7.26, δ_c 77.0 ppm for $CDCl_3$, δ_H 2.04, δc 29.8 ppm for acetone-d_6, δ_H 5.32, δc 53.8 ppm for CD_2Cl_2). For samples that encountered multiplicity problems with hydroxyl-group protons, a drop of D_2O was added for the OH-OD exchange prior to analysis. The traditional numbering system for lignins[6,12] was used rather than the systematic IUPAC numbering scheme.

3.2.2 General procedure for quinone methides preparation

Quinone methides (**QM-GG**, **QM-GH**, **QM-GS**, **QM-HG**, **QM-HH**, and **QM-H-HH$_{biphenyl}$** in **Figure 3.2** were synthesized from the corresponding six β-O-4 model compounds (**GG**, **GH**, **GS**, **HG**, **HH**, and **H-HH$_{biphenyl}$**, respectively) by a mild alkaline treatment of their benzyl bromides[1, 2, 3] which were prepared using trimethylsilyl bromide (TMSiBr) according to the method in literatures.[13-15] The general procedure for preparation of **QMs** are as follows:

General Procedure

A β-O-4 model (0.1 mmol, as a mixture of *erythro* and *threo* isomers) was placed in a small vial with a screw cap, and dissolved in 1 ml of chloroform. To this solution was added trimethylsilyl bromide (0.2 mmol), and shaken for 90 seconds at room temperature to generate the benzyl bromide. The reaction mixture was then shaken with saturated aqueous $NaHCO_3$ (1 mL) for 10 seconds. The organic layer was collected, washed with saturated NaCl, and dried over Na_2SO_4. The resulting pale yellow solution of **QM** was diluted with dioxane into a desired concentration, and used for the water addition experiment without further purification (approximately 0.1 mM or 0.8 mM **QM** based on the assumption that a β-O-4 model compound was transformed into its **QM** quantitatively). For the structural determination by NMR, the **QM** was prepared in the same way except that, instead of chloroform, deuterated chloroform was used as reaction solvent. The chloroform-*d* solution of the crude **QM** was transferred into a NMR tube and kept in liquid N_2 before NMR measurement.

Almost **QMs** (**QM-GG**, **QM-GH**, **QM-GS**, **QM-HG**, and **QM-H-HH$_{biphenyl}$**) were prepared as described above. For the preparation of **QM-HH**, dichloromethane (or dichloromethane-d_2) was used as reaction solvent instead of chloroform, which was due to the limited solubility of a β-O-4 dimer **HH** in chloroform. For all **QM** solutions, any residual NMR peak from β-O-4 model was not found

on their ^{1}H NMR spectrum (**Figure 3.5**).

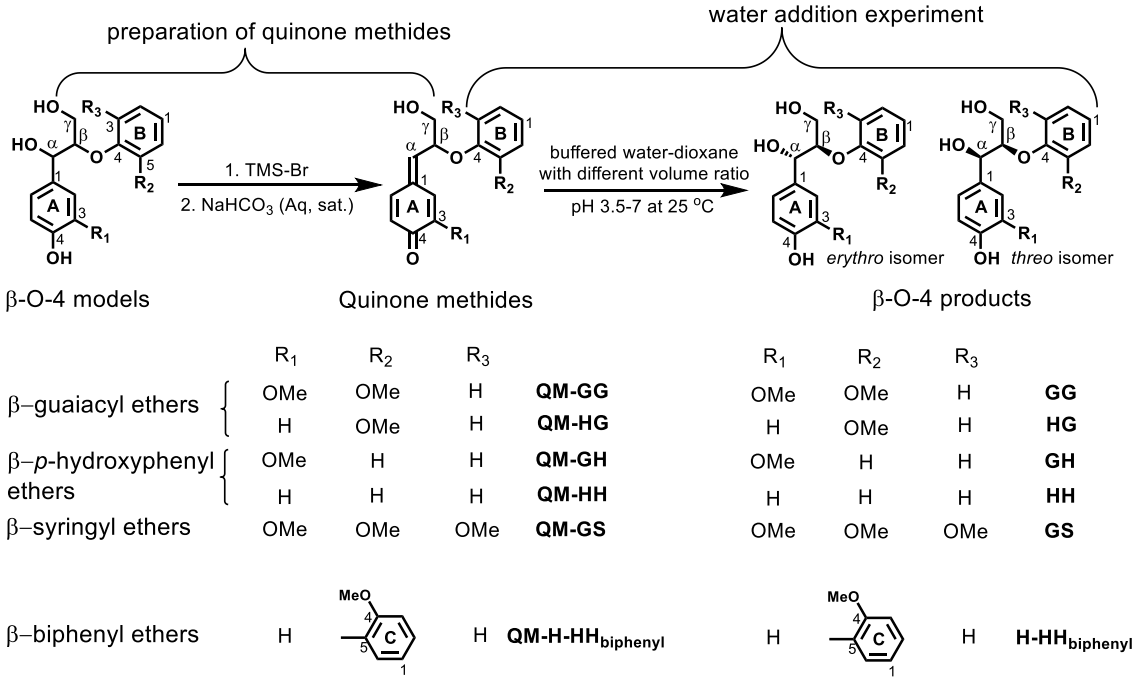

Figure 3.2 Preparation of quinone methide compounds and water addition experiment to the quinone methides to form β-O-4 products obtained as a mixture of *erythro* and *threo* isomers. The letters **H**, **G**, and **S** are used to designate the *p*-hydroxyphenyl, guaiacol, and syringyl nature of the aromatic rings, respectively. As shown in β-O-4 products, we also refer to the **A** and **B**-**rings** for aromatic ring of the phenylpropanoid skeleton and β-etherified aromatic ring, respectively (e.g. compound **GH** has a **G**-type of **A-ring** and an **H**-type of **B-ring**). Quinone methide compounds also have two rings that are labeled as **A** for quinone methide moiety and **B** for β-etherified aromatic ring. Quinone methide moiety was also categorized as **H**, **G**, and **S**-type based on the type of **A-ring** of the corresponding β-O-4 products (e.g. compound **QM-GH** has a **G**-type quinone methide moiety (**A-ring**) and a **H**-type of **B-ring**; compound **QM-H-HH$_{biphenyl}$** has a **H**-type quinone methide moiety (**A-ring**) and a **biphenyl**-type of **B-ring**)

Compound **QM-GG** (mixture of *syn*- and *anti*-isomers (7:3)): ^{1}H NMR ($CDCl_3$, 500 MHz), δ_H: *syn*-isomer, 3.72 (3H, s, A3-OMe), 3.83 (1H, broad-dd, J = 12, 3 Hz, γ_1), 3.87 (3H, s, B3-OMe), 3.94 (1H, br-dd, J = 12, 7 Hz, γ_2), 5.16 (1H, m, β), 6.31 (1H, d, J = 8.3 Hz, α), 6.42 (1H, d, J = 9.5 Hz, A5), 6.49 (1H, d, J = 2.0 Hz, A2), 6.85-6.87 (2H, m, B5 and B6), 6.92 (1H, d, J = 8.0 Hz, B2), 7.02 (1H, m, B1), 7.02 (1H, m, A6); anti-isomer, 3.75 (3H, s, A3-OMe), 3.78 (1H, m, γ_1), 3.87 (3H, s, B3-OMe), 3.88 (1H, m, γ_2), 5.19 (1H, m, β), 6.24 (1H, br-d, J = 2 Hz, A2), 6.42 (1H, m, α), 6.44 (1H, br-d, J = 10 Hz, A5), 6.85-6.87 (2H, m, B5 and B6), 6.92 (1H, d, J = 8.0 Hz, B2), 7.02 (1H, m, B1), 7.42 (1H, br-dd, J = 10, 2 Hz, A6). 13C NMR ($CDCl_3$, 125 MHz) δ_C: *syn*-isomer, 55.3 (A3-OMe), 55.8 (B3-

OMe), 64.6 (γ), 79.6 (β), 103.9 (A2), 112.2 (B2), 118.6 (B5), 121.2 (B6), 123.7 (B1), 128.3 (A5), 133.9 (A1), 141.1 (α), 141.3 (A6), 146.6 (B4), 150.5 (B3) 153.3 (A3), 181.0 (A4); anti-isomer, 55.2 (A3-OMe), 55.8 (B3-OMe), 65.0 (γ), 79.3 (β), 111.6 (A2), 112.2 (B2), 119.0 (B5), 121.2 (B6), 123.9 (B1), 129.6 (A5), 132.5 (A6), 133.7 (A1), 141.1 (α), 146.5 (B4), 150.5 (B3), 152.5 (A3), 181.3 (A4). Stereochemical assignments (*syn*- or *anti*-isomer) were made by the comparison with the reported data of the same compounds,[15] typically the chemical shift data of A2, A6, and A3-OMe protons.

Compound QM-GH (mixture of *syn*- and *anti*-isomers, major and minor isomers ratio = 6:4): ^{1}H NMR ($CDCl_3$, 500 MHz), δ_H: **major isomer**, 3.77 (3H, s, A3-OMe), 3.88 (1H, broad-dd, *J* = 12, 4 Hz, γ_1), 3.98 (1H, br-dd, *J* = 12, 7 Hz, γ_2), 5.31 (1H, m, β), 6.22 (1H, d, *J* = 8.6 Hz, α), 6.40 (1H, d, *J* = 9.5 Hz, A5), 6.59 (1H, s, A2), 6.88 (2H, br-d, *J* = 8 Hz, B3 and B5), 6.98 (1H, m, B1), 6.99 (1H, m, A6), 7.26 (2H, br-t, *J* = 8 Hz, B2 and B6); **minor isomer**, 3.73 (3H, s, A3-OMe), 3.85 (1H, br-dd, *J* = 12, 4 Hz, γ_1), 3.95 (1H, br-dd, *J* = 12, 7 Hz, γ_2), 5.35 (1H, m, β), 6.21 (1H, s, A2), 6.31 (1H, d, *J* = 8.6 Hz, α), 6.50 (1H, br-d, *J* = 10 Hz, A5), 6.88 (2H, br-d, *J* = 9 Hz, B3 and B5), 6.98 (1H, m, B1), 7.26 (2H, br-t, *J* = 9 Hz, B2 and B6), 7.54 (1H, br-d, *J* = 10 Hz, A6).^{13}C NMR ($CDCl_3$, 125 MHz) δ_C: **major isomer**, 55.4 (A3-OCH_3), 64.7 (γ), 76.5 (β), 103.7 (A2), 115.8 (B3 and B5), 122.1 (B1), 128.2 (A5), 129.7 (B2 and B6), 134.0 (A1), 141.2 (A6), 141.7 (α), 153.4 (A3), 157.3 (B4), 181.0 (A4); **minor isomer**, 55.2 (A3-OMe), 65.2 (γ), 76.1 (β), 111.5 (A2), 115.9 (B3 and B5), 122.0 (B1), 129.7 (B2 and B6), 129.8 (A5), 132.4 (A6), 133.9 (A1), 141.8 (α), 152.4 (A3), 157.2 (B4), 181.2 (A4).

Compound QM-GS (mixture of *syn*- and *anti*-isomers, major and minor isomers ratio = 7:3): ^{1}H NMR ($CDCl_3$, 500 MHz), δ_H: **major isomer**, 3.72 (3H, s, A3-OMe), 3.75 (2H, broad-d, *J* = 4 Hz, γ), 3.82 (6H, s, B3-OMe and B5-OMe), 5.07 (1H, m, β), 6.43 (1H, br-d, *J* = 10 Hz, A5), 6.56 (1H, d, *J* = 8.6 Hz, α), 6.58 (1H, br-d, *J* = 2 Hz, A2), 6.59 (1H, br-d, *J* = 8 Hz, B2 and B6), 7.04 (1H, br-t, *J* = 8 Hz, B1), 7.09 (1H, br-dd, *J* = 10, 2 Hz, A6); **minor isomer**, 3.77 (3H, s, A3-OMe), 3.75 (2H, br-d, *J* = 4 Hz, γ), 3.82 (6H, s, B3-OMe and B5-OMe), 5.09 (1H, m, β), 6.30 (1H, br-d, *J* = 2 Hz, A2), 6.43 (1H, br-d, *J* = 10 Hz, A5), 6.58 (1H, br-d, *J* = 8 Hz, B2 and B6), 6.65 (1H, d, *J* = 8.9 Hz, α), 7.03 (1H, br-t, *J* = 8 Hz, B1), 7.51 (1H, br-dd, *J* = 2, 10 Hz, A6). ^{13}C NMR ($CDCl_3$, 125 MHz) δ_C: **major isomer,** 55.1 (A3-OMe), 56.0 (B3-OMe and B5-OMe), 64.1 (γ), 80.4 (β), 104.6 (A2), 105.2 (B2 and B6), 124.8 (B1), 128.2 (A5), 133.2 (A1), 134.9 (B4), 141.7 (α), 141.9 (A6), 153.0 (A3), 153.3 (B3 and B5), 181.2

(A4); **minor isomer,** 55.2 (A3-OMe), 56.1 (B3-OMe and B5-OMe), 64.3 (γ), 79.8 (β), 105.2 (B2 and B6), 112.0 (A2), 124.7 (B1), 129.1 (A5), 133.3 (A6), 133.4 (A1), 134.8 (B4), 141.3 (α), 152.5 (A3), 153.3 (B3 and B5), 181.4 (A4).

Compound QM-HG: ^{1}H NMR ($CDCl_3$, 500 MHz), δ_H: 3.82 (1H, dd, *J* = 12.1, 4.0 Hz, γ_1), 3.87 (3H, s, B3-OMe), 3.91 (1H, dd, *J* = 12.1, 6.9 Hz, γ_2), 5.19 (1H, m, β), 6.38 (1H, broad-d, *J* = 10 Hz, A3), 6.40 (1H, br-d, *J* = 12 Hz, A5), 6.53 (1H, d, *J* = 8.6 Hz, α), 6.85-6.87 (2H, m, B5 and B6), 6.92 (1H, d, *J* = 8.0 Hz, B2), 7.03 (1H, m, B1), 7.10 (1H, br-dd, *J* = 10, 2 Hz, A2), 7.47 (1H, br-dd, *J* = 10, 2 Hz, A6). ^{13}C NMR ($CDCl_3$, 125 MHz) δ_C: 55.8 (B3-OMe), 64.8 (γ), 79.5 (β), 112.2 (B2), 119.1 (B5), 121.2 (B6), 124.1 (B1), 129.3 (A3), 130.4 (A5), 133.2 (A1), 133.2 (A6), 141.6 (A2), 144.6 (α), 146.5 (B4), 150.8 (B3), 187.0 (A4).

Compound QM-HH: ^{1}H NMR (CD_2Cl_2, 500 MHz), δ_H: 3.85 (1H, dd, *J* = 12.1, 4.0 Hz, γ_1), 3.95 (1H, dd, *J* = 12.1, 6.6 Hz, γ_2), 5.34 (1H, m, β), 6.33 (1H, broad-dd, *J* = 10, 2 Hz, A3), 6.42 (1H, br-dd, *J* = 10, 2 Hz, A5), 6.45 (1H, d, *J* = 8.9 Hz, α), 6.90 (2H, br-dd, *J* = 7, 1 Hz, B3 and B5), 6.98 (1H, br-td, *J* = 7, 1 Hz, B1), 7.10 (1H, br-dd, *J* = 10, 3 Hz, A2), 7.27 (2H, br-t, *J* = 7 Hz, B2 and B6), 7.61 (1H, br-dd, *J* = 10, 3 Hz, A6). ^{13}C NMR (CD_2Cl_2, 125 MHz) δ_C: 65.4 (γ), 76.8 (β), 116.5 (B3 and B5), 122.5 (B1), 129.5 (A3), 130.3 (B2 and B6), 130.9 (A5), 133.9 (A6), 134.0 (A1), 142.0 (A2), 146.1 (α), 158.0 (B4), 187.3 (A4).

Compound QM-H-HH$_{\text{biphenyl}}$: ^{1}H NMR ($CDCl_3$, 500 MHz), δ_H: 3.68 (2H, m, γ), 3.77 (3H, s, C4-OMe), 5.25 (1H, m, β), 6.33 (1H, d, *J* = 7.2 Hz, α), 6.37 (1H, broad-dd, *J* = 10, 2 Hz, A3), 6.40 (1H, br-dt, *J* = 10, 2 Hz, A5), 6.84 (1H, br-d, *J* = 8 Hz, B3), 7.00 (1H, br-dd, *J* = 10, 2 Hz, A2), 7.04 (1H, br-d, *J* = 8 Hz, C3), 7.08 (2H, br-t, *J* = 7 Hz, B1 and C1), 7.23 (1H, br-dd, *J* = 7, 2 Hz, C6), 7.26 (1H, br-dd, *J* = 7, 2 Hz, B6), 7.28 (1H, m, B2), 7.38 (1H, br-td, *J* = 7, 8, 2 Hz, C2), 7.46 (1H, br-dd, *J* = 10, 2 Hz, A6). ^{13}C NMR ($CDCl_3$, 125 MHz) δ_C: 56.5 (C4-OMe), 64.6 (γ), 77.4 (β), 112.2 (C3), 114.1 (B3), 121.4 (C1), 122.2 (B1), 128.0 (B5 and C5), 128.9 (A3), 129.1 (B2 and C2), 130.4 (A5), 131.5 (C6), 131.8 (B6), 133.0 (A1), 133.1 (A6), 141.5 (A2), 144.9 (α), 154.7 (B4), 156.6 (C4), 186.9 (A4).

3.2.3 General procedure for water addition to quinone methides[3]

Method 1, water addition to quinone methides in different pH condition

As shown in **Figure 3.2**, a dioxane solution of **QM** described above (approx. 0.1 mM×3ml, originating from 0.3 μmol of β-O-4 models) was placed in a 14 mL screw vial. To the **QM** solution, citrate-phosphate buffer at pH 2.4, 3.2, 3.9, 4.5, or 5.3 (3 ml) was added to start the reaction with water. This was the reaction time of 0 second. After immediately shaking the reaction mixture for few seconds to make the mixture homogeneous, an aliquot of the mixture (approx. 3 mL) was transferred in a quartz UV cell (1 cm square, TOS-UV-10, TOSHIN RIKO CO., LTD, Japan), and was placed in a UV-Visible spectrometer (Jasco V-660 model, Jasco International Co. Ltd, Tokyo, Japan) equipped with a circulating water bath (cooling-circulator CB-15, Iuchi Seieido Co. Ltd., Japan). The reaction mixture was maintained at 25°C, and the monitoring of the reaction progress was started at the reaction time of 20 sec. The citrate-phosphate buffers mentioned above were prepared by mixing 0.01 M citric acid and 0.02 M disodium phosphate in different proportions so that, after mixing with an equal volume of dioxane, the resulting buffered dioxane-water mixture (1:1, v/v) indicates the desired pH value (3.5, 4.5, 5.5, 6.0, and 7.0, respectively).

Disappearance of quinone methides and their half-life ($t_{1/2}$) in buffered dioxane-water was determined based on the decrease in UV absorbance.[2, 16, 17] The absorbance data at 304 nm was collected every 1 sec from the reaction time of 20 sec to 120 min for **QM-GG**, **-GH**, and **-GS**, and every 0.2 sec from the reaction time of 20 sec to 10 min for **QM-HG**, and **-HH**. The collected data was fitted by an exponential function to estimate the UV absorbance at reaction time of 0 sec ($Abs_{initial}$). The gram extinction coefficient of the **QM** at 304 nm was calculated with the $Abs_{initial}$. (See **Table 3.2** and **3.3** for the $Abs_{initial}$ values and pseudo-first-order reaction rate constants (k_{obs}) for the disappearance of the quinone methides.)

The disappearance of **QM-H-HH$_{biphenyl}$** was difficult to monitor by measuring the absorbance data at a specific wave number. The disappearance of **QM-H-HH$_{biphenyl}$** was judged based on the

decrease of absorbance band from 300 nm to 350 nm because the peak of **QM-H-HH$_{biphenyl}$** was overlapped with the shoulder of the peak of **QM-H-HH$_{biphenyl}$**. Thus, the half-life ($t_{1/2}$) could not be determined.

Method 2, Water addition to quinone methides in different water-dioxane ratio

A dioxane solution of **QMs** described above (approx. 0.8 mM×75μml, originating from 0.6 μmol of β-O-4 models) was diluted with dioxane to a desired volume in a 14 mL screw vial. To this **QM** solutions, different volumes of citrate-phosphate buffer at certain pH were added to start the water addition reaction. These citrate-phosphate buffers were prepared by mixing 0.01 M citric acid and 0.02 M disodium phosphate in different proportions so that, after mixing with different volume of the dioxane, the resulting buffered dioxane-water mixture indicates different dioxane to water volume ratios (1:79, 1:7, 1:5, 1:1.5, 1:1, v/v) with the same pH value (3.5, 5, or 7, respectively). Then, the work-up was same as those above described for water addition to **QMs** in different pH condition.

Work-up on quantification of the water addition reaction products

The precise concentrations of the prepared **QM** were not determined because these **QMs** were not stable enough to be purified and weighted. However, their ^{1}H-NMR spectra indicated that each crude **QM** solution was essentially pure and contains only tiny unknown products other than the peaks for **QM**. Any residual starting material (β-O-4 model) was not found on the ^{1}H NMR spectra of all the crude **QM** solutions (**Figure 3.5**). Thus, as shown in **Table 3.3** and **3.4**, the β-O-4 products yield was expressed as the yield of the successive reaction consisting of the **QM** formation (from β-O-4 dimers to **QM**) and water addition (from **QM** to β-O-4 isomers product).

The amount of the *erythro* and *threo* β-O-4 compounds in the crude products of the water addition experiments was determined by HPLC analyses. After **QM** completely disappeared, an aliquot of the reaction mixture (2 mL) was mixed with an internal standard (**IS**) of 3,4-dimethoxyacetophenone (0.1 μmol) in MeOH, and passed through a hydrophilic PTFE membrane filter (Millex-LG, 0.2 um, Millipore). The reaction mixture was analyzed by a high performance liquid chromatograph (HPLC, LC-10A, Shimadzu Co., Kyoto, Japan) equipped with an SPD-M10A detector (280 nm, Shimadzu

Co.).

The conditions for the HPLC analysis were as follows:

Column, Luna 5u C18 (2) 100 A (150 mm × 4.6 mm, Phenomenex, Inc., Torrance, CA, USA); Oven temperature, 40 °C; Eluent, degassed HPLC grade distilled water and MeOH; Flow rate, 1.0 mL min^{-1}; Analysis time, 55 min; Injected volume, 20 μl; UV response at 280 nm.

The HPLC analysis solvent system for the β-O-4 products and their corresponding calibration curves are shown in **Table 3.1**:

Table 3.1 HPLC analysis method for the water addition reaction products, for calibration curve, Y is the molar ratio of each β-O-4 model to **IS**, and X is the peak area of each β-O-4 model to **IS** (e.g., **GG** /**IS** area ratio)

β-O-4 compound	binary gradient system in HPLC	retention time for isomers and IS	calibration curves for isomers
GG	initially MeOH/H_2O (v/v) 15/85, linear over 7.5 min to 25/75, linear over 42.5 min to 35/65 (total 55 min), following an equilibration step	*erythro*: 35.8 min *threo*: 38.8 min IS: 32.4 min	Y = 2.54967X + 0.05788 (*erythro*) Y = 2.37517X + 0.04849 (*threo*)
GH	initially MeOH/H_2O (v/v) 15/85, linear over 7.5 min to 25/75, linear over 42.5 min to 35/65 (total 55 min), following an equilibration step	*erythro*: 30.0 min *threo*: 27.5 min IS: 32.4 min	Y = 3.61582X + 0.02191 (*erythro*) Y = 3.30723X + 0.0462 (*threo*)
GS	initially MeOH/H_2O (v/v) 15/85, linearly over 7.5 min to 25/75, linearly over 27.5 min to 35/65, linearly over 15 min to 75/25 (total 55 min)	*erythro*: 39.2 min *threo*: 42.1 min IS: 27.1 min	Y = 3.5562X + 0.02439 (*erythro*) Y = 3.42298X + 0.01349 (*threo*)
HG	initially MeOH/H_2O (v/v) 15/85, held isocratically for 7.5 min, linear over 27.5 min to 25/75, linear over 15 min to 35/65 (total 55 min)	*erythro*: 46.0 min *threo*: 46.8 min IS: 44.8 min	Y = 3.86212X – 0.0123 (*erythro*) Y = 3.61194X + 0.02683 (*threo*)

HH	initially MeOH/H_2O (v/v) 15/85, linear over 7.5 min to 25/75, linear over 42.5 min to 35/65 (total 55 min), following an equilibration step	*erythro*: 27.0 min *threo*: 24.6 min IS: 32.4 min	Y = 6.50908X + 0.06459 (*erythro*) Y = 6.76556X + 0.06014 (*threo*)
H-HH$_{biphenyl}$	initially MeOH/H_2O (v/v) 15/85, linear over 7.5 min to 45/55, linear over 27.5 min to 75/25, linear over 15 min to 90/10 (total 55 min), following an equilibration step	*erythro*: 21.7 min *threo*: 22.8 min IS: 13.2 min	Y = 1.92978X + 0.00819 (*erythro*) Y = 1.83235X + 0.02575 (*threo*)

3.3 Results and discussion

3.3.1 General description

A lignin model study using a β-O-4 bonded **QM** compound has been developed by Nakatsubo et al.[2] Since then, such studies have been conducted for many purposes, including the studies on the reactivity of **QMs** towards different nucleophiles,[2, 18-20] and the characterization of the *syn* and *anti* geometric isomers of 3-methoxy-substituted (**G**-type) **QM**.[21-23] The β-O-4 bonded **QM** has been used to synthesize novel lignin model compounds for lignin-carbohydrate complex (**LCC**) linkages,[24-27] dibenzodioxocin,[28] and anthrahydroquinone adducts.[29, 30]

The reaction condition of the water addition experiments to **QM** was modified by Brunow et al.[3] to be more suitable for mimicking the rearomatization step in lignin biosynthesis, and then, applied to **G**-type and 3,5-dimethoxy-substituted (**S**-type) **QMs** as the biosynthetic study of hardwood lignin. We conducted similar in vitro experiments using non-substituted (**H**-type) **QMs** basically according to the Brunow's method,[3] for mimicking the formation of β-O-4 structures in softwoods, especially in their compression wood.

Brunow et al.[3] prepared three types of β-O-4 bonded **QMs** (**QM-GG**, **QM-GS**, and **QM-SS** in **Figure 3.2**) from corresponding β-O-4 dimer models: **GG**, **GS**, and **SS**, respectively. The water addition experiments were conducted in a buffered 1:1 dioxane-water solution at a wide range of pH conditions with (pH 3-7). The *erythro*/*threo* ratios of the resultant β-O-4 dimers were higher in the

order of **SS** > **GS** > **GG** at pH 3 (the ratio was 3 for **SS**, 2 for **GS**, and 1 for **GG**). In contrast, at pH 4-7 conditions, *threo*-preferential formation was observed for the **GG** and **GS** types and no water adducts was found in the **SS** type products. The stereo-structural feature of β-O-4-structures in hardwood lignin was in line with the experimentally observed *erythro*-preferential formation at pH 3. Also, Nakatsubo et al.[2] did water addition reaction to **QM-GG** in different solvent. It was found that the *erythro*/*threo* ratio of the resultant **GG** products was influenced by difference of solvent, e.g. the amount of *erythro* isomers are higher than *threo* isomers in the case of chloroform, whereas in water-dioxane solvent mixture *threo* isomers tend to be produced more than *erythro* ones. Furthermore, the *erythro*/*threo* ratio was obtained about 0.5 in dioxane-water solution (1:9) and 0.4 in dioxane-water solution (1:1), respectively.

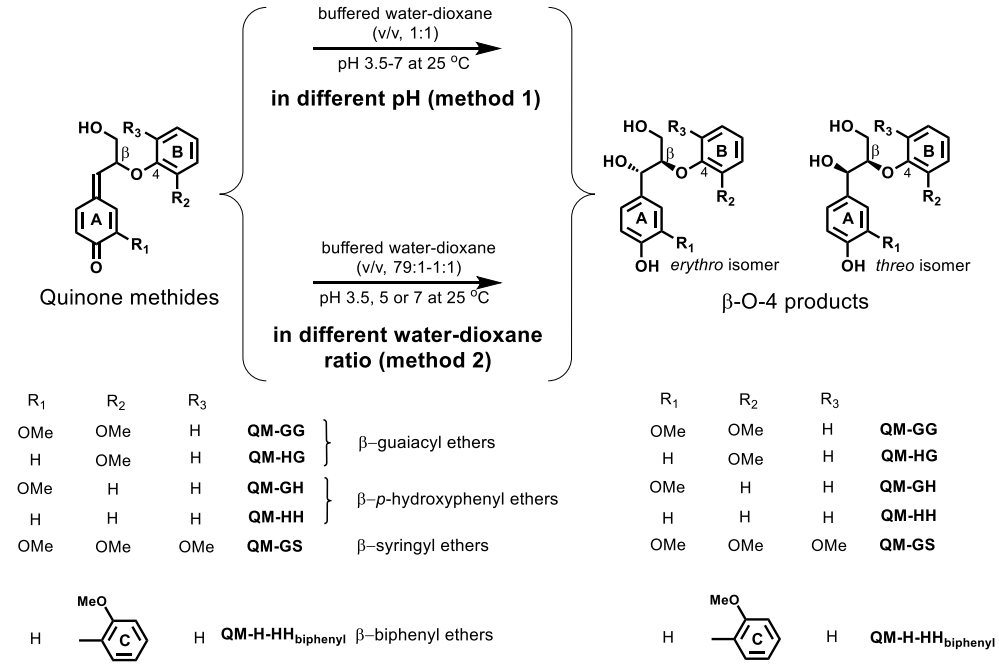

Figure 3.3 Water addition experiment in different pH and dioxane-water ratio to yield a mixture of *erythro* and *threo* isomers of β-O-4 products

We newly prepared four **QMs**, **QM-GH, -HG, -HH, and -H-HH$_{biphenyl}$** (**Figure 3.2**), from corresponding **H**-type β-O-4 model compounds: **GH**, **HG**, **HH**, and **H-HH$_{biphenyl}$**, respectively. The **QMs**, **QM-GG** and **QM-GS**, were also prepared, and subjected to the water addition experiments in different reaction condition by varying pH and dioxane-water ratio (**Figure 3.3**). Their results were

thus compared with the previous results by Nakatsubo et al. [2] and Brunow et al.[3]

The β-O-4 bonded **QMs** (**QM-GG**, **-GH**, **-GS**, **-HG**, **-HH**, or **-H-HH$_{biphenyl}$**) were allowed to react with water in the different ratio of buffered dioxane-water solution at 25°C under neutral and mild acidic conditions at pH of 3.5 to 7 (**Figure 3.3**). The reaction progress was monitored by UV absorbance at 304 nm except for **QM-H-HH$_{biphenyl}$,** which was based on the disappearance of absorbance band from 300 nm to 350 nm. **Figure 3.3** shows the spectral changes of **QMs** along the reaction time. Disappearance of the **QMs** was determined on the basis of the decrease in the absorbance at 304 nm. The β-O-4 products appeared, which can be recognized with the absorbance peaks at around 273-279 nm (see **Figure 3.4** and **Table 3.2**), but could not be quantified by UV because of the overlapping of the absorbance peak of β-O-4 products with the shoulder of intensive peak of **QMs** at this wavelength. Thus, the β-O-4 products yield was determined by the HPLC analysis, separately. The β-O-4 products yield was expressed as the yield of the successive two steps reaction consisting of the **QM** formation (from β-O-4 model to **QM**) and water addition (from **QM** to water adduct, i.e. β-O-4 products). This is due to the difficulty in the determination of the precise concentrations of the prepared **QMs** that were not stable enough to be purified and weighed. Their ^{1}H-NMR spectra indicated that each crude **QM** solution was essentially pure and contains only tiny amount of unknown products other than the peaks for **QM**. Any residual β-O-4 model, starting material, was not found on the ^{1}H NMR spectra of all the crude **QM** solutions (**Figure 3.5**). These data of β-O-4 product yield were used only for judging whether the water adducts (*erythro* and *threo* β-O-4 products) were obtained as the major products in this reaction, and were not used to draw any other conclusion.

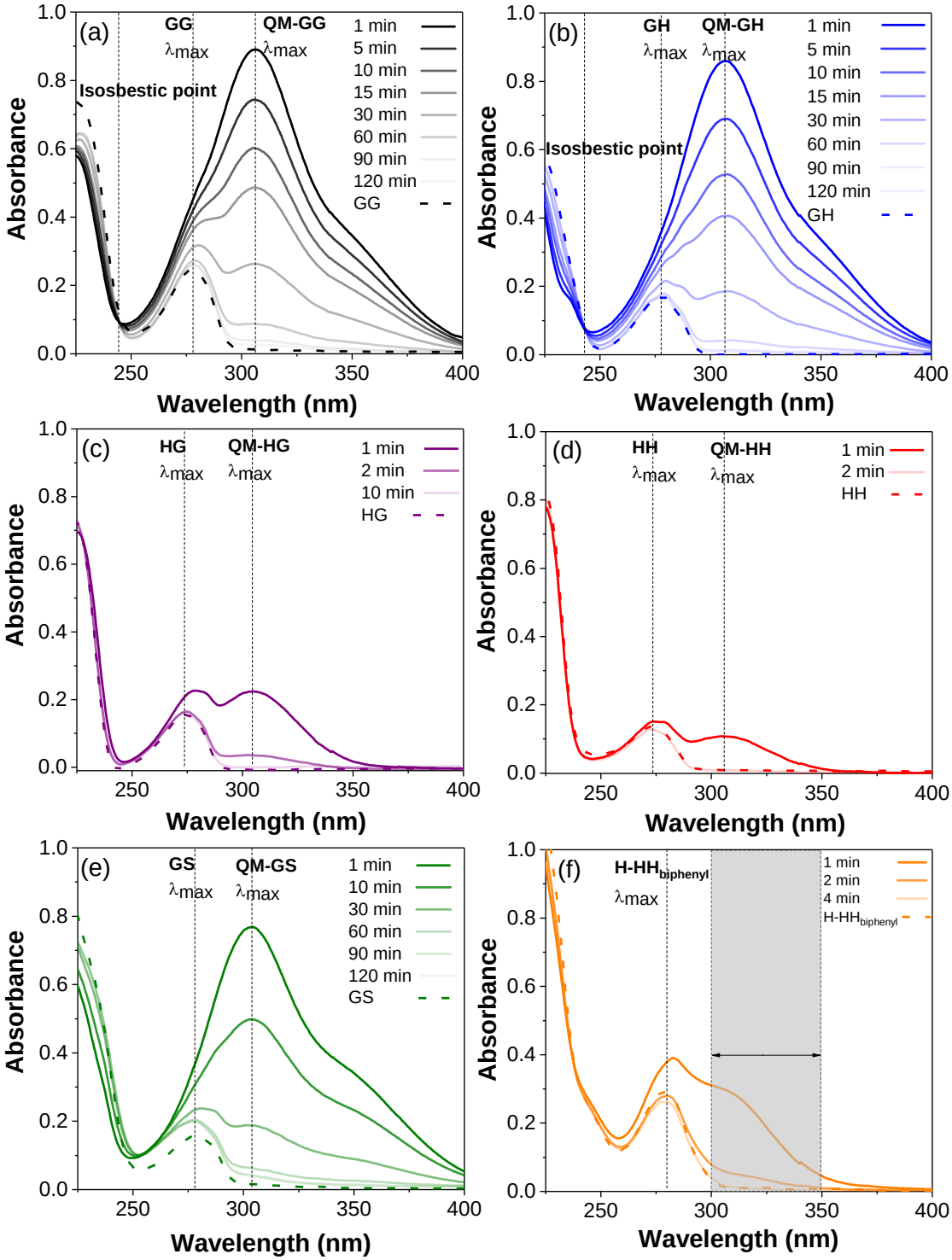

Figure 3.4 Changes in UV absorbance spectra of quinone methides in a buffered dioxane-water (1:1, v/v, pH = 7) at 25°C. a) **QM-GG**; b) **QM-GH**; c) **QM-HG**; c) **QM-HH**; e) **QM-GS**; and f) **QM-H-HH$_{biphenyl}$.**

Table 3.2 UV absorbance and specific absorption coefficient of lignin model compounds in a buffered dioxane-water (1:1, v/v, pH = 7) at 25°C.

compound		
quinone methide	$\lambda_{max.}$[a] (nm)	$\varepsilon_{304\ nm}$[b] ($g^{-1}Lcm^{-1}$)
QM-HH	306	92.8
QM-HG	304	81.5
QM-GH	307	68.4
QM-GG	306	61.2
QM-GS	304	49.9
QM-H-HH$_{biphenyl}$	NA[c]	NA[c]
β-O-4 model	$\lambda_{max.}$[a] (nm)	ε_{max}[d] ($g^{-1}Lcm^{-1}$)
HH	273	8.8
HG	276	12.1
GH	279	12.2
GG	278	15.7
GS	278	9.6
H-HH$_{biphenyl}$	279	16.0

[a]Wavelength of maximum absorbance

[b]Gram extinction coefficient of quinone methides at 304 nm are estimated from the UV absorbance data which was started collecting at the reaction time of 20 seconds. (See experimental section and **Table 3.3**).

[c]Not available. A reliable UV absorbance peak was not obtained.

[d]Gram extinction coefficient at λ_{max}.

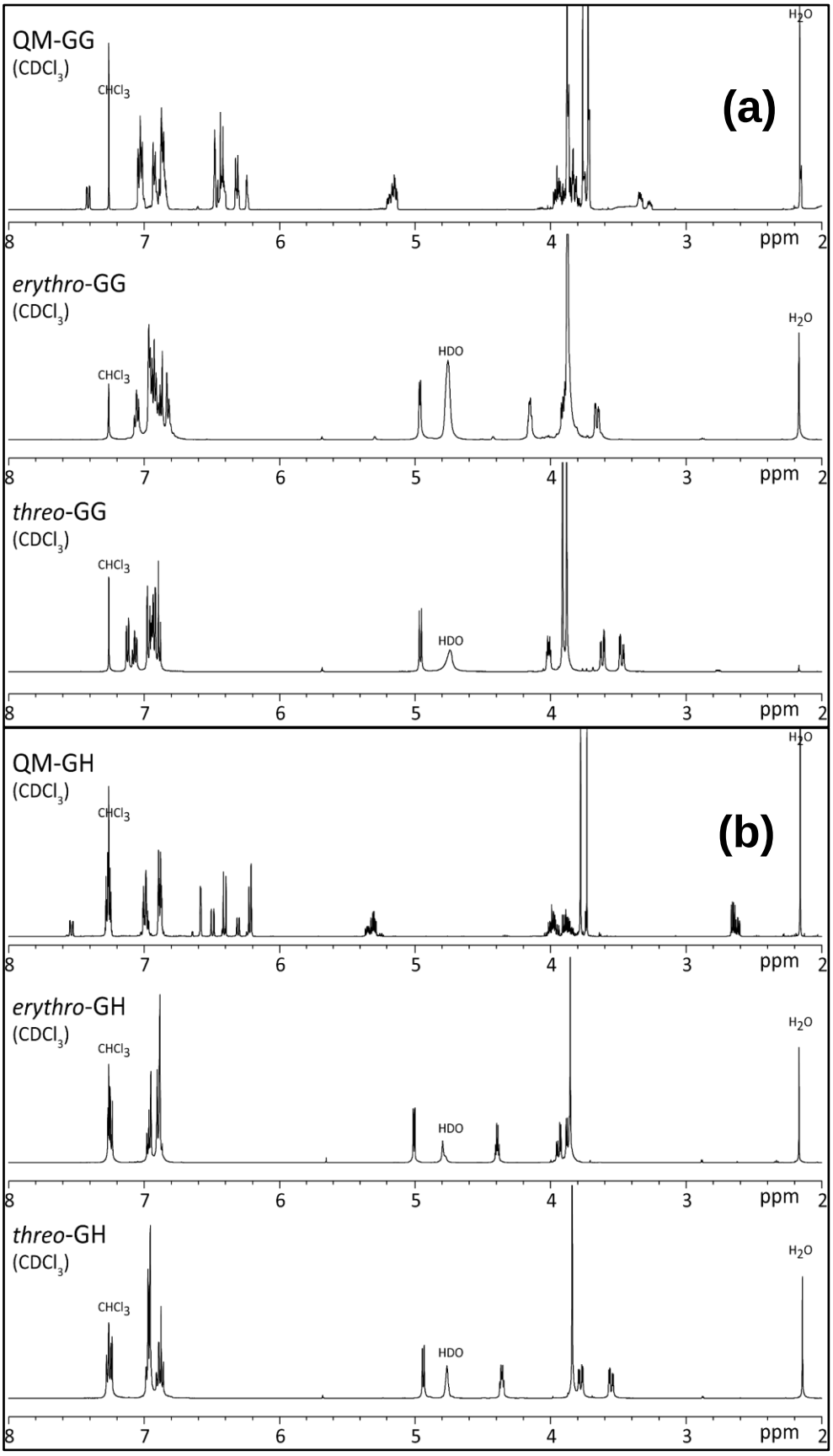
QM-GG
(CDCl3)
CHCl3
H2O
(a)
8
7
6
5
4
3
ppm
2
erythro-GG
(CDCl3)
CHCl3
HDO
H2O
threo-GG
(CDCl3)
CHCl3
HDO
QM-GH
(CDCl3)
CHCl3
H2O
(b)
erythro-GH
(CDCl3)
CHCl3
HDO
H2O
threo-GH
(CDCl3)
CHCl3
HDO
H2O

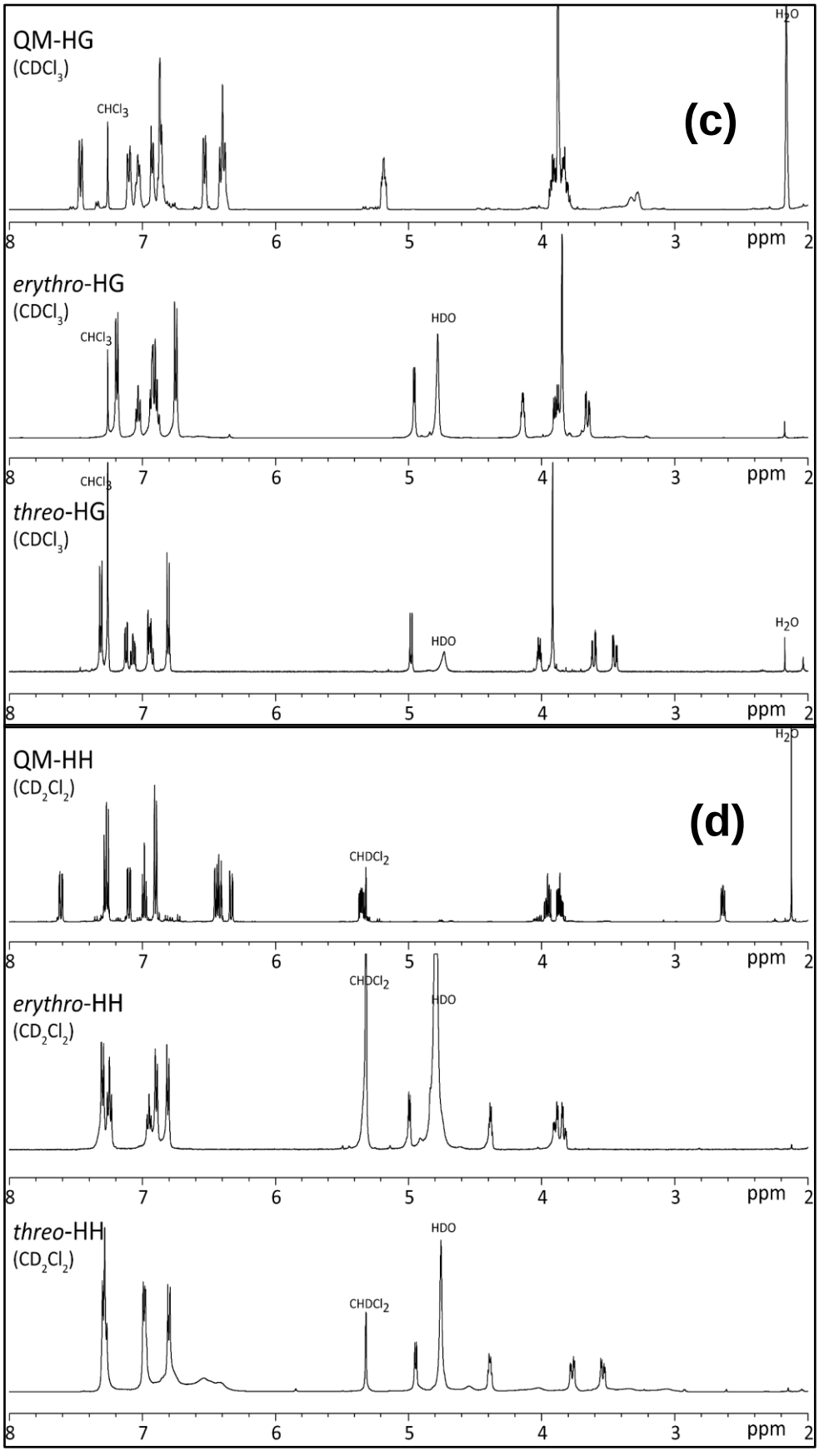
QM-HG
(CDCl3)
CHCl3
H2O
(c)
8
7
6
5
4
3
ppm
2
erythro-HG
(CDCl3)
CHCl3
HDO
threo-HG
(CDCl3)
CHCl3
HDO
H2O
QM-HH
(CD2Cl2)
H2O
(d)
CHDCl2
erythro-HH
(CD2Cl2)
CHDCl2
HDO
threo-HH
(CD2Cl2)
HDO
CHDCl2

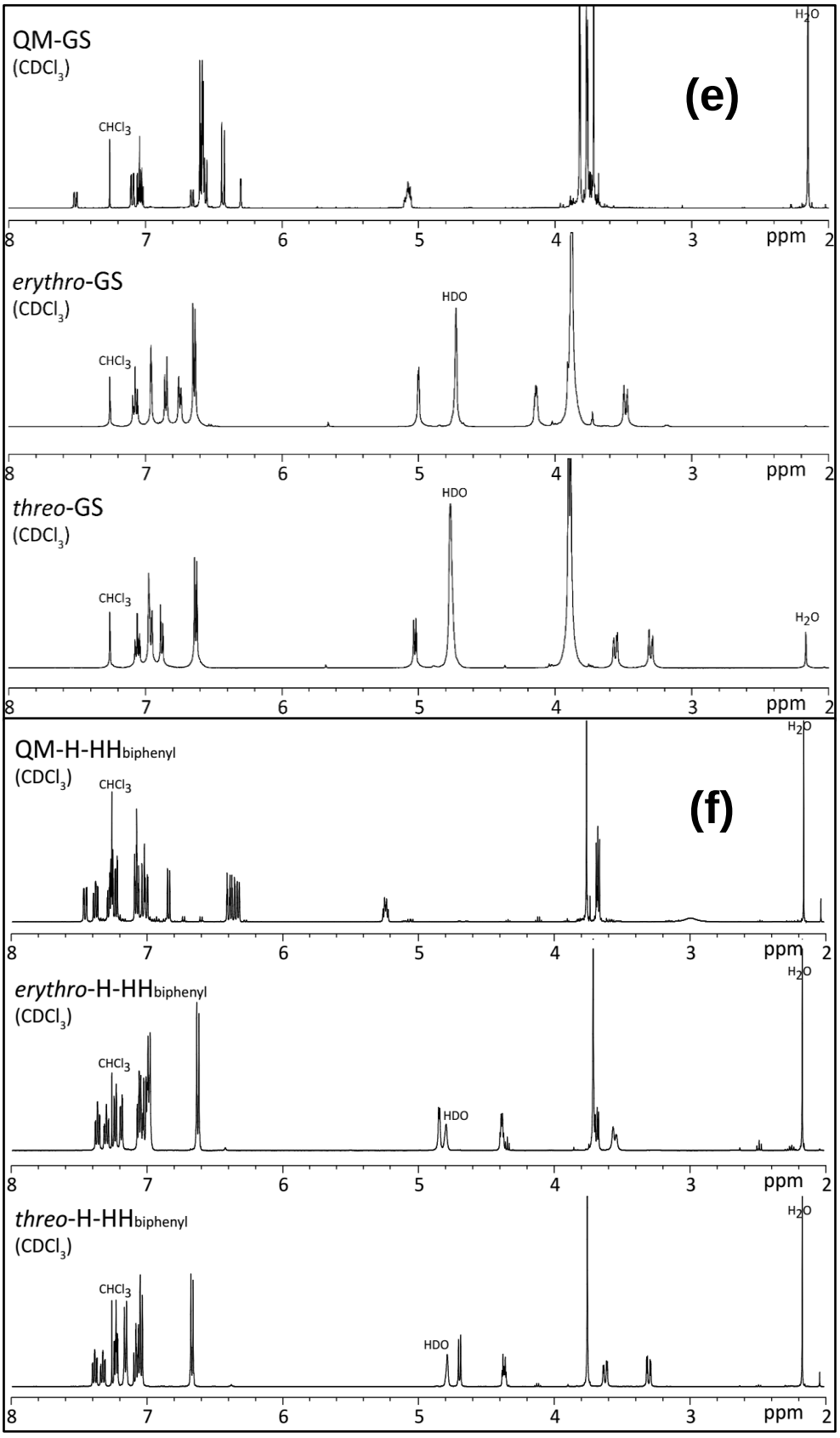

Figure 3.5 Aligned [1]H-NMR spectra of quinone methide and the *erythro*/*threo* isomers of β-O-4 models

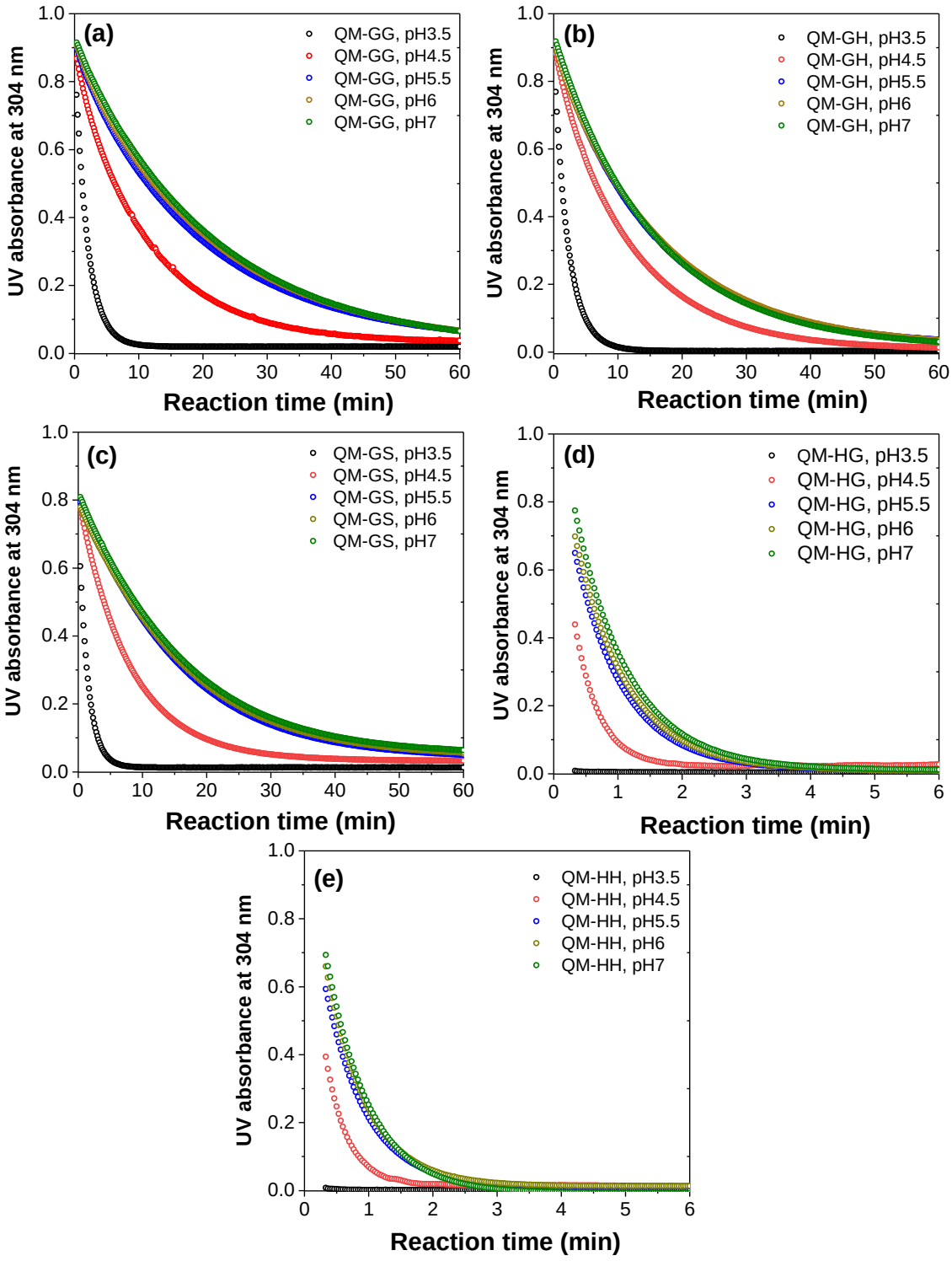

Figure 3.6 Disappearance of quinone methides in buffered dioxane-water (1:1, v/v) at 25°C under the pH condition of 3.5, 4.5, 5.5, 6, or 7. a) **QM-GG**; b) **QM-GH**; c) **QM-GS**; d) **QM-HG**; and e) **QM-HH**. Absorbance at 304 nm was monitored.

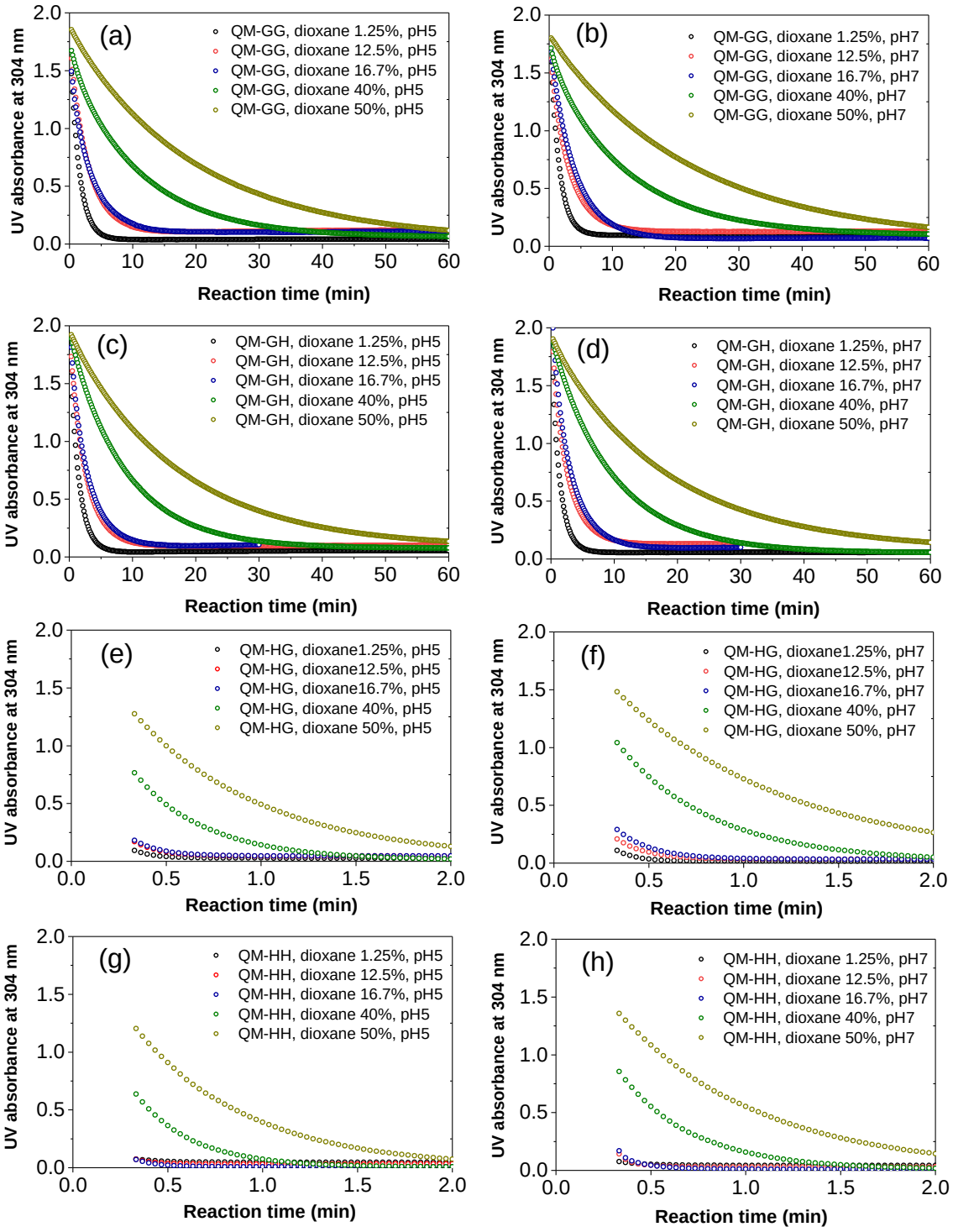

Figure 3.7 Disappearance of quinone methides in different buffered dioxane-water (1:79, 1:7, 1:5, 1:1.5, 1:1, v/v) at 25°C under the pH condition of 5 or 7. a) **QM-GG** at pH5; b) **QM-GG** at pH7; c) **QM-GH** at pH5; d) **QM-GH** at pH7; e) **QM-HG** at pH5; f) **QM-HG** at pH7; g) **QM-HH** at pH5; and h) **QM-HH** at pH7. Absorbance at 304 nm was monitored.

Table 3.3 Pseudo-first-order reaction rate constants (k_{obs}) and half-life (($t_{1/2}$)) for the disappearance of quinone methides in buffered dioxane-water (1:1, v/v) within pH 3.5-7 at 25°C.

entry	pH [a]	k_{obs} [b] ($\times 10^{-4}$ sec^{-1})	$Abs_{initial}$ (calc.)	R^2 [c]	$t_{1/2}$, sec.	Products	Yield (mol%)	E/T
QM-GG	3.5	75.7	0.86	0.99	84	**GG**	83	50/50
	4.5	15.3	0.89	0.99	460	**GG**	76	44/56
	5.5	9.16	0.91	0.99	791	**GG**	71	37/63
	6	8.85	0.92	0.99	850	**GG**	70	35/65
	7	7.93	0.93	0.99	876	**GG**	72	35/65
QM-GH	3.5	70.8	0.87	0.99	90	**GH**	91	36/64
	4.5	15.3	0.90	0.99	461	**GH**	83	30/70
	5.5	10.4	0.92	0.99	651	**GH**	75	28/72
	6	10.4	0.91	0.99	667	**GH**	76	27/73
	7	10.4	0.94	0.99	648	**GH**	73	25/75
QM-HG	3.5	127.0	0.01	0.83	<10	**HG**	87	42/58
	4.5	390.6	0.97	0.99	17	**HG**	86	38/62
	5.5	205.1	1.00	0.99	32	**HG**	77	29/71
	6	195.3	1.05	0.99	34	**HG**	74	28/72
	7	185.6	1.13	0.99	36	**HG**	76	26/74
QM-HH	3.5	371.1	0.01	0.94	11	**HH**	94	30/70
	4.5	429.7	0.95	0.99	15	**HH**	85	29/71
	5.5	253.9	0.99	0.99	17	**HH**	80	24/76
	6	244.1	1.09	0.99	17	**HH**	89	24/76
	7	244.1	1.15	0.99	18	**HH**	83	24/76
QM-GS	3.5	97.7	0.69	0.99	42	**GS**	86	64/36
	4.5	19.5	0.81	0.99	353	**GS**	61	53/47
	5.5	9.46	0.81	0.99	703	**GS**	53	40/60
	6	8.85	0.80	0.99	741	**GS**	49	41/59
	7	9.16	0.83	0.99	738	**GS**	58	36/64
QM-H-HH$_{biphenyl}$	3.5	N. D.[d]	N. D.	N. D.	N. D.	**H-HH$_{biphenyl}$**	93	70/30
	4.5	N. D.	N. D.	N. D.	N. D.	**H-HH$_{biphenyl}$**	82	66/34
	5.5	N. D.	N. D.	N. D.	N. D.	**H-HH$_{biphenyl}$**	76	57/43
	6	N. D.	N. D.	N. D.	N. D.	**H-HH$_{biphenyl}$**	75	56/44
	7	N. D.	N. D.	N. D.	N. D.	**H-HH$_{biphenyl}$**	82	56/44

[a]pH value of the buffered dioxane-water mixture. [b]$\ln(Abs_t) = -k_{obs}t + \ln(Abs_{initial})$, where Abs_t is absorbance at 304 nm at the reaction time of t second, and $Abs_{initial}$ is the absorbance at the reaction time of 0 sec. To estimate the k_{obs} and $Abs_{initial}$ values, absorbance data collected the reaction time of 20–320 sec (for **QM-GG**, **-GH**, and **-GS**), or 20–50 sec (for **QM-HG** and **-HH**) were fitted by an exponential function. [c]Square of correlation coefficient. N. D.[d], No Data.

Table 3.4 Pseudo-first-order reaction rate constants (k_{obs}) and half-life (($t_{1/2}$)) for the disappearance of quinone methides in different buffered dioxane-water ratio (1:79, 1:7, 1:5, 1:1.5, 1:1, v/v at pH 3.5, 5.0 or 7.0) at 25°C.

entry	pH [a]	Dio./ H_2O, (v/v) [b]	k_{obs} [c] ($\times 10^{-4}$ sec^{-1})	$Abs_{initial}$ (calc.)	R^2 [d]	$t_{1/2}$, sec.	Products	Yield (mol%)	E/T
QM-GG	3.5	1/79	212.9	1.77	0.99	47	**GG**	86	49:51
	5.0	1/79	107.4	1.76	0.99	81	**GG**	73	44:56
	5.0	1/7	51.3	1.70	0.99	146	**GG**	63	40:60
	5.0	1/5	46.4	1.57	0.99	157	**GG**	66	40:60
	5.0	1/1.5	17.7	1.70	0.99	448	**GG**	67	39:61
	5.0	1/1	8.9	1.87	0.99	839	**GG**	75	38:62
	7.0	1/79	97.7	1.81	0.99	84	**GG**	76	43:57
	7.0	1/7	48.8	1.70	0.99	150	**GG**	71	39:61
	7.0	1/5	41.5	1.76	0.99	182	**GG**	80	38:62
	7.0	1/1.5	15.9	1.70	0.99	501	**GG**	60	35:65
	7.0	1/1	7.6	1.81	0.99	978	**GG**	74	34:66
QM-GH	5.0	1/79	107.4	1.81	0.99	77	**GH**	81	23:77
	5.0	1/7	61.0	1.87	0.99	126	**GH**	77	25:75
	5.0	1/5	56.2	1.87	0.99	130	**GH**	79	26:74
	5.0	1/1.5	18.9	1.93	0.99	398	**GH**	75	28:72
	5.0	1/1	9.8	1.93	0.99	759	**GH**	74	29:71
	7.0	1/79	107.4	1.76	0.99	72	**GH**	86	23:77
	7.0	1/7	58.6	1.87	0.99	123	**GH**	83	24:76
	7.0	1/5	53.7	2.05	0.99	133	**GH**	81	24:76
	7.0	1/1.5	17.1	1.93	0.99	426	**GH**	68	26:74
	7.0	1/1	9.8	1.93	0.99	795	**GH**	66	27:73
QM-HG	5.0	1/79	NA[e]	NA[e]	NA[e]	28	**HG**	85	31:69
	5.0	1/7	NA[e]	NA[e]	NA[e]	29	**HG**	89	30:70
	5.0	1/5	NA[e]	NA[e]	NA[e]	29	**HG**	84	30:70
	5.0	1/1.5	429.7	1.87	0.99	36	**HG**	83	31:69
	5.0	1/1	234.4	2.05	0.99	49	**HG**	84	31:69
	7.0	1/79	NA[e]	NA[e]	NA[e]	26	**HG**	84	30:70
	7.0	1/7	NA[e]	NA[e]	NA[e]	28	**HG**	90	29:71
	7.0	1/5	NA[e]	NA[e]	NA[e]	29	**HG**	87	28:72
	7.0	1/1.5	332.0	1.99	0.99	41	**HG**	85	27:73
	7.0	1/1	175.8	2.12	0.99	59	**HG**	79	27:73
QM-HH	5.0	1/79	NA[e]	NA[e]	NA[e]	＜20	**HH**	88	20:80
	5.0	1/7	NA[e]	NA[e]	NA[e]	＜20	**HH**	86	21:79
	5.0	1/5	NA[e]	NA[e]	NA[e]	25	**HH**	87	22:78
	5.0	1/1.5	546.9	1.93	0.99	32	**HH**	86	25:75
	5.0	1/1	273.4	2.05	0.99	45	**HH**	87	26:74
	7.0	1/79	NA[e]	NA[e]	NA[e]	＜20	**HH**	87	19:81
	7.0	1/7	NA[e]	NA[e]	NA[e]	24	**HH**	86	20:80
	7.0	1/5	NA[e]	NA[e]	NA[e]	24	**HH**	87	21:79
	7.0	1/1.5	429.7	1.99	0.99	36	**HH**	82	23:77
	7.0	1/1	214.9	2.12	0.99	51	**HH**	78	23:77

[a]pH value of the buffered dioxane-water mixture. [b]the volume ratio of dioxane and water in buffered mixture. [c]$\ln(Abs_t) = -k_{obs}t + \ln(Abs_{initial})$, where Abs_t is absorbance at 304 nm at the reaction time of t second, and $Abs_{initial}$ is the absorbance at the reaction time of 0 sec. To estimate the k_{obs} and $Abs_{initial}$ values, absorbance data collected the reaction time of 20–220 sec (for **QM-GG** and **-GH**), or 20–30 sec (for **QM-HG** and **-HH**) were fitted by an exponential function.[d]Square of correlation coefficient. [e]Not Available. A reliable data was not obtained.

3.3.2 Reactivity of quinone methides with water

On the basis of correlation coefficients and pseudo-first-order reaction rate constants **in Table 3.3, 3.4**, the disappearance of the **QM**, which was monitored by the absorption at 304 nm (**Table 3.2**, **Figure 3.6** and **Figure 3.7**), was fitted well with exponential function in most cases of the reactions. The comparison of the reaction rates was made based on the half-life ($t_{1/2}$) of the **QMs** (**Table 3.5**). The β-O-4 products were obtained in satisfactory yields in the cases of these five **QMs** carrying **H-**, **G-** or **biphenyl-**type units (70-94% yield), indicating that water addition was the main reaction in these experiments although minor unknown side-reactions must have been accompanied. Relatively clear presence of isosbestic point in the spectral change during the progress of water addition to **QM-GG**, **-GH** (see **(a)** and **(b)** in **Figure 3.3**, for other **QM**s carrying **H**-type **QM** moiety, their reactivity with water were so fast that we did not have enough time to observe the isosbestic point in their UV absorbance spectra) suggesting that conversion of **QM-GG** and **-GH** to corresponding β-O-4 product **GG** and **GH** proceeded rather quantitatively. Thus, it is possible to compare the reaction rate of water addition on the basis of the disappearance rate of **QMs**.

As shown in **Figure 3.6** and **Table 3.3**, the **QMs**, as being expected, disappeared faster in a more acidic condition in all the cases of our experiment. While noticeable differences in $t_{1/2}$ were found among QMs with different aromatic ring types and structures of **QM** moiety.

Effect of aromatic ring type and the structures of quinone methide moiety on the reactivity

As illustrated in **Table 3.3**, water addition occurs to **G-**type **QMs** (**QM-GG** and **-GH**) with a half-life of 1.4–15 min to form guaiacylglycerol-β-aryl ethers (**GG** and **GH**). In contrast, the **H**-type **QMs** (**QM-HH** and **-HG**) were very labile, and transformed into *p*-hydroxyphenylglycerol-β-aryl ethers (**HH** and **HG**) with a half-life of 10–40 seconds. The half-life ($t_{1/2}$) tended to be shorter in the order of **QM-HH** < **QM-HG** < **QM-GH** < **QM-GG** at any pH condition.

As well as the structural difference in **QM** moiety (**A-ring**), the type of β-etherified ring (**B-ring**) also influenced the reaction rates. By replacing the **B-ring** from the *p*-hydroxyphenyl to the guaiacyl

ring, the half-life became longer regardless of the type of **A-ring** ($t_{1/2}$: **QM-XH** < **QM-XG**, where **X** is either **H** or **G**). In detail, in the case of the 3-methoxy-substituted **QMs** (**G**-type), the half-life of the β-O-4-guaiacyl ether **QM** was up to 1.2–1.4 times longer than the β-O-4-*p*-hydroxyphenyl ether **QM** ($t_{1/2}$: **QM-GH** < **QM-GG**) at pH of 5.5–7 although they have a similar half-life at pH 3.5 and 4.5. A similar trend was also observed for non-substituted **QMs**, in which the half-life was 1.1–2 times longer in the β-O-4-guaiacyl ether **QM** in the range of pH 5.5-7.0 ($t_{1/2}$: **QM-HH** < **QM-HG**).

However, the reaction rate was more influenced by the type of **QM** moiety (**A-ring**) ($t_{1/2}$: **QM-HX** < **QM-GX**, where **X** is either **H** or **G**). In detail, the β-O-4-guaiacyl ether **QM** became less reactive by replacing the non-substituted **QM** moiety with the 3-methoxy-substituted one at any pH condition, and the half-life was up to 27 times longer ($t_{1/2}$: **QM-HG** < **QM-GG**). Also in the β-O-4-*p*-hydroxyphenyl ether **QMs**, the 3-methoxy-substituted **QM** reacted much slower at any pH condition with up to 39 times longer half-life at pH 5 ($t_{1/2}$: **QM-HH** < **QM-GH**). The water addition reaction apparently became slower owing to the methoxy group at the 3-position of **QM** moiety, of which stabilizing electronic effect and possible steric effect might oppose the requirements of the water addition reaction.

It is appeared that the methoxy groups play an important role on the reactivity of **QM**. Hemmingson et al.[31] ever reported one kind of 3-methoxy-substituted **QM** reacts 15-16 times faster than the other kind of 3, 5-dimethoxy-substituted **QM** with hydroxyl compound in the same reaction condition. Also, both the formation and subsequent adduct reaction of **QMs** had previously demonstrated to be highly responsive to the presence of electron-withdrawing and -donating groups when studying a series of *ortho*-**QM** models with a variety of substituents.[32,33] Electron-donating groups like methoxy group, greatly facilitate initial **QM** generation and its stability. Conversely, electron-withdrawing groups greatly suppress initial formation of **QM** and its regeneration from corresponding adduct products.

Effect of solvent condition on the reactivity

As shown in **Table 3.4**, interestingly, the reactivity of all **H**-type **QMs** with water increases as the decreasing concentration of dioxane in the reaction solution with the same pH condition. However, the disappearance of **QM** (**Figure 3.7**) was still fitted well with exponential function in most cases of

the reactions (See **Table 3.4** for the correlation coefficient and also the pseudo-first-order reaction rate constants.). Also, the water addition to **QMs** is the main reaction in solutions with any ratios of dioxane to water (v/v) on the basis of the satisfactory yield (64%-90%) of β-O-4 products from all **QMs**. Moreover, the higher reactivity in the lower pH condition (pH5＞pH7) and the order of faster water addition to **QMs** (**QM-HH**＞**QM-HG**＞＞**QM-GH**＞**QM-GG**), described above, can be found in the water addition to **QMs** in different dioxane-water ratios. When the volume percentage of dioxane in solutions decreased from 50% to 1.25%, the half-life of the **H**-type **QMs** decreased by around 2-folds, and the **G**-type **QMs** decreased around ten times. If we set the pH condition as 3.5, the **QM-GG** can quickly disappear with half-life, 47 seconds in the solution containing around 1% volume of dioxane. By contrast, the half-life of **QM-GG** is 84 sec for the solution with 50 % volume of dioxane at pH 3.5 is 84 sec. Nakatsubo et al. also reported the similar results that the dioxane to water ratio can influence the reactivity of QM. When the **QM-GG** was added into the dioxane-water solution, the bright yellow color of **QM-GG** disappeared after 15 min in dioxane/water (1:9) and 4 hours in dioxane/water (1:1), respectively.[2]

Implication from the rapid aromatization in *p*-hydroxyphenyl-type QMs

Using wide range of pH conditions for water addition experiments, we tried to cover the possible pH range assumed for extracellular sites in cell walls as much remains unknown about the reaction condition where lignification occurs. As mentioned above, the half-life time of **QMs** was shorter in the order of **QM-HH** < **QM-HG** << **QM-GH** < **QM-GG**. This result imply that, when a new β-O-4-linkage is introduced at the end of a growing lignin by a radical coupling reaction with a monolignol, a non-substituted **QM** moiety (**H**-type) derived from *p*-coumaryl alcohol is rearomatized faster than the methoxy-substituted **QMs** (**G**-type) from coniferyl alcohol, which will result in the sooner formation of a new phenolic end, thereby getting ready for being further oxidized and coupled with a new monolignol for the subsequent chain extension reaction. In this way, the rapid aromatization in the **H**-type **QM** may possibly contribute to the demand on the rapid lignin deposit in compression wood.

Compression wood is known to be more active in the production of tracheid, major tissues of softwood xylem, than normal wood. The production rate from vascular cambium was two times higher in compression wood than in the opposite wood of Chamaecyparis obtuse Endl.[34] A tracheid differentiation takes around 3 weeks, including the cell production, expansion of the cell size, secondary wall thickening, and maturation by lignin deposition.[34] In the maturation step, whereas *p*-hydroxyphenyl units are deposited in compound middle lamella on the early stage of cell wall formation in normal woods,[35] they are distributed both in the compound middle lamella and the secondary wall in compression wood, which results in the highly lignified compression wood tissues.[10, 36-38] Taken together, these present knowledge suggest that *p*-hydroxyphenyl units play a role in the rapid lignin deposition.

In horseradish peroxidatse-H_2O_2 system, *p*-coumaryl alcohol (**H**-type) has slower reaction rate than coniferyl alcohol (**G**-type).[39] Measurement of oxidation potentials of monolignols with cyclic voltammetry also revealed that *p*-coumaryl alcohol can be less oxidized than coniferyl alcohol.[39] On the basis of these results of the oxidizability of monolignols, *p*-coumaryl alcohol does not seem to have an advantage over coniferyl alcohol for driving the lignin polymerization cycle efficiently.

However, once a radical coupling reaction occurs to produce a **QM** structure at the growing end of a lignin chain, it is reasonably assumed that subsequent aromatization will proceed faster in the **H**-type **QM** moiety than in the **G**-type one based on the results of the water addition experiments (**Table 3.4** and **Table 3.5**). Since the rapid water addition means the rapid aromatization and re-generation of phenolic hydroxy group which is essential for further polymerization, **H**-type **QM** may possibly contribute to the efficient lignin polymerization and the development of compression wood in response to the growing stress.

Considering that the re-generation of phenolic hydroxy group by aromatization of **QM** is a crucial step in the lignin polymerization cycle, the study on the reactivity of lignin-related **QMs** will be more important for understanding the lignification process and predicting the structural features of lignins.

3.3.3 Stereo-preferential formation of β-O-4 structures

The *threo* isomer of β-O-4 dimer was obtained more than the *erythro* isomer by the water addition experiment to **QM-HH**, **-HG**, **-GH**, and **-GG** in almost all pH conditions with only one exception that 50:50 of *erythro*: *threo* ratio was obtained from **QM-GG** at pH condition of 3.5. These results are clearly different from the results of **QM-GS**, and **-SS** previously reported by Brunow et al.[3] in which the *erythro* isomers of β-O-4 dimers were preferentially obtained by water addition under pH 3. By using **QM-GS**, we confirmed the reproducibility of the results of Brunow's group.[3] The **QM-GS** was preferentially transformed to the *erythro* isomer of the β-O-4 product at pH 3.5 and 4.5 conditions, whereas **QM-GG** did not exhibit *erythro*-preferential formation at any pH condition.

However, in the respect of a novel **H**-type lignin **QM** model β-etherified with a **biphenyl** unit (**QM-H-HH$_{biphenyl}$**), the *erythro*-preferential formation was observed in the water addition at every pH conditions examined.

Based on the structural characterization of lignins by ozonation method, the *erythro* form was slightly predominant in the β-O-4-structures of the compression wood lignins that consist of **G** unit and a substantial amount of **H** units, but no **S** unit.[10,11] Therefore, we assumed that non-substituted **QM** or β-O-4-*p*-hydroxyphenyl ether **QM** could undergo *erythro*-preferential water addition. In the present study by the use of **QM** model compounds, however, *erythro*-preferential formation was not found in the water addition to normal three types of **QM** dimers, **QM-HH**, **-HG**, and **-GH**, at any conditions employed here. The *threo* selective formation was also reported for *in vitro* enzymatic dehydrogenation of a *p*-hydroxyphenyl-type monolignol;[40] β-O-4 dilignols (*p*-hydroxyphenylglycerol-β-*p*-coumaryl ether) were isolated from the coupling products of *p*-coumaryl alcohol obtained in peroxidase and H_2O_2 system, and the *erythro*: *threo* ratio was 1:4.7. Whereas, *erythro*-preferential water addition occurred to an **H**-type **QM** trimer composing of etherified biphenyl structure as **B-ring** never reported before. Although there is still a gap for the *erythro/threo* ratios of β-O-4 structure obtained between our present model experiment and the previous analysis of compression wood lignin, the result for our experiment would give us some clues to imagine and assume the condition in cell wall for lignification.

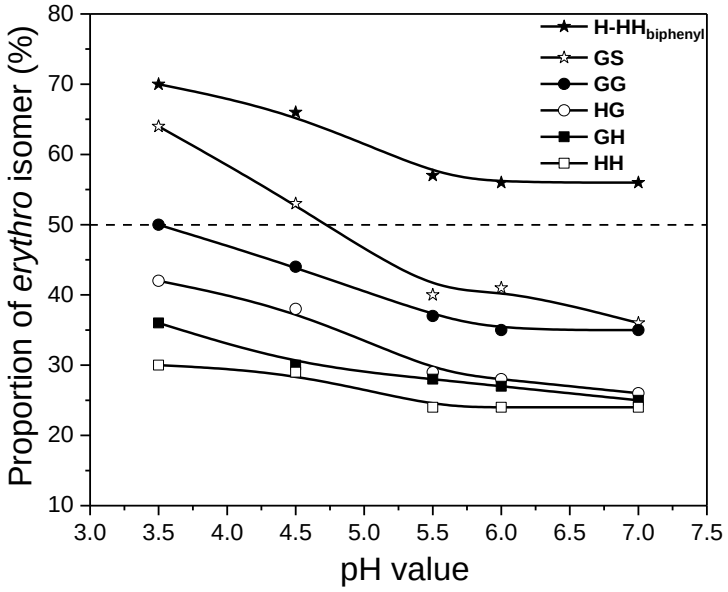

Figure 3.8 The proportion of *erythro* to *threo* isomers of β-O-4 products obtained by water addition to quinone methides (around 0.3 μmol) at different pH condition.

Effect of pH condition on the *erythro*/*threo* ratio

Throughout all experiments conducted here, the *erythro*/*threo* ratio varied widely and tended to be higher at a more acidic condition within the pH 3.5 to 7.0 (**Figure 3.8**). This result was in line with the results of the previous study on **S**-type **QMs** by Brunow's group,[3] i.e., this pH-dependent trend is common in **H**-, **G**-, and/or **S**-type lignin-related **QMs**, even in our novel **QM** trimer β-etherified with a **biphenyl** unit. Also, as referred to **Figure 3.8**, the *erythro/threo* ratio varied widely but tended to be stable within the neutral condition (pH 5.5 to pH 7).

Effect of aromatic nucleus structures on the *erythro*/*threo* ratio

At any pH condition employed, the ratio of *threo* isomer in the β-O-4 dimer products was always higher in the order of **HH** > **GH** > **HG** > **GG**. In details, a higher *threo*-selectivity was obtained by replacing the β-etherified aromatic nucleus of the **QMs** (**B-ring**) from **G**-type to **H**-type. This phenomenon was obtained from both non-substituted and 3-methoxy-substituted **QMs** in the any pH condition (comparison of **QM-GG** with **QM-GH**, and **QM-HG** with **QM-HH**).

The structural type of the quinone methide moiety (**A-ring**), which governs the reactivity of the

QMs, also influenced the stereo-selectivity to smaller extents. A higher *threo*-selectivity was obtained by replacing the quinone methide moiety from methoxy-substituted (**G-**) type to non-substituted (**H-**) one in the every pH condition. But the effect of this replacement was moderate (comparison of **QM-GG** with **QM-HG**, and **QM-GH** with **QM-HH**). The structural type of β-etherified ring influenced the *erythro/threo* ratio more than that of the quinone methide moiety did (**B-ring** effect > **A-ring** effect).

To investigate the effect of **B-ring** in more detail, a novel **QM-H-HH$_{biphenyl}$** was subjected to the water addition. The **QM-H-HH$_{biphenyl}$** disappeared as fast as the **H-type QM** at the different pH conditions (pH 3.5 to 7), and gave **β-O-4** products (**H-HH$_{biphenyl}$**) in satisfactory yields (75-93%, **Table 3.4, 3.5**). Interestingly, as shown in **Figure 3.8,** the *erythro*-preferential formation was observed in the water addition at any pH examined. The *erythro*-selectivity was also higher under more acidic condition up to the *erythro*:*threo* = 70: 30. It was evidenced that *erythro*-preferential water addition can occur to a **QM** composing of only H-units although the reaction mechanism causing the stereo-preference remains unknown.

Effect of dioxane to water ratio on the *erythro*/*threo* ratio

As illustrated in **Figure 3.9**, the results suggest that *erythro/threo* ratio is also determined by the volume ratio of dioxane to water, whereas we still did not get the *erythro*-preferential formation of β-O-4 dimer products. By changing the volume percentage of dioxane in reaction solution from 1.29% to 50%, the *erythro/threo* ratio varied and tended to different trend depending on the β-etherified ring (B-ring) of **QM**. At the same time, both higher *erythro/threo* ratio was obtained in a lower pH condition (e.g. pH5 > pH7) and *erythro/threo* was higher in the order **QM-GG＞QM-GH＞QM-HG＞QM-HH** can be observed for water addition in every dioxane to water ratio. This is consistent with what we found for water addition experiment in different pH condition in above.

For the buffered dioxane-water solution at the same pH condition (pH 5 or 7), the *erythro/threo* ratio obtained by water addition to **QM** with β-etherified guaiacyl ring (**G**-type) increased with a decrease of volume percentage of dioxane. On the contrary, the *erythro/threo* ratio of **QM** with β-etherified *p*-hydroxyphenyl ring (**H**-type) decreased with a decrease of the dioxane concentration. However, the **QMs** with different **QM** moiety (**A-ring**) have no clear response to the stereo-preference

with water as the change of dioxane-water ratio. In details, in the cases of β-O-4-guaiacyl ether QMs, **QM-XG** (where **X** is either **H** or **G**), the proportion of *erythro* isomer was lowered by Δ6-9% for **GG** and Δ0-3% for **HG** by changing the dioxane volume percentage from 1.25% to 50%. In contrast, for β-O-4-*p*-hydroxyphenyl ether QMs, **QM-XH** (where **X** is either **H** or **G**), the proportion of *erythro* isomer became higher by changing the dioxane volume percentage from 1.25% to 50% (+Δ4-6% for **HH** and +Δ4-6% for **GH**).

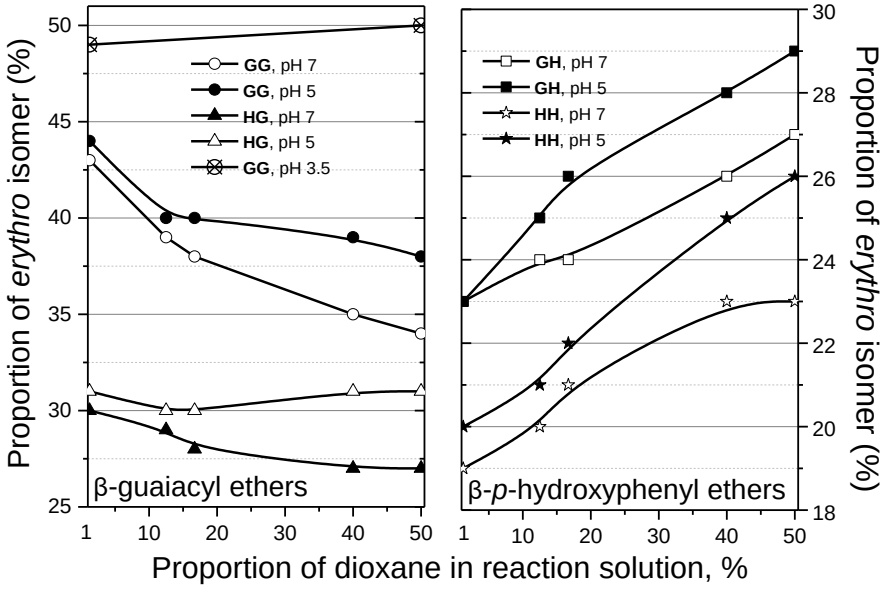

Figure 3.9. The proportion of *erythro* to *threo* isomers of β-O-4 products obtained by water addition to quinone methides (around 0.6 μmol) in different ratio of dioxane to water, left picture for the results from water addition to β-O-4-guaiacyl ether **QMs**, right picture for the results from water addition to β-O-4-*p*-hydroxyphenyl ether **QMs**

In the previous literature, different *erythro/threo* ratios of **GG** obtained from water addition to **QM-GG** in two different solvent conditions have been reported.[2] The slightly *erythro*-preferential formation of β-O-4 products, **GG** were obtained from water addition experiment in chloroform, whereas in water-dioxane solvent *threo* isomers tended to be produced more than *erythro* ones. Specifically, the *erythro/threo* ratio of **GG** products from **QM-GG** in dioxane/water solvent (1:9, v/v) was reported to be 0.5 and 0.4 for dioxane/water solvent (1:1, v/v), respectively.[2] This trend that the *erythro*/*threo* ratio of **GG** products from **QM-GG** preferentially decreased as the increase of volume ratio of dioxane/water during water addition reaction was same as the result of our experiment. As the reason for variations of *erythro/threo* ratio by the difference of solvent condition, Nakatsubo et al.[2]

proposed that the formation of some attracting force between water and QM molecules on the transition state of reaction, such as hydrogen bond controls water addition to the planar **QM** from the favorable side. Different reaction solvent may result different type and number of attracting force, which could lead to different *erythro*/*threo* ratio of β-O-4 products during water addition experiment.

In our water addition experiment on **QM-GG** by varying the pH condition (3.5-7) in the same buffered dioxane to water (1:1, v:v) or varying volume percentage of dioxane from 1% to 50% in solution at the pH 5, both the *erythro/threo* ratio of **GG** products was higher under the lower pH up to the *erythro*: *threo* = 50:50 and under the lower volume percentage of dioxane up to the *erythro*: *threo* = 44:56. On the basis of this, we assumed that if we add the effect of pH and dioxane to water ratio together to perform the water addition experiment on **QM-GG**, the *erythro*-preferential formation of **GG** could be obtained in the solution with 1% volume of dioxane under pH condition of 3.5. However, the similar result as the previous water addition experiment for **QM-GG** in solutions with 50% volume of dioxane under pH condition of 3.5 was observed in here (*erythro/threo* = 49/51, **Figure 3.9**). Therefore, under the pH 3.5, it is appeared that the effect of volume percentage of dioxane does not work so well on the stere-preferential water addition to **QM-GG**. Whereas, for all the QM dimers used in here, the effect of pH on the *erythro*/*threo* ratio of their corresponding water addition β-O-4 products get larger by changing the volume percentage of dioxane in reaction solution from 1% to 50 % dioxane. As shown in **Figure 3.9** and **Table 3.4**, when the pH condition was changed from 7 to 5, the proportion of *erythro* isomer was increased by Δ1% for **GG**, Δ1% for **HG**, Δ0% for **GH** and Δ1% for **HH** in the solution with 1% dioxane (or 99% water). In contrast, for the solution with 50% dioxane (or 50% water), the proportion of *erythro* isomer was increased by Δ4% for **GG**, Δ4% for **HG**, Δ2% for **GH** and Δ3% for **HH** by changing pH condition from 7 to 5. Even by lowering the pH from 7 to 3.5, the increasing degree on the proportion of *erythro* isomer of **GG** products from water addition to **QM-GG** was smaller in the solution with 1% dioxane than in the solution with 50% dioxane (Δ6%＜Δ16%).

Implication from the *erythro*/*threo* ratio of water adducts

Yeh et al. and Nawawi et al.[10,11] reported that the *erythro/threo* ratio of β-O-4 structures in compression wood is slightly but clearly higher than 1.0 whereas the ratio in opposite wood is exactly 1.0.[10, 11] Our attempts to obtain *erythro* preferential formation of **H**-type β-O-4 products from

corresponding **QM** models (**QM-HH**, **-HG**, **-HH**) were not successful. This would be either because the model dimers chosen did not sufficiently closely model the structure in compression wood lignin and/or because the reaction condition for rearomatization step in lignin biosynthesis may not be perfectly mimicked.

However, there are still lots of information valuable for the understanding the ligninficaiton for compression wood. For example, the *erythro*/*threo* ratio obtained in a lower pH condition was closer to the values reported for compression wood lignins, rather than the ratio obtained in higher pH condition was. In this viewpoint, the results in the present study are in line with the proposal by Brunow et al.[3] that "the pH of the medium in which lignin biosynthesis occurs is lower than has been assumed until now". This statement was made for guaiacyl and/or syringyl lignins.

On the other hand, low pH condition seems to be strict for the cell wall condition during lignification. Our study for the influence of solvent on the stereo-selectivity of water addition to QM suggest that the effect of pH on the *erythro*/*threo* ratio of their β-O-4 products became smaller by changing the volume percentage of water in reaction solution from 50% to 99 %. Additionally, a higher *erythro*/*threo* ratio of **GG** was obtained up to the *erythro*: *threo* = 45:55 from the **QM-GG** in the solution with higher volume percentage of water under pH 5. Nakatsubo et al.[2] also concluded that solvent condition affected the *erythro/threo* ratio of a β-O-4 structure obtained by water addition to the **QM-GG**. Therefore, *erythro*/*threo* ratio of **GG** products approaching to the value reported for the softwood lignin also could be obtained in a water media condition with pH 5. This would be used to establish a more reliable reaction condition to get the *erythro*-preferential rearomatization in **H**-type **QM**, which was observed in the analysis of compression wood lignin.

Model compounds for quinone methides used in previous studies are fairly simple models, which have a β-O-4 linkage but the structure etherified at β-position (**B-ring**) is pretty simple and does not have a side chain structure. Based on the observation that *erythro*-selectivity became higher by replacing the β-etherified aromatic rings of **QMs** from non-substituted type (**H**-type) with *o*-methoxy-substituted one (**G**-type or **S**-type), it is deserved to consider the role of the methoxy group at the 3, or 5-position of β-etherified aromatic rings during *erythro* preferential formation. As lignification progresses, a 4-O-coupling between phenoxy radical on a biphenyl (5-5 structure)[11] or diaryl ethers

(4-O-5 structure)[41] structures and a monolignol radical at its side-chain β-position could produce a quinone methide intermediate, in which the 3-posiiton of β-etherified aromatic ring is substituted with a phenyl unit or a phenoxy unit. Even though, to date detailed studies on their corresponding rearomatization structure and quantitative evaluation have not been reported, we assumed they might exist as excess *erythro* form. Therefore, a novel **H**-type lignin **QM** model β-etherified with a **biphenyl** unit was designed and subjected to water to obtain expected *erythro* selectivity in any pH condition. This is a good trial, which gives us more details on the effects of β-etherified structures and their size during *erythro*-preferential formation in **H**-type **QM**.

3.4 Conclusions

This work presented in this chapter is the first step towards a comprehensive understanding of the reactivity of **H**-type **QMs**, and by using **QM** models a potential role of the **H**-units in compression wood lignin was proposed. A *p*-hydroxyphenyl **QM**, resulting from a radical coupling reaction of *p*-coumaryl alcohol with a growing lignin, can be aromatized faster than guaiacyl-type ones during lignin biosynthesis, which was suggested by the water addition experiments using different β-O-4-aryl ether **QM** models. The reaction rates of water addition were largely dependent on the structural type of the **QM** moiety, whereas the stereo-selectivity was affected by the β-etherified aromatic ring structure greater than the type of the **QM** moiety. The β-O-4-aryl ether **QMs** bearing β-etherified guaiacyl ring yielded higher proportion of *erythro* isomer than ones carrying β-etherified *p*-hydroxyphenyl ring within the *threo*-selective aromatization for all normal β-O-4-aryl ether **QM** dimer. However, *erythro*-preferential water addition can occur to a **H**-type **QM** trimer β-etherified with a **biphenyl** unit, which is same as the expectation based on the previous observation of the slight but clear *erythro* preference of β-O-4 structures in compression wood lignins.

For the solvent condition in the water addition, both lower pH condition and higher volume percentage of water in reaction solution can accelerate the reaction rate of water addition to any lignin-related **QMs**. We still cannot get the *erythro*-selectivity formation by changing the solvent condition in our experiment. However, the pH condition influenced the *erythro/threo* ratio of β-O-4 structures, which became greater under more acidic conditions. The *erythro/threo* ratio also varied significantly in the solvent with different volume percentage of water, but opposite changing trends of *erythro/threo* ratio were observed between β-*p*-hydroxyphenyl ethers **QMs** and β-guaiacyl ethers **QMs**. The solvent dependency was suggested to be an important factor for understanding and reproducing the lignification condition in cell walls.

3.5 References

[1] Ralph, J., Schatz, P. F., Lu, F., Kim, H., Akiyama, T., Nelsen, S. F. 2009. Quinone methides in lignification. In Quinone methides, Rokita, S., Ed., John Wiley & Sons, Hoboken, NJ, pp. 385-420.

[2] Nakatsubo, F., Sato, K., Higuchi, T., 1976. Enzymic dehydrogenation of *p*-coumaryl alcohol, 4: Reactivity of quinonemethide. Mokuzai Gakkaishi, 22, 29-33.

[3] Brunow, G., Karlsson, O., Lundquist, K., Sipilä, J., 1993. On the distribution of the diastereomers of the structural elements in lignins: the steric course of reactions mimicking lignin biosynthesis. Wood Science and Technology, 27(4), 281-286.

[4] Akiyama, T., Goto, H., Nawawi, D. S., Syafii, W., Matsumoto, Y., Meshitsuka, G. 2005. *Erythro*/*threo* ratio of β-O-4 structures as an important structural characteristic of lignin. Part 4: Variation in the *erythro*/*threo* ratio in softwood and hardwood lignins and its relation to syringyl/guaiacyl ratio. Holzforschung, 59(3), 276-281.

[5] Nawawi, D. S., Syafii, W., Tomoda, I., Uchida, Y., Akiyama, T., Yokoyama, T., Matsumoto, Y. 2017. Characteristics and reactivity of lignin in Acacia and Eucalyptus woods. Journal of Wood Chemistry and Technology, 37(4), 273-282.

[6] Ralph, J., Lundquist, K., Brunow, G., Lu, F., Kim, H., Schatz, P. F., ..., Boerjan, W. 2004. Lignins: natural polymers from oxidative coupling of 4-hydroxyphenyl-propanoids. Phytochemistry Reviews, 3(1-2), 29-60.

[7] Hauteville, M., Lundquist, K., von Unge, S. 1986. NMR studies of lignins. 7. ^{1}H NMR spectroscopic investigation of the distribution of *erythro* and *threo* forms of β-O-4 structures in lignins. Acta Chemica Scandinavica, B40, 31-35.

[8] Nimz, H. H., Tschirner, U., Stähle, M., Lehmann, R., Schlosser, M. 1984. Carbon-13 NMR spectra of lignins, 10.1 comparison of structural units in spruce and beech lignin. Journal of Wood Chemistry and Technology, 4(3), 265-284.

[9] Bardet, M., Robert, D., Lundquist, K., von Unge, S. 1998. Distribution of *erythro* and *threo* forms of different types of β-O-4 structures in aspen lignin by ^{13}C NMR using the 2D INADEQUATE experiment. Magnetic Resonance in Chemistry, 36(8), 597-600.

[10] Nawawi, D. S., Akiyama, T., Syafii, W., Matsumoto, Y. 2017. Characteristic of β-O-4 structures in different reaction wood lignins of Eusideroxylon zwageri T. et B. and four other woody species. Holzforschung, 71(1), 11-20.

[11] Yeh, T. F., Braun, J. L., Goldfarb, B., Chang, H. M., Kadla, J. F. 2006. Morphological and chemical variations between juvenile wood, mature wood, and compression wood of loblolly pine (Pinus taeda L.). Holzforschung, 60(1), 1-8.

[12] Sarkanen, K. V., Hergert, H. L. 1971. In lignins: occurrence, formation, structure, and reactions, Wiley-Interscience: New York, pp 43−94.

[13] Brunow, G., Sipilä, J., Mäkelä, T. 1989. On the mechanism of formation of non-cyclic benzyl ethers during lignin biosynthesis. Part 1. The reactivity of β-O-4 quinone methides with phenols and alcohols. Holzforschung, 43(1), 55-59.

[14] Diehl, B. G., Watts, H. D., Kubicki, J. D., Regner, M. R., Ralph, J., Brown, N. R. 2014. Towards lignin-protein crosslinking: amino acid adducts of a lignin model quinone methide. Cellulose, 21(3), 1395-1407.

[15] Ralph, J. 1982. Reactions of lignin model quinone methides and NMR studies of lignins. Ph. D. thesis, University of Wisconsin—Madison, pp 199−204.

[16] Tobimatsu, Y., Takano, T., Kamitakahara, H., Nakatsubo, F. 2010. Reactivity of syringyl quinone methide intermediates in dehydrogenative polymerization I: high-yield production of synthetic lignins (DHPs) in horseradish peroxidase-catalyzed polymerization of sinapyl alcohol in the presence of nucleophilic reagents. Journal of Wood Science, 56(3), 233-241.

[17] Tobimatsu, Y., Takano, T., Kamitakahara, H., Nakatsubo, F. 2008. Studies on the dehydrogenative polymerization of monolignol β-glycosides: part 5. UV spectroscopic monitoring of horseradish peroxidase-catalyzed polymerization of monolignol glycosides. Holzforschung, 62(5), 501-507.

[18] Sipilä, J., Brunow, G. 1991. On the mechanism of formation of non-cyclic benzyl ethers during lignin biosynthesis. Part 2. The effect of pH on the reaction between a β-O-4-type quinone methide and vanillyl alcohol in water-dioxane solutions. The stability of non-cyclic benzyl aryl ethers during lignin biosynthesis. Holzforschung, 45, 275-278.

[19] Sipilä, J., Brunow, G. 1991. On the mechanism of formation of non-cyclic benzyl ethers during

lignin biosynthesis. Part 4. The reactions of a β-O-4-type quinone methide with carboxylic acids in the presence of phenols. The formation and stability of benzyl esters between lignin and carbohydrates. Holzforschung, 45, 9-14.

[20] Sipilä, J., Brunow, G. 1991. On the mechanism of formation of non-cyclic benzyl ethers during lignin biosynthesis Part 3. The reactivity of a β-O-4-type quinone methide with methyl-α-D-glucopyranoside in competition with vanillyl alcohol. The formation and the stability of benzyl ethers between lignin and carbohydrates. Holzforschung, 45, 3-7.

[21] Ralph, J., Adams, B. R. 1983. Determination of the conformation and isomeric composition of lignin model quinone methides by NMR. Journal of Wood Chemistry and Technology, 3(2), 183-194.

[22] Ede, R. M., Main, L., Ralph, J. 1990. Evidence for increased steric compression in *anti* compared to *syn* lignin model quinone methides. Journal of Wood Chemistry and Technology, 10(1), 101-110.

[23] Ralph, J., Young, R. A. 1983. Stereochemical aspects Op addition reactions involving lignin model quinone methides. Journal of Wood Chemistry and Technology, 3(2), 161-181.

[24] Tanbda, H., Nakano, J., Hosoya, S., Chang, H. M. 1987. Stability of α-ether type model compounds during chemical pulping processes. Journal of Wood Chemistry and Technology, 7(4), 485-497.

[25] Kishimoto, T., Ikeda, T., Karlsson, O., Magara, K., Hosoya, S. 2002. Reactivity of secondary hydroxyl groups in methyl β-d-xylopyranoside toward a β-O-4-type quinone methide. Journal of Wood Science, 48(1), 32-37.

[26] Toikka, M., Sipilä, J., Teleman, A., Brunow, G. 1998. Lignin–carbohydrate model compounds. Formation of lignin–methyl arabinoside and lignin–methyl galactoside benzyl ethers via quinone methide intermediates. Journal of the Chemical Society, Perkin Transactions 1, (22), 3813-3818.

[27] Toikka, M., Brunow, G. 1999. Lignin–carbohydrate model compounds. Reactivity of methyl 3-O-(α-l-arabinofuranosyl)-β-d-xylopyranoside and methyl β-d-xylopyranoside towards a β-O-4-quinone methide. Journal of the Chemical Society, Perkin Transactions 1, (13), 1877-1884.

[28] Karhunen, P., Rummakko, P., Pajunen, A., Brunow, G. 1996. Synthesis and crystal structure determination of model compounds for the dibenzodioxocine structure occurring in wood lignins. Journal of the Chemical Society, Perkin Transactions 1, (18), 2303-2308.

[29] Landucci, L. L., Ralph, J. 1982. Adducts of anthrahydroquinone and anthranol with lignin model quinone methides. 1. Synthesis and characterization. The Journal of Organic Chemistry, 47(18), 3486-3495.

[30] Ralph, J., Landucci, L. L., Nicholson, B. K., Wilkins, A. L. 1984. Adducts of anthrahydroquinone and anthranol with lignin model quinone methides. 4. Proton NMR hindered rotation studies. Correlation between solution conformations and X-ray crystal structure. The Journal of Organic Chemistry, 49(18), 3337-3340.

[31] Hemmingson, J. A., Leary, G. 1975. The chemistry of reactive lignin intermediates. Part II. Addition reactions of vinyl-substituted quinone methides in aqueous solution. Journal of the Chemical Society, Perkin Transactions 2, (14), 1584-1587.

[32] Weinert, E. E., Dondi, R., Colloredo-Melz, S., Frankenfield, K. N., Mitchell, C. H., Freccero, M., Rokita, S. E. 2006. Substituents on quinone methides strongly modulate formation and stability of their nucleophilic adducts. Journal of the American Chemical Society, 128(36), 11940-11947.

[33] Toteva, M. M., Moran, M., Amyes, T. L., Richard, J. P. 2003. Substituent effects on carbocation stability: The pK_R for *p*-Quinone Methide. Journal of the American Chemical Society, 125(29), 8814-8819.

[34] Fujita, M., Saiki, H., Sakamoto, J., Araki, N., Harada, H. 1979. The secondary wall formation of compression wood tracheid. IV: Cell wall structure of transitional tracheids between normal wood and compression wood, 51, 247-256.

[35] Fukushima, K., Terashima, N. 1991. Heterogeneity in formation of lignin. Wood Science and Technology, 25(5), 371-381.

[36] Lapierre, C., Monties, B., Rolando, C. 1988. Thioacidolyses of diazomethane-methylated pine compression wood and wheat straw in situ lignins. Holzforschung, 42(6), 409-411.

[37] Timell, T. E. 1986. Compression wood in gymnosperms. Springer-Verlag, Berlin, vol. 1, pp. 289-408.

[38] Nanayakkara, B., Manley-Harris, M., Suckling, I. D., Donaldson, L. A. 2009. Quantitative chemical indicators to assess the gradation of compression wood. Holzforschung, 63(4), 431-439.

[39] Kobayashi, T., Taguchi, H., Shigematsu, M., Tanahashi, M. 2005. Substituent effects of 3, 5-

disubstituted *p*-coumaryl alcohols on their oxidation using horseradish peroxidase–H_2O_2 as the oxidant. Journal of Wood Science, 51(6), 607.

[40] Nakatsubo, F., Higuchi, T. 1975. Enzymic dehydrogenation of *p*-coumaryl alcohol.: III. Analysis of dilignols by gas chromatography and NMR spectrometry. Wood Research, 58, 12-19.

[41] Li, Y., Akiyama, T., Yokoyama, T., Matsumoto, Y. 2016. NMR assignment for diaryl ether structures (4-O-5 structures) in pine wood lignin. Biomacromolecules, 17(6), 1921-1929.

Chapter 4

Preparation and Characterization of Dehydrogenation Polymers (DHP) from *p*-coumaryl alcohol

4.1 Introduction

To explore a reaction condition that leads *erythro*-selective formation in **H**-type **QM** during lignin formation in cell wall, in vitro synthesis of lignin, so called dehydrogenation polymers (DHP), was achieved from *p*-coumaryl alcohol by using peroxidase and hydrogen peroxide in different reaction conditions. The DHP contains the same major structural units as nature lignin but the structure and molecular weight of the DHP differ from molecular weight and structures of milled wood lignin (MWL).[1-4] For instance, DHPs have a lower number of β-O-4-linkage and more β-5- and β-β-linkage than natural lignin.[3,5] This, however, seems to be unavoidable, because the characteristics of DHPs vary with reaction condition and the polymerization conditions are different from those in the cell wall.[3,6] Much attentions have been paid to understand the reaction condition in cell wall by comparing the structure of natural lignin with that of DHPs prepared in different conditions. These reaction conditions include solvent, pH, oxidation rate of monolignols, and rates of supply of substances.[4,7]

In a similar approach, reliable experiment condition for the water addition to **H**-type **QM** models in the Chapter 3 might contribute to get the **H**-type DHP with *erythro* dominated β-O-4 structures. In detail, it is expected that DHP with higher *erythro/threo* ratio will be prepared in the lower pH condition and lower volume percentage of dioxane. Moreover, during the cross-coupling between monomer radicals and dimers or higher oligomers, the influence of the β-etherified structure (originated from the dimers or higher oligomers) and its size will be studied in detail, which might result the *erythro* preferential formation of β-O-4 structure.

Therefore, in this study, varied DHP samples were prepared in different conditions and characterized, subsequently to be determined the *erythro/threo* ratio of β-O-4 structure by ozonation analysis.

4.2 Experimental

4.2.1 General

Reagents and solvents were purchased from Fujifilm Wako Pure Chemical Co. (Osaka, Japan),

Tokyo Chemical Industry Co., Ltd. (Tokyo, Japan) or Sigma-Aldrich (Tokyo, Japan), and used as received. The pH values of buffers were measured with a HORIBA F-52 pH meter with JF15 electrode (Horiba, Kyoto, Japan). The NMR spectra of synthesized compounds were recorded with a JEOL JNM-A500 500 MHz spectrometer. The standard JEOL programs of one- and two-dimensional (proton, carbon, DEPT-135, and ^{1}H-^{13}C HSQC) NMR experiments were performed for the structural elucidation and assignment of newly synthesized compounds. The central peak of the residual solvent was used as an internal reference (δ_H 7.26, δc 77.0 ppm for $CDCl_3$, δ_H 2.04, δc 29.8 ppm for acetone-d_6). Samples with multiplicity problems with OH–OD exchange were exchanged by the addition of a drop of D_2O prior to measurements. The traditional numbering system [1, 8] for lignin was used rather than the systematic IUPAC numbering scheme.

4.2.2 General procedure for preparation of artificial lignin

Synthetic dehydrogenation polymers (DHP) are useful to verify the factors influencing the proportion of *erythro* and *threo* form of β-O-4 structure from quinone methide through mimicking the lignin biosynthesis. They were prepared via horseradish peroxidase (HRP)-catalysed polymerization using an end-wise polymerization (*Zutropfverfahren* method) or a bulky polymerization (*Zulaufverfahren* method).[9-13] The sample codes of the synthetic DHP, for example, **H-Zutropf-5-30** representing that the DHP was prepared from *p*-coumaryl alcohol with *Zutropfverfahren* method in pH 5 citrate-phosphate buffer mixed with 30 ml of dioxane; **G-Zulauf-6-30** representing that the DHP was prepared from coniferyl alcohol with *Zulaufverfahren* method in pH 6 citrate-phosphate buffer mixed with 30 ml of dioxane.

According to the previous references,[7,14] coniferyl alcohol and *p*-coumaryl alcohol was separately synthesized by DIBAL-H reduction of methyl ferulate and methyl *p*-coumarate which was prepared from the corresponding ferulic acid and *p*-coumaric aicd. Their corresponding NMR data is shown in below:

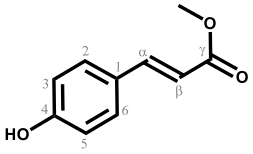

Compound methyl *p*-coumarate. ^{1}H NMR (acetone-d_6 +D_2O (1 drop), 500 MHz), δ_H: 3.71 (3H, s, γ-OMe), 6.34 (1H, broad-d, J = 16 Hz, β), 6.88 (2H, m, H3 and H5), 7.53 (2H, m, H2 and H6), 7.59 (1H, br-d, J = 16 Hz, α). ^{13}C

NMR (acetone-d_6, 125 MHz) δ_C: 51.6 (γ-OMe), 115.4 (β), 116.8 (3), 116.8 (5), 127.1 (1), 131.0 (2), 131.0 (6), 145.4 (α), 160.6 (4), 167.9 (γ).

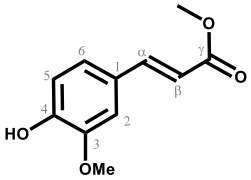

Compound methyl ferulate. ^{1}H NMR ($CDCl_3$, 500 MHz), δ_H: 3.79 (3H, s, γ-OMe), 3.91 (3H, s, H3-OMe), 6.29 (1H, broad-d, J = 16 Hz, β), 6.91 (1H, br-d, J = 8 Hz, H5), 7.01 (1H, br-d, J = 1 Hz, H2), 7.06 (1H, br-dd, J = 8, 1 Hz, H6), 7.62 (1H, br-d, J = 16 Hz, α). ^{13}C NMR ($CDCl_3$, 125 MHz) δ_C: 51.6 (γ-OMe), 55.9 (H3-OMe), 109.3 (2), 114.7 (β), 115.1 (5), 123.0 (6), 126.9 (1), 144.9 (α), 146.7 (3), 147.9 (4), 167.7 (γ).

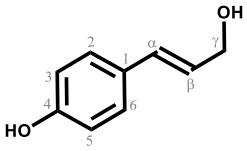

Compound *p*-coumaryl alcohol. ^{1}H NMR (acetone-d_6 +D_2O (1 drop), 500 MHz), δ_H: 4.18 (2H, broad-dd, J = 5, 1 Hz, γ), 6.19 (1H, br-dt, J = 16, 5 Hz, β), 6.50 (1H, br-d, J = 16 Hz, α), 6.78 (2H, m, H3 and H5), 7.26 (2H, m, H2 and H6). ^{13}C NMR (acetone-d_6, 125 MHz) δ_C: 63.5 (γ), 116.3 (3), 116.3 (5), 127.9 (β), 128.5 (2), 128.5 (6), 129.9 (1), 130.2 (α), 157.9 (4).

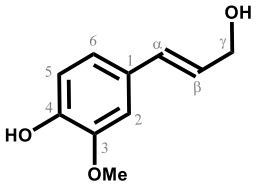

Compound coniferyl alcohol. ^{1}H NMR ($CDCl_3$, 500 MHz), δ_H: 3.89 (3H, s, H3-OMe), 4.30 (2H, broad-dd, J = 6, 1 Hz, γ), 5.72 (1H, s, γ-OH), 6.22 (1H, br-dt, J = 16, 6 Hz, β), 6.53 (1H, br-d, J = 16 Hz, α), 6.86 (1H, br-d, J = 8 Hz, H5), 6.88 (1H, br-d, J = 2 Hz, H2), 6.90 (1H, br-dd, J = 8, 2 Hz, H6). ^{13}C NMR ($CDCl_3$, 125 MHz) δ_C: 55.8 (H3-OMe), 63.8 (γ), 108.3 (2), 114.4 (5), 120.3 (6), 126.1 (β), 129.2 (1), 131.3 (α), 145.5 (4), 146.6 (3).

Preparation of DHP from *p*-coumaryl alcohol in different pH condition with *Zutropfverfahren* method

As shown in **Figure 4.1**, 200 mg of *p*-coumaryl alcohol was dissolved in dioxane (30 ml) and diluted with 70 ml of distilled water (flask ＃A). 20 ml of the diluted H_2O_2 solution (1.77 mmol) was prepared as flask ＃B. Horseradish peroxidase (3.3 mg; 454 units/mg solid, Oriental yeast CO., LTD) was prepared in 20 ml of distilled water (flask ＃C). Flask ＃A was added by a syringe pump for 25

h. at room temperature to a 500 ml three necks flask containing 100 ml of 0.5 M citrate-phosphate buffer at pH 3.5, 4.5, 5, 6 and 7. Flask ＃B and ＃C were independently pumped for 25 h. into the three necks flask with a two-channel syringe pump at a rate of 0.8 mL/h. Flasks were covered with aluminum foil to limit light during the reaction. Once all of the solution in Flask ＃A was pumped into the reaction suspension, the reaction is stopped by addition of 36 g NaCl powder and 1mmol of sodium thiosulfate solution. Then a light-brown colored product was collected by filtration with a hydrophilic PTFE membrane filter (ADVANTEC, 0.2 μm) for sample from pH 4.5 and 6 or filter paper for samples from pH 3.5, 5 and 7), and washed with distilled water.

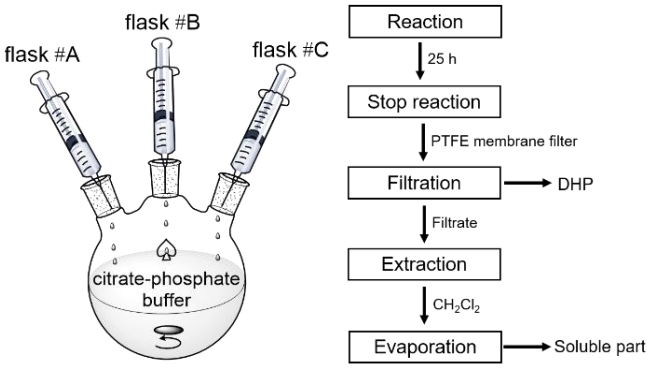

Figure 4.1 Schematic diagram of preparation of DHP samples

Preparation of DHP from *p*-coumaryl alcohol in different solvent condition with *Zutropfverfahren* method

Same as the above method, 200 mg of *p*-coumaryl alcohol was dissolved in different volumes of dioxane (10, 30 and 100 ml) and diluted with 90, 70 and 0 ml of distilled water, respectively (flask ＃A). 20 ml of the diluted H_2O_2 solution (1.77 mmol) was prepared as flask ＃B. Horseradish peroxidase (3.3 mg; 454 units/mg solid, Oriental yeast CO., LTD) was prepared in 20 ml of distilled water (flask ＃C). Flask ＃A was added by a syringe pump for 25 h. at room temperature to a 500 ml three necks flask containing 100 ml of 0.5 M citrate-phosphate buffer at pH 5.0. Flask ＃B and ＃C were independently pumped for 25 h. into the three necks flask through using a two-channel syringe pump at a rate of 0.8 ml/h. Flasks were covered with aluminum foil to limit light during the

reaction. Once all of the solution in Flask ＃A was pumped into the reaction suspension, the reaction is stopped by addition of 36 g NaCl powder and 1mmol of sodium thiosulfate solution. Then a light-brown colored product was collected by filtration with a hydrophilic PTFE membrane filter (ADVANTEC, 0.2 μm), and washed with distilled water.

Preparation of DHP from coniferyl alcohol with *Zutropfverfahren* method

The **G**-type DHP was used as a controlled experiment and prepared in the same condition as the above. It was prepared by slow independent addition of coniferyl alcohol solution (200 mg dissolved in 30 ml dioxane and 70 ml distilled water), H_2O_2 solution (0.0885 mmol/ml×20ml) and horseradish peroxidase solution (0.165mg/ml×20ml; 454 units/mg) via syringe pumps to pH 6.0 citrate-phosphate buffer (100 ml) for 25 h. at room temperature.

Preparation of DHP from *p*-coumaryl alcohol and coniferyl alcohol with *Zulaufverfahren* method

The same solutions as above, *p*-coumaryl alcohol or coniferyl alcohol solution (200 mg dissolved in 30 ml dioxane and 70 ml distilled water), H_2O_2 solution (0.0885 mmol/ml×20ml) and horseradish peroxidase solution (0.165mg/ml×20ml; 454 units/mg), were mixed at once in pH 6.0 citrate-phosphate buffer (100 ml) for 1 h. at room temperature. The reaction is stopped by addition of 36 g NaCl powder and 1mmol of sodium thiosulfate solution to reaction suspension. Then a light-brown colored product was collected by filtration with a hydrophilic PTFE membrane filter (ADVANTEC, 0.2 μm), and washed with distilled water.

4.2.3 Acetylation of the DHP samples, *p*-coumaryl alcohol and HH type β-O-4 dimer

To a 20 mg starting material (DHP samples, *p*-coumaryl alcohol or **HH** type β-O-4 dimer) dissolved in pyridine (1.5 ml) in a 10 ml of round bottom flask, 0.5 ml acetic anhydride was added at room temperature. The reaction mixture was stirred overnight. After reaction, the pyridine was

removed by repeated addition of EtOH and evaporation under vacuum at 45 °C (1 ml×4). At last, the acetylated samples were kept in vacuum oven setting at 40 °C to dryness overnight.

4.2.4 HSQC experiments of DHP samples

One-bond adiabatic ^{1}H-^{13}C correlation (HSQC) was performed to check and confirm the structure of DHP samples prepared in different pH and solvent condition. The resultant acetylated-DHP samples have different dissolving ability in $CDCl_3$. The 20mg of acetylated **H-Zutropf-3.5-30**, **H-Zutropf-4.5-30**, **H-Zutropf-5-30**, **H-Zutropf-5-10**, **H-Zulauf-6-30** and **G-Zulauf-6-30** were fully soluble in $CDCl_3$ (0.6 ml). The 40 mg acetylated **H-Zutropf-6-30**, **H-Zutropf-7-30** and **H-Zutropf-5-100** were not fully soluble in $CDCl_3$. After ultrsonicating in $CDCl_3$ (1 ml), the suspension was filtered with glass wood yielding around 10 mg of soluble acetylated DHP. The acetylated **G-Zutropf-6-30** was scarcely dissolved in any solvent and therefore, its NMR structure could not be measured by HSQC. However, the **G-Zutropf-6-30** seems to be a very high polymer and the molecular weight may be close to that of natural lignin. In the HSQC experiment, 1024 data points were acquired from 10 to 0 ppm in F2 (^{1}H), with an acquisition time of 140 ms, and from 200 to 0 ppm in F1 (^{13}C) with 256 increments, 16−48 scans, and a 1.5 s interscan delay, with a total acquisition time of 3 h 50 min to 11 h 28 min depending on the number of scans used. Processing the final matrix to 2 k by 1 k data points was performed by means of an Exponential in both F2 and F1. Correlation peaks appearing in the aliphatic region of the HSQC spectrum of acetylated DHP samples ($CDCl_3$) were assigned based on the NMR data of acetylated lignin model compounds ($CDCl_3$) reported in the NMR database of lignin model compounds and previous studies. The # refers to the library number of the NMR database:[15] in the case of β-O-4 (#225, #268, #269, #270, #271),[16, 17] β−β (#109 and #123), β-5 (#267), arylglycerol (#240, #272, #285, #160), and cinnamyl alcohol (#151, #2003, #222, #219, #220).

4.2.5 Dissolvability of prepared DHP samples in different solvents

Solvent systems examined in this experiment were mixtures of dioxane and water (dioxane/H_2O) (96/4, v/v), dimethylsulfoxide (DMSO), tetrahydrofuran (THF) and chloroform ($CHCl_3$). The DHP

and acetylated DHP samples were suspended into the above solvent systems with different concentrations (dioxane/H_2O — 5 mg/ml, DMSO — 1 mg /ml, THF — 1 mg/ml, $CHCl_3$ — 20 mg/ml) and stirred continuously at room temperature for 24 h. Detailed information is shown in **Table 4.1**.

Table 4.1. Solvent systems examined for the dissolution of DHP samples

	Dioxane-H_2O (96:4, V:V)		DMSO		DMSO (acetylated[c])		THF (acetylated[c])		$CHCl_3$ (acetylated[c])	
	S[a]	C[b](mg/ml)	S[a]	C[b](mg/ml)	S[a]	C[b](mg/ml)	S[a]	C[b](mg/ml)	S[a]	C[b](mg/ml)
H-Zutropf-3.5-30	●	5	●	1	●	1	●	1	●	20
H-Zutropf-4.5-30	●	5	●	1	●	1	●	1	●	20
H-Zutropf-5.0-10	●	5	●	1	●	1	●	1	●	20
H-Zutropf-5.0-30	○	5	●	1	●	1	●	1	●	20
H-Zutropf-5.0-100	○	5	○	1	○	1	╳	1	○	20
H-Zutropf-6.0-30	╳	5	○	1	○	1	╳	1	○	20
H-Zulauf-6.0-30	●	5	●	1	●	1	●	1	●	20
H-Zutropf-7.0-30	╳	5	○	1	○	1	╳	1	○	20
G-Zutropf-6.0-30	╳	5	╳	1	╳	1	╳	1	╳	20
G-Zulauf-6.0-30	●	5	●	1	●	1	●	1	●	20

Note: S[a], solubility. C[b], concentration. acetylated[c], acetylated DHP. ● — soluble, ○ — mostly soluble, ╳ — slightly soluble.

4.2.6 Analytical Gel permeation chromatography

For making molecular weight calibration curve, twelve standards with different molecular weight (2.5 mg) were assigned to four groups (A, B, C, D) in the 20 ml of vial with a teflon cap as shown in **Table 4.2**. The degassed HPLC grade inhibitor free THF (5 mL) was used as solvent, and resulting four kinds of solution mixtures were kept overnight. All standard solutions were filtered with a 0.45 μm filter (PTFE) before analysis with Gel permeation chromatography (GPC). This analysis was performed by a Shimadzu HPLC/GPC system equipped with LC-20AD pumps and SPD-20A UV-Vis detector using the following conditions:

column, Shodex GPC KF-802 and KF-802.5 (300mm×8.0mm); eluent, degassed HPLC grade inhibitor free THF; flow rate, 1 mL/min; analysis time, 50 min; injected volume, 20 μl; column oven temperature, 40 °C.

Table 4.2 The types of standard assigned to four groups and their corresponding relative molecular weight (M.W.)

Standard groups	The types of standard and their corresponding M.W.
A	Polystyrene (M.W. 482000, 9960), acetylated HH (M.W. 386)
B	Polystyrene (M.W. 133500, 2980), acetylated *p*-coumaryl alcohol (M.W. 234)
C	Polystyrene (M.W. 70500, 1220), propylbenzene (M.W. 120)
D	Polystyrene (M.W. 34800, 940), benzene (M.W. 78)

To determine the relative molecular weight distribution of six soluble DHP samples in THF (**H-Zutropf-3.5-30**, **H-Zutropf-4.5-30**, **H-Zutropf-5-30**, **H-Zutropf-5-10**, **H-Zulauf-6-30** and **G-Zulauf-6-30**), 2.5 mg of these acetylated DHP samples were separately dissolved in degassed HPLC grade inhibitor free THF (5 mL) and the solution was kept overnight. All DHP samples were filtered (0.45 μm, PTFE) before analysis with GPC. The analysis condition was same as the standard mixture samples. The wavelengths used for analysis were 250 nm and 280 nm. Data acquisition and computation was done using Shimadzu LCsolution v. 5.73 software.

4.2.7 Analytical Ozonation

The *erythro*/*threo* ratio of β-O-4-structures in DHP samples were determined by ozonation analysis according to the method of Akiyama et al.[18-20] Fine DHP samples (20 mg) were suspended in 30 ml of AcOH-H_2O-MeOH (80: 15: 5 by volume) in an ice bath. Oxygen containing ca. 3% ozone (type ON-3-2, Nippon ozone) was bubbled into the suspension at a rate of 0.5 L/min for 2 h with stirring. After removing the residual ozone, 0.1 M sodium thiosulfate (300 μl) was added. The solvent was removed under reduced pressure at 40 ˚C and traces of acetic acid were removed by repeated evaporation by adding small amounts of water (1 ml×3). The products were saponified with 0.1 M NaOH (20 ml) at room temperature overnight. Erythritol (2 μmol) was added as an internal standard. The product solution was then passed through a column filled with 10–15 ml of cation-exchange resin (Dowex-50W-X4, NH_4^+ form), and the column was washed with water until the pH of the eluent was 7–8. A 0.1 M ammonia solution (1ml) was added to the eluent, and diluted with water to adjust the total volume of the eluent into 100 ml. An aliquot of the eluent (2 ml) was concentrated and dried in *vacuo* at 40 ˚C, then dissolved in dimethylsulfoxide (300 μl), and trimethylsilylated with

hexamethyldisilazane (200 μl) and trimethylchlorosilane (100 μl) at 60°C for 30 min. The trimethylsilyl derivatives in the upper layer were subjected to gas chromatography (GC-FID: Shimadzu 17A) with an InertCap-1 column (GL Science NB1, 0.25mm i.d. ×30m) to determine the yields of erythronic acid (**E**) and threonic acid (**T**) in the ozonation product. The analytical conditions were as follows:

GC-FID: Oven temperature program: 120 ˚C, 5 min-4 ˚C /min→170 ˚C -10 ˚C /min→280 ˚C.

Injection tem. 250 ˚C; Detector temp. 280 ˚C; Column flow rate of He gas 1.9 ml/min; Splitting ratio 60:1; Injection volume 2 μl.

The calibration curves of commercial erythronic and threonic acid models with erythritol as an internal standard are shown in **Figure 4.2**.

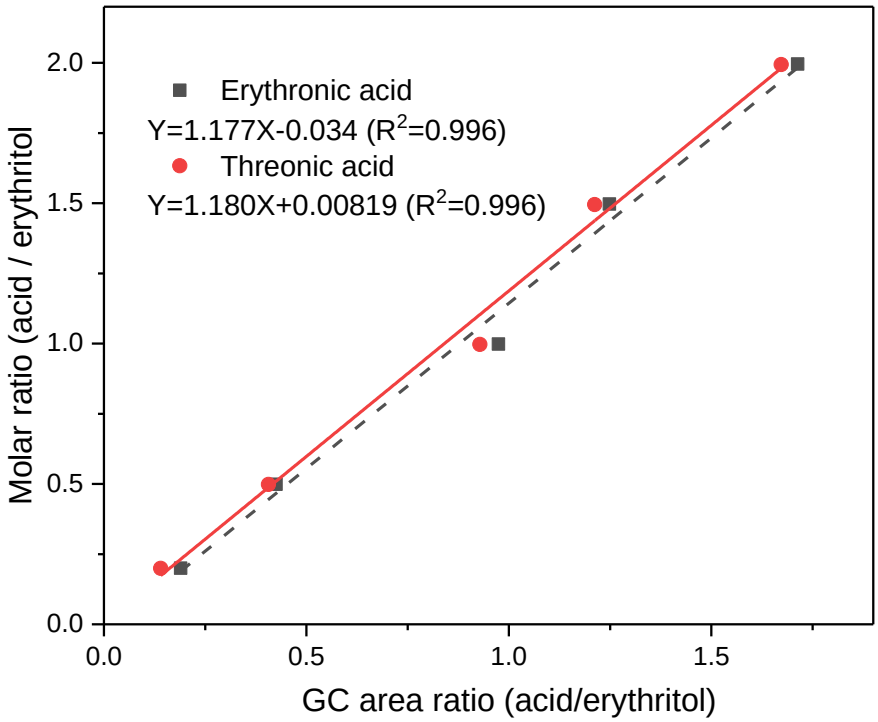

Figure 4.2 Calibration curves of erythronic and threonic acids with erythritol as internal standard (retention time in GC chorography: erythronic acid = 16.7 min, threonic acid = 17.2 min, erythritol = 15.8 min)

4.3 Results and discussion

4.3.1 General description

To examine lignin polymerization in vitro, dehydrogenation experiments with lignin precursors have carried out by Freudenberg et al.[21] The DHPs render it possible to elucidate most of the known structural detail of lignins based on the understanding of coupling modes of monolignols and of nucleophilic addition reactions to quinone methides intermediate. However, the characteristics of DHP samples vary with reaction conditions.[3,6] The rate of addition of monolignol to the dehydrogenative experiment is the key parameter for the structure of DHP.[22] The slow feeding method, known as *Zutropfverfahren*, gives rise to an "end-wise" polymerization with a higher molecular weight and higher amount of β-O-4 linkages in the DHP (more similar to native lignin). While the *Zulaufverfahren* method, which is feeding all monolignols at once, predominately produce the β–β or β-5 dilignols.[13] Also, it is reported that the DHP formed at pH 4–5 is more similar to native lignins than that at pH around 6–7. Regarding the enzyme, the highest oxidizing ability is at pH 4.5; however, acidic pH is not very favorable for its stability.[3,4] The discovery that the number of radical coupling and the formation of β-O-4 bonds increased as the proportion of organic solvent increased. Furthermore, there was a positive correlation between the ratio of organic solvent and the Molecular Weight (M. W.) of DHP.[3,5]

According to the model experiment involving the addition of water to **H**-type and **G**-type **QMs** in the Chapter 3, there is a gap between compression wood lignin analysis and model experiment results: *threo*-preferential formation, not the *erythro*-preferential was found in the water addition reaction with **QM-HH**, **QM-HG** and **QM-GH** compound. However, it would be worth exploring the effect of the solvent conditions, like lower pH condition or higher proportion of organic solvent on the stereoselective formation of β-O-4 structure from **QM**. Especially, the effect of β-etherified structure and its size may play an important role on that during the end-wise cross-coupling, where the monomer lignol radical, instead of dimerizing, reacts with phenolic structures on the growing chain. We conducted in vitro synthesis of lignin from **H**-type monolignols according to the improved

Zutropfverfahren method in different solvent condition to mimic the lignin polymerization in cell walls (**Figure 4.3**).

In this regard, we expected that β-O-4 structures in prepared **H**-type DHPs could undergo *erythro*-preferential formation from water addition to **QM** intermediate. To improve the *Zutropfverfahren* method used in this experiment, we consider from the following three perspective based on our model water addition experiment; a) to successfully obtain the DHP from *p*-coumaryl alcohol in the acidic condition; b) to successfully collect high yield of DHP from the organic solvent; c) to get an ideal DHP produced from end-wise cross-coupling reaction between monolignol and dimer or oligomer, instead of coupling between two growing chains. In the respect of typical *Zutropfverfahren* method, peroxidase was directly dissolved in buffer solution and generally accepted the supply of monolignol and H_2O_2 solutions. However, this operation is hardly realized in the acidic condition, especially at pH 3.5 due to the inactivation of enzyme.[3,22] Thus, we designed that peroxidase dissolved in small amount of water was added slowly at the same pace with feeding of monolignol and H_2O_2 solutions into pH 3.5 of buffer solution. In this way, there is enough time for the fresh peroxidase to oxidize the substrates before inactivation, then new peroxidase will be supplied continually to push the polymerization. Our improved *Zutropfverfahren* method in nature is also end-wise coupling.

As referred the **Figure 4.3**, if our assumption that the β-etherified structures with big size could result *erythro* form of β-O-4 structures in excess were true, there should be a positive relationship between the M.W. and *erythro/threo* ratio in DHP produced by end-wise coupling. Therefore, continually supply of *p*-coumary alcohol is very important in our experiment. Once we stop supplying the *p*-coumary alcohol into the end-wise polymerization, the experiment also should be stopped by adding the reductant to consume the H_2O_2 in case two growing chain would couple with each other through the biphenyl linkage or diaryl ethers linkage. This could influence the expected result due to the increased M.W. of DHP by two folds without the attendance of end-wise coupling. Another important consideration is the solvent condition. In convenient for comparison, we conducted similar buffered water-dioxane reaction condition as previous water addition to QMs experiment. Furthermore, to collect high yield of DHP product, it is necessary to collect the low molecular weight of DHP dissolving in dioxane by adding the NaCl powders into the reaction system to decrease the solubility

of DHP in the solvent system, then filtrate them by the hydrophilic PTFE membrane filter. Through in such procedures, an ideal **H**-type DHP could be obtained for satisfy our experimental requirement.

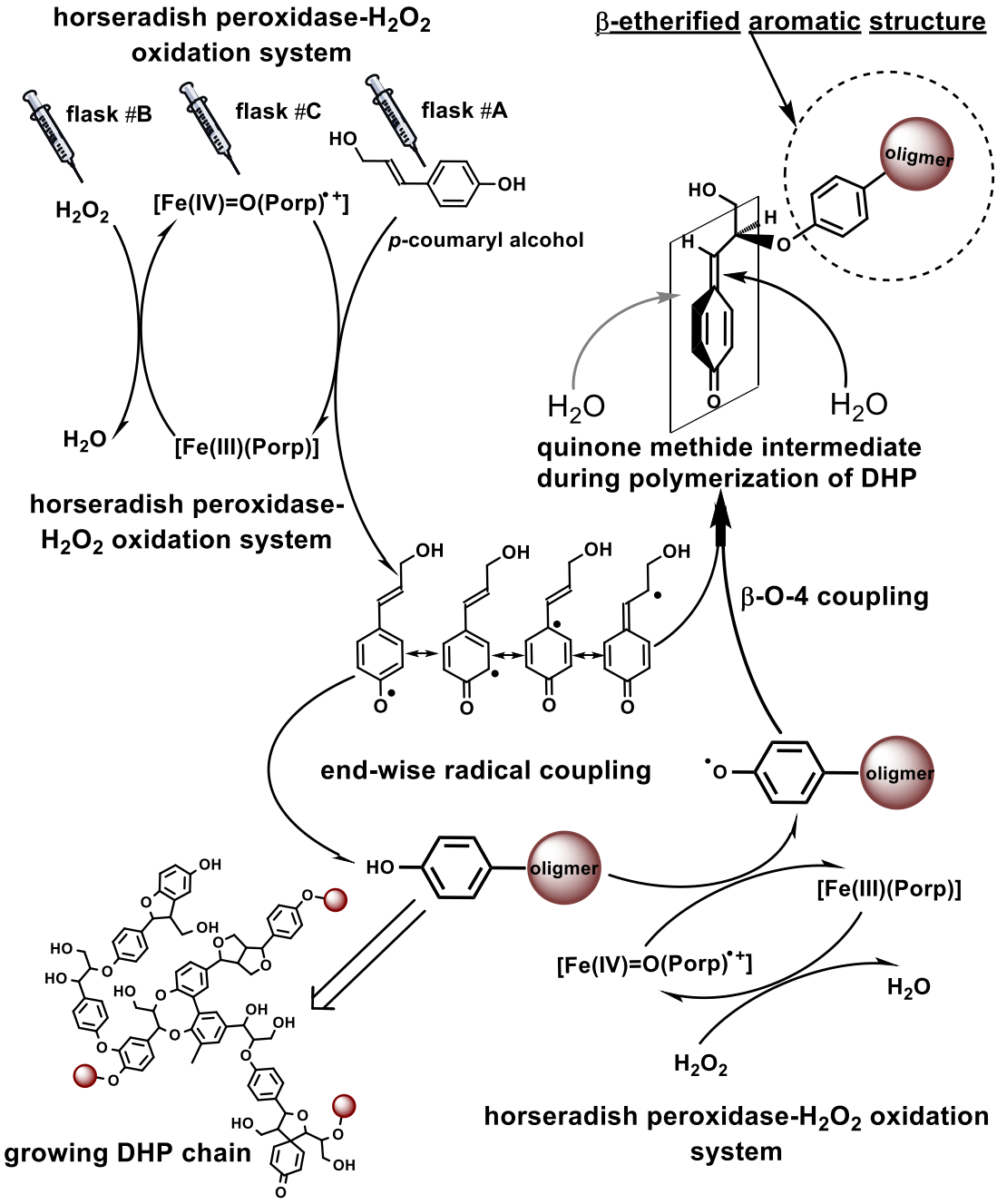

Figure 4.3 The formation of DHP from *p*-coumaryl alcohol through the end-wise radical coupling reaction

According to the structural characterization of DHP samples by the ozonation method (**Table 4.3**), even though the *erythro/threo* ratio of β-O-4 structure in all **H**-type DHP samples was higher than that of β-O-4 dimer from water addition to **H**-type **QMs**, *erythro* form of β-O-4 structure was not obtained

more than the *threo* form in the preparation of **H**-type DHP samples under any of the conditions employed here. It is worth noting that there are no significant differences between the distributration of *erythro* and *threo* forms in all **H**-type DHPs prepared with end-wise polymerization within the *threo*-dominated rang of 36/64 to 38/62.

Table 4.3. The ozonation analysis results for DHP samples prepared in different condition

DHP samples	pH	E+T (μmol/mg)	Percentage of E and T in the DHP	E/(E+T)	The volume of dioxane, ml	Dioxane/water (v/v)	Yield
H-Zutropf-3.5-30	3.5	0.288	5.75 %	37%	30	1:7	65.9 %
H-Zutropf-4.5-30	4.5	0.313	6.26 %	37%	30	1:7	97.8 %
H-Zutropf-5.0-30	5.0	0.346	6.91 %	36%	30	1:7	99.4 %
H-Zutropf-6.0-30	6.0	0.253	5.06 %	36%	30	1:7	99.6 %
H-Zulauf-6.0-30	6.0	0.094	1.88 %	32%	30	1:7	86.9 %
H-Zutropf-7.0-30	7.0	0.265	5.30 %	38%	30	1:7	100.7 %
H-Zutropf-5.0-10	5.0	0.323	6.47 %	36%	10	1:23	102.5 %
H-Zutropf-5.0-100	5.0	0.309	6.18 %	38%	100	1:1.4	52.0 %
G-Zutropf-6.0-30	6.0	0.977	19.54 %	55%	30	1:7	75.6 %
G-Zulauf-6.0-30	6.0	0.613	12.26 %	65%	30	1:7	59.5 %

By preparing the controlled **G**-type DHP sample from the coniferyl alcohol, we confirmed that the *erythro/threo* ratio of the **G**-type β-O-4 structure is higher than that of **H**-type β-O-4 structure, which is same as our water addition model experiment. The *erythro* form was slightly predominant in the β-O-4 structure of the prepared **G-Zutropf-6.0-30**. This was also ever reported for in vitro enzymatic dehydrogenation of a guaiacyl-type monolignol by Yelle et al., and the *erythro/threo* ratio was 51:49.[11]

The *erythro/threo* ratio of DHPs prepared with bulky polymerization (**H-Zulauf-6.0-30** and **G-**

Zulauf-6.0-30) are also listed in **Table 4.3**. The *erythro/threo* ratio of **H-Zulauf-6.0-30** (32/68) is lower than 36/64 for **H-Zutropf-6.0-30** prepared with end-wise polymerization. A similar β-O-4 dilignols with *erythro/threo* ratio, 18/82, in reference [23] were isolated from the coupling products of the *p*-coumaryl alcohol with bulky polymerization. Therefore, for preparing the **H**-type DHP, the end-wise polymerization is appeared to obtain higher *erythro/threo* ratio than the bulky polymerization. However, the opposite result was observed in the **G**-type DHP (**G-Zulauf-6.0-30)** prepared with bulky polymerization. Its *erythro/threo* ratio (65/35) is higher than 55/45 for **G-Zutropf-6.0-30** prepared with end-wise polymerization. The mechanism reason is still unknown for us.

4.3.2 Dissolvability of prepared DHP samples

The solubility of various DHP samples in different solvents are listed in **Table 4.1**. In general, the solubility of DHP samples prepared in the pH 3.5-5 is better than that from the pH 6 and 7; the solubility of DHP samples prepared in the solvent containing low volume of dioxane is better than that containing high volume of dioxane; for DHP samples prepared with the end-wise polymerization method, the solubility of **H**-type DHP is better than **G**-type DHP; the solubility of DHP prepared with bulky polymerization method is better than DHP prepared with end-wise polymerization. This is mainly due to the fact that they have different molecular weight, which will be discussed details in Section 4.3.4. Especially, it is unexpected that **G-Zutropf-6.0-30** prepared with improved end-wise polymerization method was very high polymer and its solubility in varied solvents was very low lever. Whereas normal **G**-type DHP has been conducted for many purposes with good solubility, such as studies on the diastereoselective microbial degradation of lignin and the characterization of wood lignin. A similar high polymer, of which molecular weight may be closed to that of natural lignin, was prepared with a dialysis membrane by Tanahashi et al.[13] That was also scarcely dissolved in any solvent.

4.3.3 HSQC spectra of DHP samples

In this work, we used HSQC spectroscopy to obtain further detailed structural characterization of the **H**-type DHP samples prepared in different reaction condition (**Figure 4.3**). It was confirmed that the **H**-type DHP sample prepared in the present study had an interunit linkage distribution typical of conventional DHP.[9] The HSQC peak patterns of the acetylated **H**-type DHP samples ($CDCl_3$ solvent) were extremely similar to each other, sharing different correlation peaks that can be assigned for β−O−4 **A**, β−5 (phenylcoumaran) **B**, and β−β (resinol) **C** in its aliphatic region. However, according to the contour level of correlation peaks for each linkages, DHP samples still rarely form β-O-4 linkages, so instead, monolignol radicals predominately produce β–β or β−5 linkages. The correlation peaks for dibenzodioxocins (5−5/β−O−4), which was an eight-membered ring structure resulting from radical coupling of a monolignol with a 5-5- coupled end unit, producing mainly threonic acid through ozonation[24], were not found in all HSQC spectra. The cinnamyl alcohol end groups **D**, arisen from monomer-monomer coupling and were therefor indicating the degree of polymerization: the strong $\mathbf{D}_{\beta}$- and $\mathbf{D}_{\gamma}$-C/H correlation peaks implied that the degree of end-wise polymerization in these DHP samples may still not as high as the nature lignin. Note, in addition, that the arylglycerol structures **E** observed in the DHP samples are also present in the HSQC spectra of MWL, as noted previously. It was suspected that this structures not only can be produced in DHP under oxidative coupling reaction conditions, but also they may be, at least in part, authentic units in the native lignin.[9] Thus, we need take lots of attention on discussion about *erythro*/*threo* ratio of β−O−4 in DHP samples because this structure also could yield erythronic and threonic aicds through ozonation.

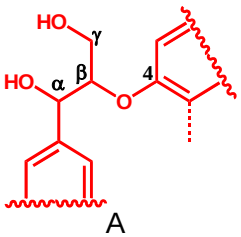

A
ß-aryl ether (ß-O-4)

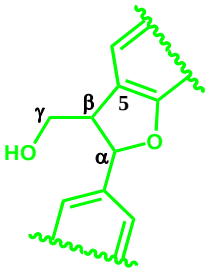

B
phenylcoumaran (ß-5)

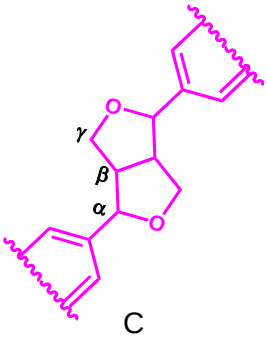

C
resinol (ß-ß)

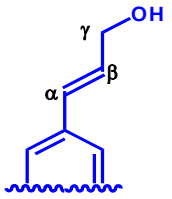

D
cinnamyl alcohol

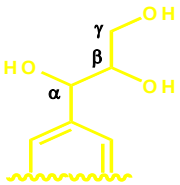

E
arylglycerol

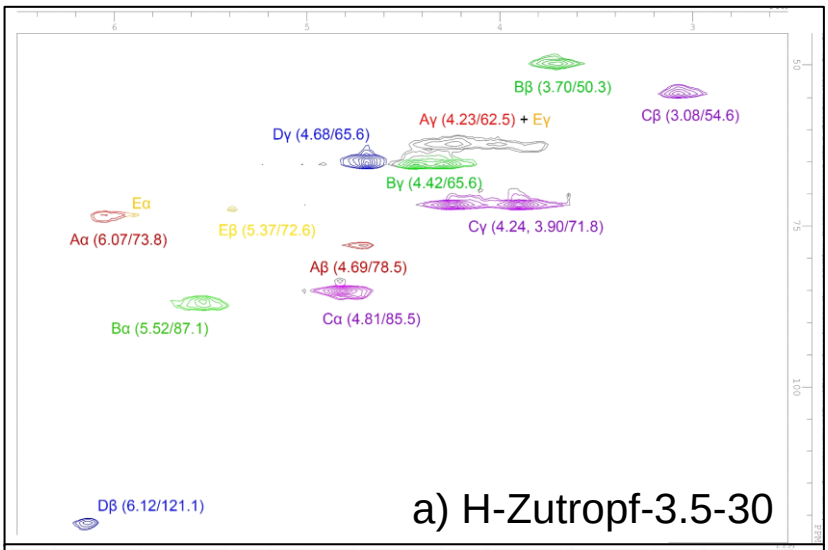

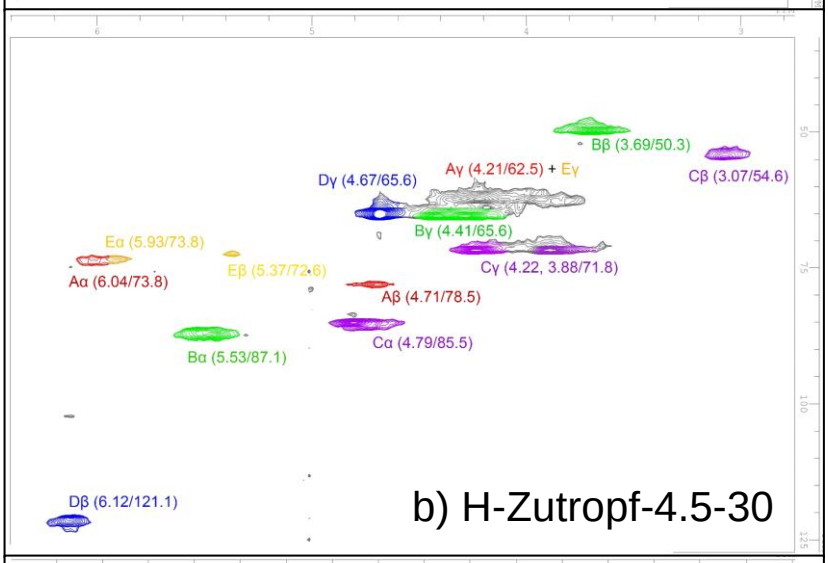

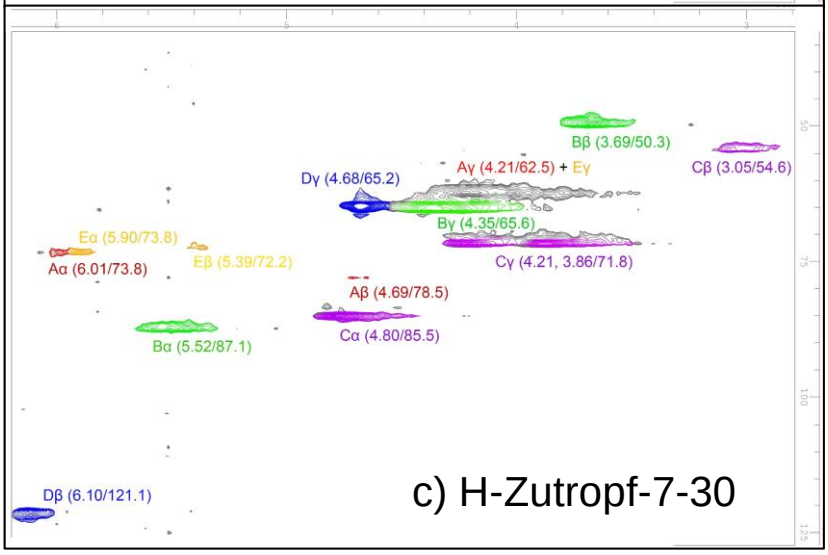

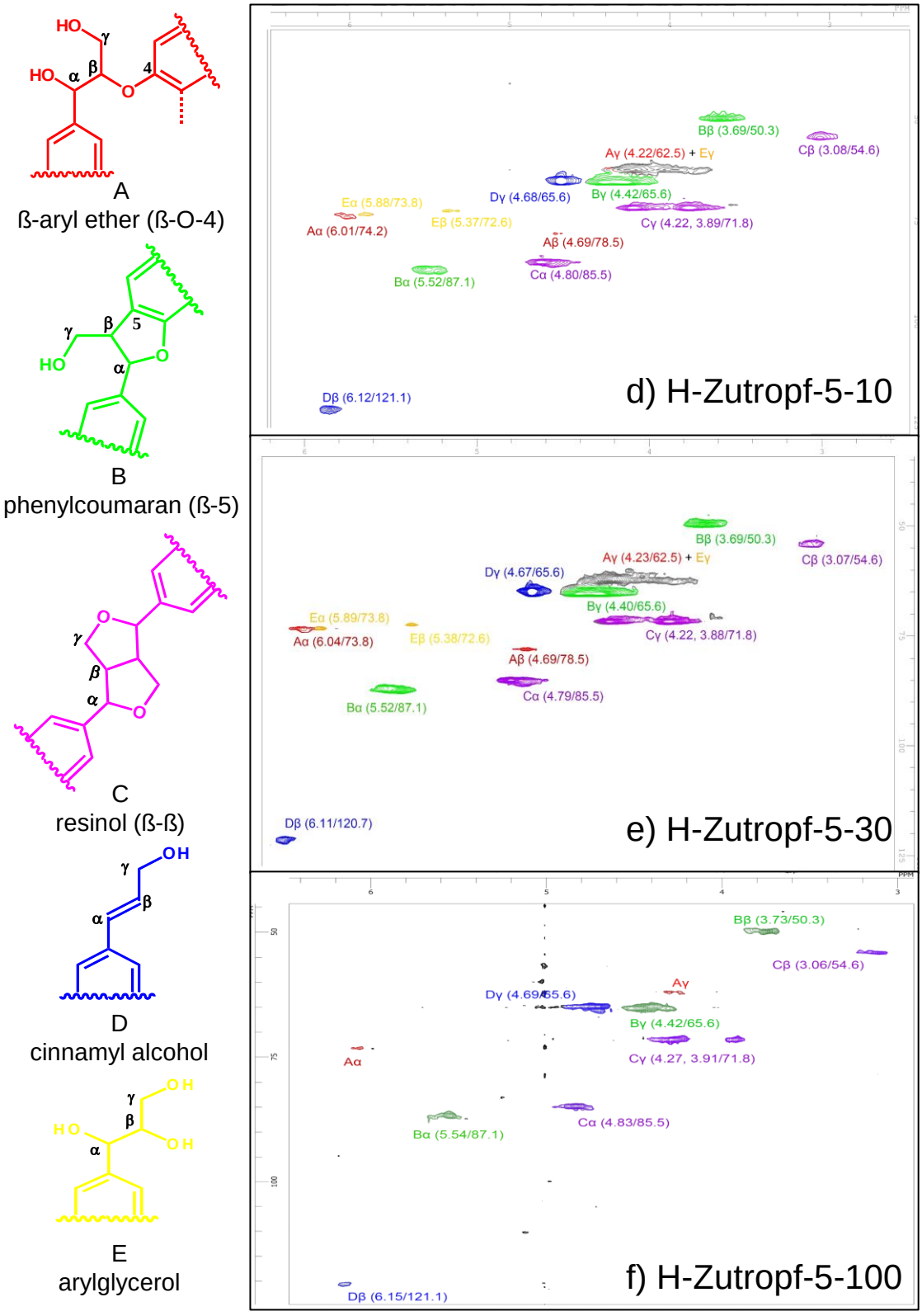

Figure 4.3 Side chain regions of short-rang ^{13}C-^{1}H correlation (HSQC) spectra of the acetylated **H**-type DHP samples.

4.3.4 GPC analysis of soluble prepared DHP samples

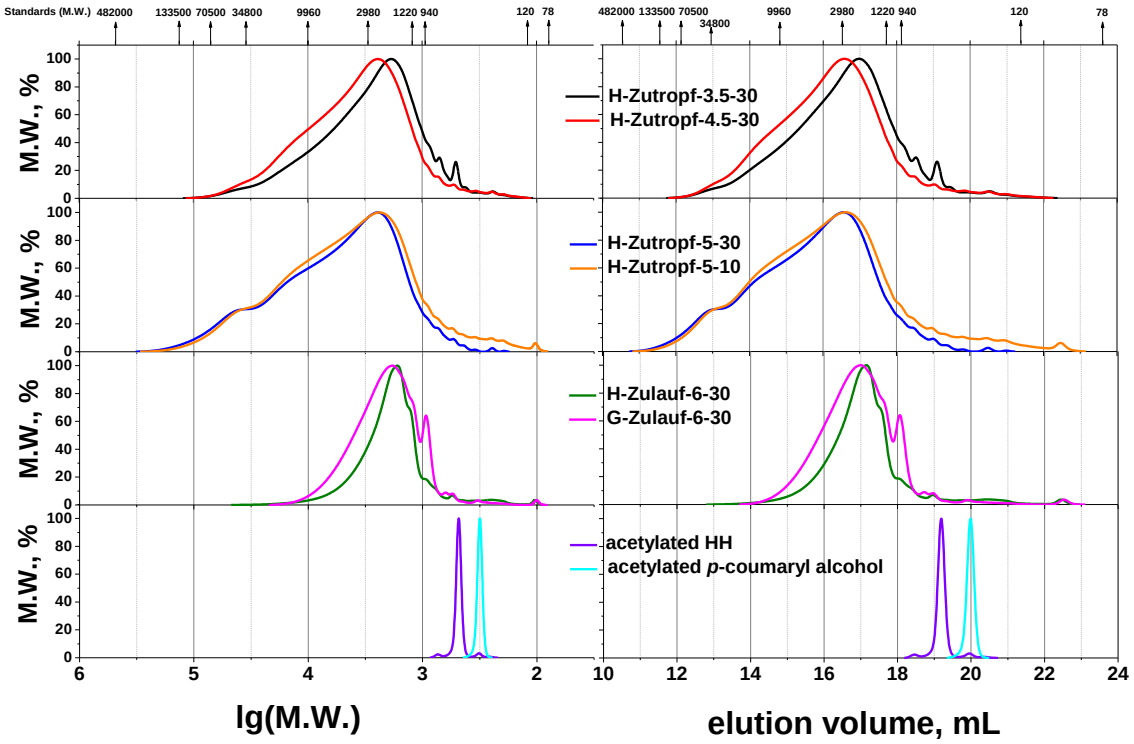

Figure 4.4 GPC spectra of THF-soluble acetylated DHP samples at 280 nm.

The GPC spectra of THF-soluble acetylated DHP samples are shown in **Figure 4.4**. The average molecular weights and polydispersity index are shown in **Table 4.4**. GPC analysis showed that pH condition had a clear effect on the degree of polymerization (**Table 4.4**). Higher weight average molecular weight (Mw) DHPs were produced under pH of 3.5 to 5 and also higher order of polydispersity (PDI) values were obtained in the pH5＞pH 4.5＞pH 3.5 which indicates that very heterogeneous distributions were obtained. The pH effects on molecular weight of DHPs have been proposed that the enzymatic deactivation happened in the acidic condition and neutral condition was very favorable for stability of enzyme, thus resulting the higher molecular weight of DHP generated in the higher pH condition.[3] By combining this molecular weight increasing trend as pH and the dissolution of DHPs prepared in different pH (**Table 4.1**), DHPs prepared in pH 6 and 7 with end-wise polymerization method (**H-Zutropf-6-30** and **H-Zutropf-7-30**) should be higher in molecular weight than those prepared in pH 5, 4.5 and 3.5 (**H-Zutropf-3.5-30**, **H-Zutropf-4.5-30** and **H-Zutropf-5-30**).

This analysis also indicated that DHPs (**H-Zutropf-3.5-30**, **H-Zutropf-4.5-30** and **H-Zutropf-5-30**) were higher in molecular weight and polydispersity than DHPs (**H-Zulauf-6-30** and **G-Zulauf-7-30**). We thus can conclude the average molecular weights of DHP prepared with bulky polymerization method (**H-Zulauf-6-30** and **G-Zulauf-6-30**) are smaller than the average molecular weights for DHPs prepared with end-wise polymerization method (**H-Zutropf-6-30** and **G-Zutropf-6-30**), although none of molecular weight results for their THF-insoluble acetylated derivatives were shown in here. To evaluate the effect of the solvent on the degree of polymerization for DHP, only one pH condition (pH=5) was chosen as if the pH condition goes beyond 5, DHP with bad dissolution in THF will be prepared. The **H-Zutropf-5-30** prepared in 12.5% dioxane solution had higher molecular weights than **H-Zutropf-5-10** prepared in 4% dioxane solution. This is easily understood to mean that DHPs are precipitated in the low volume ratio of dioxane to water during polymerization, which prevents further radical coupling from producing high molecular weight of DHP.[5] Thus, it is able to imagine that the molecular weight of **H-Zutropf-5-100** is higher than that of **H-Zutropf-5-30** and **H-Zutropf-5-30** due to the bad dissolution of **H-Zutropf-5-100** in varied solvents (**Table 4.1**).

Table 4.4 Average molecular weights and polydispersity indices of soluble prepared DHP samples

	H-Zutropf-3.5-30	H-Zutropf-4.5-30	H-Zutropf-5-30	H-Zutropf-5-10	H-Zulauf-6-30	G-Zulauf-6-30
Mn	1642	2022	2780	1593	1278	1507
Mw	4715	5959	11099	9296	2250	2460
Mp	1866	2437	2455	2401	1655	1839
Mw/Mn	2.87	2.95	3.99	5.84	1.76	1.63

4.3.5 *erythro*/*threo* ratio of β-O-4 structures in DHP samples

On the basis of the total yields of erythronic (**E**) and threonic (**T**) acids obtained by ozonation, the β-O-4 structures in the DHP samples were further characterized (**Table 4.3**). The total yields of the ozonation products (**E**+**T**) from **H**-type DHP samples prepared by end-wise polymerization were 0.25-0.35 mmol g^{-1} DHP, whereas the yield of the ozonation products ((**E**+**T**) of **H-Zulauf-6-30** prepared with bulky polymerization was much lower (0.09 mmol g^{-1} DHP). For the **G**-type DHP (**G-Zutropf-6-30**), which was prepared by end-wise polymerization method, was very high (0.93 mmol g^{-1} DHP).

However, the **G-Zulauf-6-30** prepared with bulky polymerization was also lower at total yields of the ozonation products (**E**+**T**) than **G-Zutropf-6-30.** This result was consistent with literature report [4] that end-wise polymerization can produce DHP with more β-O-4 structures than bulky polymerization does.

Effect of pH condition on the *erythro*/*threo* ratio

Under all pH conditions used, the trend that the *erythro/threo* ratio tended to be higher under more acidic condition, which we found in our model water addition to QMs experiment, was not observed in the **H**-type DHP samples within the pH rang of 3.5 to 7. The interpretation is that the effect of pH on **H**-type DHP is limited based on the previous water addition result: a higher *erythro*-selectivity was obtained on **QM-HH** by changing the pH from 7 to 3.5 with +Δ6% *erythro* isomer for **HH**. This pH effect may be easily negligible during producing **H**-type DHP because of its low amount of β-O-4 structures. The total yields of erythronic (**E**) and threonic (**T**) acids from β-O-4 structures in **H**-type DHP samples were from 5.8% to 6.9% (assuming that the C9 units have a molecular weight of 200).

Effect of solvent condition on the *erythro*/*threo* ratio

In this experiment, three **H**-type DHP samples (**H-Zutropf-5-10**, **H-Zutropf-5-30** and **H-Zutropf-5-100**) were synthesized from *p*-coumaryl alcohol in a mixture of buffer and dioxane with volume ratios of 10:230, 30:210, and 100:140 in the presence of horseradish peroxidase and H_2O_2 at pH 5 condition. As shown in **Table 4.3**, the total yields of erythronic (**E**) and threonic (**T**) acids from ozonation of these three **H**-type DHP samples were almost constant, from 6.2% to 6.9%. Interestingly, when the ratio of dioxane/buffer increased, that is, the *erythro/threo* ratio of corresponding DHP samples increased slightly from 36/64 to 38/62 (**Table 4.2**). This result could be related to the trend we found in our previous water addition to **QM-HH** experiment in different dioxane/water ratio condition: the *erythro/threo* ratio of **QM** with β-etherified *p*-hydroxyphenyl ring increased as the increasing volume percentage of dioxane in reaction solution. Thus, the observed increasing *erythro/threo* ratio may be the result of stereo-selective water addition to a non-substituted quinone methide intermediate (**H**-type **QM**) during biosynthesis, and the selectivity is different for **H**-type β-

etherified structure in different dioxane/water ratio condition. However, as shown in **Table 4.4**, it is also possible related to the higher molecular weight of DHP prepared in higher volume of dioxane. As a consequence, the addition of solvent increases the polymer's molecular weight by increasing its solubility during polymerization and inducing formation of more *erythro* form of β-O-4 structures.

4.3.6 Implications from the *erythro/threo* ratio of DHP samples

Continuing our previous water addition experiment with simple dimer or trimer **QM** compounds, a more complicate and similar lignin models, DHP, were used to further understanding of the relationship between lignin aromatic type (guaiacyl- or *p*-hydroxyphenyl type) and the yield of *erythro* and *threo* form of β-O-4 structures during lignin biosynthesis. The **H**-type DHP and **G**-type DHP were separately prepared from *p*-coumaryl alcohol and coniferyl alcohol in the similar reaction condition with previous used on water addition to **H**-type QM or **G**-type **QM** models. These DHP samples were further characterized by same ozonation method with the wood meals analysis.[18-20] The amount of β-O-4 structures and their *erythro*/*threo* ratios were calculate based on the yields of erythronic and threonic acids, which were released from the side-chain of the β-O-4 structures by ozonation. In all DHP samples, the total yield of erythronic and threonic acid of the **G**-type DHP was higher than that of the yield of the **H**-type DHP (see **Table 4.3**). The interpretation is that β-O-4 structures are much more abundant in the **G**-type DHP than those in the **H**-type DHP. Similar results were also found in compression wood lignin analysis, e.g. the erythronic and threonic acids yields from pine samples are negatively correlated with the corresponding proportion of **H**-units detected by the alkaline NBO method.[19] These imply that the frequency of the β-O-4 coupling reaction during lignin polymerization is low when the proportion of **H**-units is high.

If a comparison was focused on the *erythro/threo* ratio, the *erythro/threo* ratio obtained from both of **H**-type DHP and **G**-type DHP was higher than that obtained from water addition to **H**-type and **G**-type **QM** dimers, and closer to the ratio found in compression wood. The proportion of *erythro* and *threo* forms of β-O-4 structures was nearly 38:62 in the **H-Zutropf-7.0-30**, but the proportion of the *erythro* form was slightly higher than *threo* form in the **G-Zutropf-6.0-30**: the *erythro*/*threo* ratio was 55:45. In the previous ozonation analysis of five gymnosperm species that are mostly composed of G-

type aromatic structures, the proportion of *erythro* form in the total amount of β-O-4 structures was within the 50.0%±0.6% range.[18] The *erythro/threo* ratio in the **G-Zutropf-6.0-30** was outside this range, thus indicating that it is possible even for the **G**-type QM to obtain the *erythro*-preferential formation of β-O-4 structure without the attendance of **S**-type units. The *erythro/threo* ratio of β-O-4 structures in DHP samples seems to be related to their molecular weight. For example, the **H-Zutropf-6.0-30** prepared by end-wise polymerization with higher molecular weight produce higher *erythro/threo* ratio of β-O-4 structures than the **H-Zulauf-6.0-30** prepared by bulky polymerization. Also, the DHP samples (**H-Zutropf-5.0-100** and **H-Zutropf-7.0-30**) with high *erythro/threo* ratio of β-O-4 structures have much high molecular weight. This may be under the effect of the β-etherified structures and their size in the QM intermediate during DHP synthesis. Although in this case of **H**-type DHP, the formation of the *erythro* configuration was not dominating during cross coupling between a monolignol radical and phenolic structures on the growing chain. In the previous model experiment with the similar reaction condition as preparation of **H**-type DHP, however, water addition to an **H**-type QM with a 3-methoxyphenyl-substituted β-etherified aromatic ring (**QM-H-HH$_{biphenyl}$** model in chapter 3) promoted the *erythro* form. It was suggested that local steric hindrance by the β-etherified structures may be present in the β-O-4 ether quinone methide intermediate and that the possibility for *erythro* preferential formation of β-O-4 structures during the water addition has to be considered. It also means that the degree of stereo-selectivity was according on the position difference of substituents on the β-etherified structures, e.g. the β-etherified structures with the 3- or 5-substitutions have more chances than 1-substitutions to result the *erythro* form.

4.4 Conclusions

By using the improved *Zulaufverfahren* and *Zulaufverfahren* method, a series of **H**-type DHP samples and controlled **G**-type DHP samples were prepared from *p*-coumaryl alcohol and coniferyl alcohol, respectively, in different reaction condition. We thus propose the potential role of the reaction solvent and β-etherified structures and its size in stereo-selectivity of water addition to β-O-4 ether quinone methide intermediate during lignin polymerization. Based on the ozonation method, even though both the *erythro/threo* ratio of **H**-type DHP and **G**-type DHP were improved by comparison of the results from water addition experiments using different β-O-4-aryl ether QM models, the *threo* form of β-O-4 structures were still produced in excess during the polymerization of **H**-type DHP in any conditions employed here. The proportion of *erythro* form of β-O-4 structures was relatively same in the pH rang 3.5-7. This pH-dependent trend was not consistent with findings from the previous study on **H**-, **G**-, and **S**-type lignin-related quinone methide models. Whereas, the solvent-dependent trend was in line with observations from the previous study on non-substituted quinone methides, e.g. the proportion of *erythro* isomer was higher at a higher volume percent of dioxane in aqueous condition. The β-etherified structures of β-O-4-aryl ether quinone methide intermediate, especially its 3- or 5- substituted groups was suggested to be an important factor in understanding the mechanism of stereo-selective water addition to different types of quinone methide intermediate during lignin polymerization.

4.5 References

[1] Ralph, J., Lundquist, K., Brunow, G., Lu, F., Kim, H., Schatz, P. F., ... & Boerjan, W. 2004. Lignins: natural polymers from oxidative coupling of 4-hydroxyphenyl-propanoids. Phytochemistry Reviews, 3(1-2), 29-60.

[2] Landucci, L. L. 2000. Reaction of *p*-hydroxycinnamyl alcohols with transition metal salts 3. Preparation and NMR characterization of improved DHPs. Journal of Wood Chemistry and Technology, 20(3), 243-264.

[3] Taboada-Puig, R., Lú-Chau, T. A., Moreira, M. T., Feijoo, G., Lema, J. M., Fagerstedt, K., & Tamminen, T. 2018. Polymerization of coniferyl alcohol by Mn^{3+}-mediated (enzymatic) oxidation: Effects of H_2O_2 concentration, aqueous organic solvents, and pH. Biotechnology Progress, 34(1), 81-90.

[4] Shigeto, J., Honjo, H., Fujita, K., & Tsutsumi, Y. 2018. Generation of lignin polymer models via dehydrogenative polymerization of coniferyl alcohol and syringyl alcohol via several plant peroxidases involved in lignification and analysis of the resulting DHPs by MALDI-TOF analysis. Holzforschung, 72(4), 267-274.

[5] Hwang, H., Moon, S. J., Won, K., Kim, Y. H., & Choi, J. W. 2015. Parameters affecting in vitro monolignol couplings during dehydrogenative polymerization in the presence of peroxidase and H_2O_2. Journal of Industrial and Engineering Chemistry, 26, 390-395.

[6] Yoshida, S., Chatani, A., Tanahashi, M., Honda, Y., Watanabe, T., & Kuwahara, M. 1998. Preparation of synthetic lignin by manganese peroxidase of Bjerkandera adusta in organic solvents. Holzforschung, 52(3), 282-286.

[7] Kobayashi, T., Taguchi, H., Shigematsu, M., & Tanahashi, M. 2005. Substituent effects of 3, 5-disubstituted *p*-coumaryl alcohols on their oxidation using horseradish peroxidase–H_2O_2 as the oxidant. Journal of Wood Science, 51(6), 607.

[8] Sarkanen, K. V., Hergert, H. L. 1971. In lignins: occurrence, formation, structure, and reactions, Wiley-Interscience: New York, pp 43−94.

[9] Ralph, J., Akiyama, T., Kim, H., Lu, F., Schatz, P. F., Marita, J. M., & Dixon, R. A. 2006. Effects

of coumarate 3-hydroxylase down-regulation on lignin structure. Journal of Biological Chemistry, 281(13), 8843-8853.

[10] Terashima, N., Akiyama, T., Ralph, S., Evtuguin, D., Neto, C. P., Parkås, J., & Ralph, J. 2009. 2D-NMR (HSQC) difference spectra between specifically ^{13}C-enriched and unenriched protolignin of Ginkgo biloba obtained in the solution state of whole cell wall material. Holzforschung, 63(4), 379-384.

[11] Yelle, D. J., Kapich, A. N., Houtman, C. J., Lu, F., Timokhin, V. I., Fort, R. C., & Hammel, K. E. 2014. A highly diastereoselective oxidant contributes to ligninolysis by the white rot basidiomycete Ceriporiopsis subvermispora. Applied and Environmental Microbiology, AEM-02111.

[12] Bonawitz, N. D., Im Kim, J., Tobimatsu, Y., Ciesielski, P. N., Anderson, N. A., Ximenes, E., & Chapple, C. 2014. Disruption of Mediator rescues the stunted growth of a lignin-deficient Arabidopsis mutant. Nature, 509(7500), 376.

[13] Tanahashi, M., Higuchi, T. 1981. Dehydrogenative polymerization of monolignols by peroxidase and H_2O_2 in a dialysis Tube. I.: preparation of highly polymerized DHPs. Wood Research No. 67, 29-42.

[14] Quideau, S., Ralph, J. 1992. Facile large-scale synthesis of coniferyl, sinapyl, and *p*-coumaryl alcohol. Journal of Agricultural and Food Chemistry, 40(7), 1108-1110.

[15] Ralph, S. A., Ralph, J., Landucci, L. L. 2009. NMR database of lignin and cell wall model compounds, https://www.glbrc.org/ databases_and_software/nmrdatabase/.

[16] Hauteville, M., Lundquist, K., Von Unge, S. 1986. NMR studies of lignins. 7. ^{1}H NMR spectroscopic investigation of the distribution of *erythro* and *threo* forms of β-O-4 structures in lignins. Acta Chemica Scandinavica, 31-35.

[17] Sipilä, J., Syrjänen, K. 1995. Synthesis and ^{13}C NMR spectroscopic characterisation of six dimeric arylglycerol-β-aryl ether model compounds representative of syringyl and *p*-hydroxyphenyl structures in lignins. on the aldol reaction in β-ether preparation. Holzforschung-International Journal of the Biology, Chemistry, Physics and Technology of Wood, 49(4), 325-331.

[18] Akiyama, T., Goto, H., Nawawi, D. S., Syafii, W., Matsumoto, Y., Meshitsuka, G. 2005. *Erythro*/*threo* ratio of β-O-4 structures as an important structural characteristic of lignin. Part 4:

Variation in the *erythro*/*threo* ratio in softwood and hardwood lignins and its relation to syringyl/guaiacyl ratio. Holzforschung, 59(3), 276-281.

[19] Nawawi, D. S., Akiyama, T., Syafii, W., Matsumoto, Y. 2017. Characteristic of β-O-4 structures in different reaction wood lignins of Eusideroxylon zwageri T. et B. and four other woody species. Holzforschung, 71(1), 11-20.

[20] Akiyama, T., Sugimoto, T., Matsumoto, Y., Meshitsuka, G. 2002. *Erythro*/*threo* ratio of β-O-4 structures as an important structural characteristic of lignin. I: Improvement of ozonation method for the quantitative analysis of lignin side-chain structure. Journal of Wood Science, *48*(3), 210-215.

[21] Freudenberg, K. 1968. The constitution and biosynthesis of lignin. In: Constitution and Biosynthesis of Lignin. Eds. Freudenberg, K. and Neish, A.C. Springer, Berlin, pp. 47–122.

[22] Taboada-Puig, R., Lú-Chau, T., Moreira, M. T., Feijoo, G., Martínez, M. J., Lema, J. M. 2011. A new strain of Bjerkandera sp. production, purification and characterization of versatile peroxidase. World Journal of Microbiology and Biotechnology, 27(1), 115-122.

[23] Nakatsubo, F., Higuchi, T. 1975. Enzymic dehydrogenation of *p*-coumaryl alcohol. III. Analysis of dilignols by Gas Chromatography and NMR spectrometry. Wood Research No. 58, 12-19.

[24] Lundquist, K., Langer, V., Li, S., Stomberg, R. 2003. Lignin stereochemistry and its biosynthetic implications. In 12th International Symposium on Wood and Pulping Chemistry, Madison, Wisconsin, USA, June 9-12 2003 (Vol. 1, pp. 239-244).

Chapter 5

Summary

Water addition to *p*-quinone methide (**QM**) intermediate is the post-coupling rearomatization reaction to form the β-O-4 structure during lignification. The resultant β-O-4 structure has two distinct, chemically different, isomeric forms, commonly known as *erythro* (**E**)- and *threo* (**T**)-forms. Previous studies of reaction wood lignin showed that β-O-4 structures in compression wood were slightly predominant in *erythro* form whereas the *erythro/threo* (**E**/**T**) ratio in the opposite wood was 50:50.[1, 2] The distribution of the **E**/**T** ratio in the reaction wood disc was positively correlated with that of *p*-hydroxyphenyl/guaiacyl (**H**/**G**) ratio, implying that the *erythro*-preferential formation occurred during lignin biosynthesis, and is related to the H-unit of aromatic ring type. However, this phenomenon has never been studied in detail by model study.

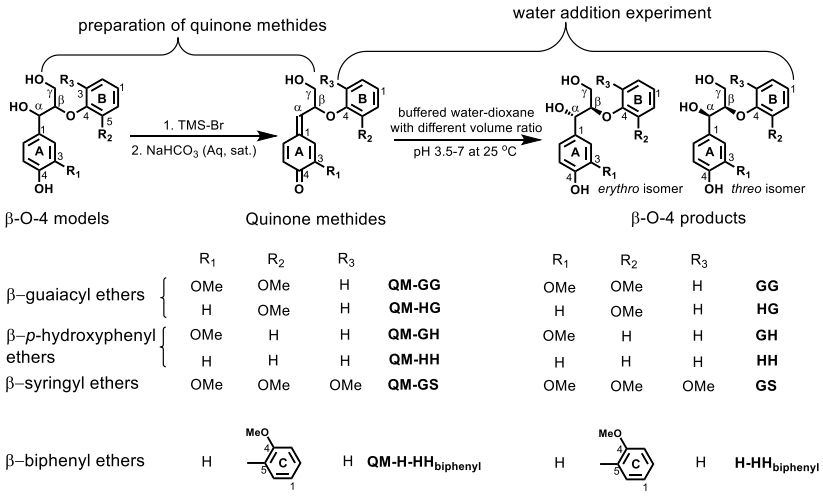

Scheme 1 Water addition experiment on quinone methides

In this study, model experiments mimicking the **E**/**T** ratio determining-step for β-O-4 structures during lignin biosynthesis were performed to characterize lignin formation in compression wood. Five types of quinone methides (**QM-GG**, **QM-GH**, **QM-HG**, **QM-HH**, and **QM-H-HH$_{biphenyl}$)** were synthesized from corresponding β-O-4 models carrying **H**-, **G**-, and **biphenyl**-units [**GG**, **GH**, **HG**, **HH**, and **H-HH$_{biphenyl}$**, respectively. (ex. **GH**: guaiacylglycerol-β-*p*-hydroxyphenyl ether, **H-HH$_{biphenyl}$**: *p*-hydroxyphenyl glycerol-β-biphenyl ether)]. As shown in **Scheme 1**, the water addition to the **QMs** was examined in different buffered dioxane-water solution (pH varying: 3-7 or dioxane/water ratios varying: 1/79-1/1, v/v). Then, the reactivity and stereo-selectivity of these QMs with water under the influence of pH and dioxane-water ratio were separately discussed in Chapter 3.

To confirm the above results from water addition to **QMs** more, a series of **H**-type **DHP** (dehydrogenation polymers) and controlled **G**-type **DHP** samples were prepared from *p*-coumaryl alcohol and coniferyl alcohol, respectively, in different reaction condition (pH varying: 3-7 or dioxane/water ratios varying: 1/23-1/1.4, v/v) by using the end-wise and bulky polymerization in Chapter 4. Their chemical structures, molecular weight distribution and **E**/**T** ratio of β-O-4 structures were determined.

5.1 Reactivity of quinone methides with water

As discussed in Chapter 3, the β-O-4 dimer products were obtained from these five **QMs** in satisfactory yield (70-94% yield), indicating that the water addition was the main reaction in these experiments. The half-lives ($t_{1/2}$) of the **QMs** were used to compare the reaction rates of water addition to **QMs**. In the respect of reaction condition for the water addition, either lowing pH condition or lowing volume percentage of dioxane in reaction solution can accelerate the reaction rate of water addition to any **QM** models. However, under every reaction condition, the half-lives ($t_{1/2}$) of **QMs** tended to be shorter in the order of **QM-HH** < **QM-HG** < **QM-GH** < **QM-GG.** Thus, the structural type of both a **QM** moiety and a β-etherified aromatic ring structure seem to affect the reaction rate, but the effect of the **QM** moiety is larger than that of a β-etherified aromatic ring structure. Moreover, noticeable differences in the $t_{1/2}$ were found between **QMs** carrying **H**-type aromatic nucleus and **G**-type aromatic nucleus. This is because of the methoxy group at the 3-position of the aromatic nucleus.

5.2 Stereo-preferential formation of β-O-4 structures from quinone methide

In the present study, *erythro*-preferential formation, which we assumed based on the previous result of chemical analysis of compression wood lignin, [1, 2] was not found in the β-O-4 products from neither water addition to **QM** dimers (Chapter 3) nor **H**-type **DHP** samples (Chapter 4) at any conditions employed here, *threo*-preferential formation was unexpectedly observed from them. However, in Chapter 3, the proportion of *erythro* form could be improved by changing the pH

condition, solvent condition and aromatic nucleus structures of **QM** models. Furthermore, *erythro*-preferential water addition can occur to a novel **H**-type **QM** β-etherified by a biphenyl structure (**QM-H-HH$_{biphenyl}$**) although the reaction mechanism causing the stereo-preference remains unknown.

The effect of pH condition

Throughout all water addition to **QMs** experiments conducted in Chapter 3, the *erythro/threo* ratio varied significantly, and tended to be higher at a lower pH condition within the pH 3.5 to 7.0. This pH-dependent trend for **H**-, **G**-type is consistent with the syringyl (**S)**-type **QMs** reported by Brunow et al..[3] However, this trend was not observed in Chapter 4 through preparing **H**-type **DHPs** from *p*-coumaryl alcohol under different pH conditions. The proportion of *erythro* form of β-O-4 structures in these **H**-type **DHPs** were relatively same in the pH 3.5 to pH 7.0.

The effect of solvent condition

From the Chapter 3, the *erythro/threo* ratio of β-O-4 products from water addition to **QMs** is also influenced by the presence of dioxane. By changing the volume percentage of dioxane in solution from 1% to 50%, the *erythro/threo* ratio of β-O-4 products varied and tended to different trend depending on the β-etherified aromatic ring structure of corresponding **QMs**. In other words, the effect of the volume percentage of dioxane on the stereo-preference of **QMs** with water is related to their β-etherified aromatic ring structures regardless of the **QM** moiety structures. For the water addition experiment in dioxane-buffered solution at a same pH condition, the *erythro/threo* ratio of β-O-4 products from **QMs** with β-etherified guaiacyl unit decreased as an increase of volume percentage of dioxane. In contrast, the *erythro/threo* ratio of β-O-4 products from **QMs** with β-etherified *p*-hydroxyphenyl ring showed an increasing trend. Even though the effect of pH on the stereo-preferential formation of β-O-4 structures from **QMs** can be observed in every solution with different volume percentage of dioxane, such effect is larger in the solution containing 50% of dioxane than 1% of dioxane. However, same as the effect of pH on the **H**-type DHP, the clear relationship between the **E**/**T** ratio of β-O-4 structures in **H**-type **DHPs** and dioxane/water ratios was not found in Chapter 4.

The effect of aromatic nucleus structures

As described in Chapter 3, the *threo*-selectivity was always higher in the order of **QM-HH**>

QM-GH＞**QM-HG**＞**QM-GG** at any reaction condition used in here. In detail, the formation of *threo*-isomer was more favorable in the **H**-type **QM** (**QM-HH**, **QM-HG**) than the **G**-type one (**QM-GH**, **QM-GG**), and in the β-O-4 *p*-hydroxyphenyl ether **QM** (**QM-HH**, **QM-GH**) than in the guaiacyl ether **QM** (**QM-HG**, **QM-GG**). Both the **QM** moiety and β-etherified aromatic ring structures influenced the *threo*-selectivity, but the effect of β-etherified aromatic ring was larger than that of **QM** moiety. To investigate the effect of β-etherified aromatic ring and its size in more detail, a novel **H**-type lignin **QM** model β-etherified with a biphenyl unit (see **Scheme 1**, **QM-H-HH$_{biphenyl}$**) was subjected with water in the Chapter 3, and **H**-type **DHPs** were produced by the end-wise and bulky polymerization methods in Chapter 4. Interestingly, *erythro*-selective water addition can occur to the novel lignin-related **QM-H-HH$_{biphenyl}$** trimer, which is same as our expectation based on the previous observation of the slight but clear *erythro* preference of β-O-4 structures in compression wood lignins. [1, 2] While, in the respect of **QM** intermediates derived from β-O-4-coupling (of monolignols or/and the phenolic end of the growing polymer) during polymerization of **H**-type **DHP**, even though the *erythro/threo* ratios of **H**-type **DHP** were improved in comparison with the results from water addition to **QM-HH** dimer in Chapter 3, the *threo* form of β-O-4 structures were still produced in excess in any reaction conditions. Additionally, considering that the **H**-type **DHP** with large molecular weight prepared from end-wise polymerization contains higher **E**/**T** ratio of β-O-4 structures than that with small molecular weight prepared from bulky polymerization, it is appeared that there is a relationship between the size of β-etherified moiety of **QM** and stereo-preferential formation of its corresponding β-O-4 product.

5.3 Implication from this model experiment

As mentioned in Chapter, the **H**-type **QM** reacted faster than the **G**-type **QM**. This result implies that the rapid aromatization in **H**-type **QMs** may provide an advantage over **G**-type one for efficiently driving the lignin polymerization cycle, which possibly contributes to the development of highly lignified compression wood in nature.

This model experiment may not perfectly mimic the rearomatization step in lignin biosynthesis.

The *erythro/threo* ratios obtained in the present models differed from the ratio of β-O-4 structures for compression wood lignins[1, 2] with only one exception (an *erythro*-preference was obtained from **QM-H-HH$_{biphenyl}$** at any pH in Chapter 3), whereas the proportion of *erythro* form of β-O-4 products from water addition experiment still can be improved by changing the pH, the dioxane/water ratio in solution or the structure of β-O-4 aryl ether **QMs,** especially structures of its β-etherified aromatic ring and corresponding size. In more detail, the β-etherified aromatic ring of **QMs** have more chances with the *ortho*-substitutions than *para*-substitutions to result the *erythro* form of β-O-4 structures during water addition.

Such experiments in this paper may help us to further understanding of condition in cell walls for lignification. Notably, the pH, water-media solvent and *ortho*-position or size of β-etherified aromatic ring in **QM** intermediate play an important role on the lignin polymerization.

5.4 References

[1] Nawawi, D. S., Akiyama, T., Syafii, W., Matsumoto, Y. 2017. Characteristic of β-O-4 structures in different reaction wood lignins of Eusideroxylon zwageri T. et B. and four other woody species. Holzforschung, 71(1), 11-20.

[2] Yeh, T. F., Braun, J. L., Goldfarb, B., Chang, H. M., Kadla, J. F. 2006. Morphological and chemical variations between juvenile wood, mature wood, and compression wood of loblolly pine (Pinus taeda L.). Holzforschung, 60(1), 1-8.

[3] Brunow, G., Sipilä, J., Mäkelä, T. 1989. On the mechanism of formation of non-cyclic benzyl ethers during lignin biosynthesis. Part 1. The reactivity of β-O-4 quinone methides with phenols and alcohols. Holzforschung, 43(1), 55-59.

Acknowledgement

Thanks to this great research platform, I can smoothly finish my doctoral research work. I would like to express my sincerely appreciation to the following people in here.

At my laboratory (Wood Chemistry Laboratory): Professor Matsumoto Yuji, my supervisor; for his professional advice, constant inspiration, patient instruction and kindly caring not only in my study but also in my life in Japan. I also remember the moment four year ago, how exciting I was when I received the accepting letter from Prof. Matsumoto. My deeply grateful again to him for accepting me as a member of this big family. Besides, I would like to express my deepest respect and gratitude to Dr. Akiyama Takuya for his strong support of my Ph.D study: Thanks for his immense knowledge and directed-teaching at the experiment desk, I could begin my study in a short time; Thanks for his patient and extensive discussions with me, I could efficiently settle experimental problems and not lose myself; Thanks for his great help of writing scientific papers, my study work could be admitted quickly by peer review; Thanks for his warm suggestion on how to balance the life and research, I could enjoy a good time for these years in Japan. I want to extend my grateful to Associate Professor Yokoyama Tomoya for his valuable comments and suggestions throughout this research. Thanks for his teaching on lots of organic chemistry. Thanks for his important help on dealing with so many affairs in our laboratory, like reimbursement for the cost of our business trip and chemicals' purchase. I would like to express my thankful to the members of my laboratory. I really enjoyed our discussion on experimental problems, techniques, new ideas and new knowledge. Special thanks to Hada Naoki for gifts of coniferyl alcohol compound.

I would also like to thank the Forestry Chemistry Laboratory for sharing the UV spectrometer with me. Thanks to the big help from Mr. in the NMR analysis room of this school.

Sincere thanks for my wife, Sese, for her accompany, endless encouragement and understanding; for her sharing every happy and sad moment with me; especially for putting up with me during the graduating period. My sincere appreciation to my parents for giving me opportunities, optimistic attitude and freedom to pursue my dream and interest.

Finally, I am grateful to the China Scholarship Council (CSC) for financial support of my study and life abroad.

List of Publications

Journal articles

- ✧ **Zhu Xuhai**, Akiyama Takuya, Yokoyama Tomoya, Matsumoto Yuji. (2019). Lignin-biosynthetic study: Reactivity of quinone methides in the diastereopreferential formation of *p*-hydroxyphenyl- and guaiacyl-type β-O-4 structures. *Journal of Agricultural and Food Chemistry*, DOI: 10.1021/acs.jafc.8b06465.
- ✧ **Zhu Xuhai**, Akiyama Takuya, Yokoyama Tomoya, Matsumoto Yuji. (2019). Stereopreferential formation of β-O-4 structures mimicking softwood lignin biosynthesis: Effects of solvent and the structure of quinone methide lignin models. **(submitted to Biomacromolecules**)

Conference paper

- ✧ **Zhu Xuhai**, Akiyama Takuya, Yokoyama Tomoya, Matsumoto Yuji. (2018). Stereo-preferential formation of *p*-hydroxyphenyl- and guaiacyl-type β-O-4 structures from the quinone methides. *Proceeding of the 5th International Conference on Pulping, Papermaking and Biotechnology*, Nanjing, China. (**Oral presentation**)
- ✧ **Zhu Xuhai**, Akiyama Takuya, Yokoyama Tomoya, Matsumoto Yuji. (2018). Stereo-preferential formation of *p*-hydroxyphenyl-type β-O-4 structures from the quinone methides: Part 2. Water addition to a quinone methide β-etherified with a biphenyl unit. *Proceeding of the 85th Pulp and Paper Research Conference*, Tokyo, Japan. (**Oral presentation**)
- ✧ **Zhu Xuhai**, Akiyama Takuya, Yokoyama Tomoya, Matsumoto Yuji. (2018). Stereo-preferential formation of *p*-hydroxyphenyl-type β-O-4 structures from the quinone methides: Part 2. Water addition to a quinone methide β-etherified with a biphenyl unit. *Proceeding of the 68th Japan wood research society conference*, Kyoto, Japan. (**Poster presentation**)
- ✧ **Zhu Xuhai**, Akiyama Takuya, Yokoyama Tomoya, Matsumoto Yuji. (2017). Stereo-preferential formation of *p*-hydroxyphenyl-type β-O-4 structures from the quinone methides. *Proceeding of the 62nd Lignin Symposium*, Nagoya, Japan. (**Oral presentation**)